A DIRECT METHOD FOR THE DETERMINATION OF EARTH PRESSURES ON RETAINING WALLS

By

ASSAD F. ABDUL-BAKI

Bachelor of Science
Oklahoma State University
Stillwater, Oklahoma
1955

Master of Science
Oklahoma State University
Stillwater, Oklahoma
1956

Submitted to the Faculty of the Graduate
School of the Oklahoma State University
in partial fulfillment of the
requirements for the degree of
DOCTOR OF PHILOSOPHY
May, 1966

A DIRECT METHOD FOR THE DETERMINATION
OF EARTH PRESSURES ON RETAINING WALLS

Thesis Approved:

J. V. Parcher

Thesis Adviser

Roger L. Flanders

Robert G. McIntyre

J. W. Boggs

Dean of the Graduate School

ACKNOWLEDGEMENT

The author, in completing the final phase of his work, wishes to express his gratitude and sincere appreciation to the following individuals:

To his major professor and adviser, Professor J. V. Parcher, for his valuable suggestions and his inspiring method of teaching.

To his committee members, Professors R. L. Flanders, M. Abdel-Hady and R. G. McIntyre.

To Professors J. J. Tuma and D. M. MacAlpine for their assistance and encouragement to pursue graduate work.

To his uncle and aunt, Mr. and Mrs. J. M. Abdul-Baki, who fully supported his undergraduate education.

To his brother, Showky, for his financial help during the last three years.

To his friends, Mr. W. G. Henderson and Mr. E. Citipitioglu.

To his parents and to his wife, Wafiah, to his daughters, Ghada and Feriale, for the many sacrifices which they have made over the past several years to enable the author to continue his work to completion. This represents a personal debt which the author will never be able to repay.

To Mrs. Peggy Harrison for her careful typing of this dissertation.

May, 1965
Stillwater, Oklahoma

A. A. B.

TABLE OF CONTENTS

LIST OF ILLUSTRATIONS

NOMENCLATURE

C_s	Resultant cohesive force along the curved portion of the slip line.
C_w	Resultant adhesive force along the back of the retaining wall.
c	Cohesion in Coulomb's equation
c_a	Adhesion between cohesive soil and the back of the wall
c_o	Cohesion equal to 100 psf
E_A, E_A''	Active force exerted by the wedge
E_A'	Active resistance due to cohesion and surcharge
E_P, E_P''	Passive force exerted by the wedge
E_P'	Passive resistance due to cohesion
F	Total internal force due to friction in cohesionless backfill
F'	Internal force due to cohesion in cohesive backfill
F''	Internal force due to friction in cohesive backfill
H, h	Height of retaining wall
K	Ratio between c_o and c
K_A	Coefficient in Coulomb's equation
P_A	Active earth pressure on retaining walls with cohesionless backfill or sum of P_A' and P_A'' in cohesive backfill.
P_A'	Component of active earth pressure on retaining walls due to cohesion and adhesion

P''_A	Component of active earth pressure on retaining walls due to friction
P_p	Passive earth pressure on retaining walls with cohesionless backfill or sum of P'_p and P''_p in cohesive backfill
P'_p	Component of passive earth pressure on retaining walls due to friction
P''_p	Component of passive earth pressure on retaining walls due to adhesion and cohesion
p_a	Active stress on an element adjacent to the wall
p_p	Passive stress on an element adjacent to the wall
q	Surcharge
W	Weight per unit of length
Z	Arbitrary depth
α_1, α_2	Angles
$\alpha^A_1, \alpha^A_2, \alpha^P_1, \alpha^P_2$	Inclinations of the slip line and its conjugate with respect to the surface of a sloping semi-infinite cohesionless mass, in the active and passive cases.
β	Inclination of semi-infinite soil mass with respect to the horizontal
γ	Unit weight of soil
δ	Angle of wall friction
ϵ	Unit strain
λ, ν	Angles
σ	Total normal stress
τ	Shearing stress
φ	Angle of internal friction or of shearing resistance

ψ_1	Slope of the slip line with respect to the horizontal in a simi-infinite sloping cohesionless mass
ψ_A	Slope of the slip line at the toe of the wall, with cohesive backfill, in the active case
ψ_{A1}	Slope of the slip line at the toe of the wall, with cohesionless backfill, in the active case
ψ_P	Slope of the slip line at the toe of the wall, in the passive case
ω	Angle

CHAPTER I

INTRODUCTION

Earth pressure problems encountered in engineering practice are concerned with the determination of internal stresses acting on the soil masses or the stresses between the soils and the contiguous structures.

The major purpose of this thesis is to deal with a direct solution of the lateral earth pressure on retaining walls holding either cohesionless or cohesive soils. The work will be limited to the case of a rigid wall that will undergo only rotation about its toe.

A historical review of the concepts of earth pressure theory will be helpful in bringing up a wider and clearer picture of its present state of development; also analyses and comparisons of the advantages and disadvantages of the various methods will be facilitated.

The first classical method in earth pressure theory was presented by Coulomb[1], 1776, who assumed that the lines of rupture are straight, and that the shearing resistance: $\tau = c + \mu \sigma$, where μ equals the tangent of the apparent angle of friction.

In 1857, Rankine[2] investigated the conditions of equilibrium by considering an element from a semi-infinite soil mass which is subjected to uniform deformation in a direction parallel to the surface of the mass. Assuming a straight strength line, he was able to formulate the state of failure (plastic equilibrium) for active and passive pressures.

Kötter[3], in 1892, derived a differential equation expressing the stresses along a curved surface of sliding in cohesionless masses. But the difficulties encountered in solving this equation under specific boundary conditions made its application rather impractical.

Jaky[4] (1936) showed that Kötter's equation is also valid for cohesive soil, whereas Ohde[5] (1938) and Hansen[6] (1953) used the equation to determine the distribution of horizontal soil pressure on a yielding vertical wall.

The theory of plasticity was first applied to soil by Prandtl[7] (1920); using Kötter's equation and assuming the soil to be weightless, he found the rupture-figure consists of a system of straight lines through the apex and a system of logarithmic spirals with the apex as their pole. Recently, with the progress accomplished in the field of plasticity, many investigators, including Sokolovski[8] (1960), Freudenthal[9] (1950), Nadai[10] (1950), Drucker and Prager[11] (1950-51), have applied the theory of plasticity to earth pressure and foundation problems.

The work mentioned in the preceeding paragraphs was theoretical. For experimental studies much credit should be accorded the remarkable work done by Terzaghi[12] (1934, 1936), Tschebotarioff[13] (1948-51) and Rowe[14] (1952).

In the literature of earth pressure theory, the names of many other contributors appear, but much of the work was inspired by the efforts of those mentioned above, who made important contributions in the area of study embraced by this thesis.

CHAPTER II

METHODS OF CALCULATING EARTH PRESSURES ON RETAINING WALLS

The different methods used in earth pressure calculations can be classified into three major groups:

1. Extreme method
2. Theories of plasticity
3. Empirical methods

2-1. Extreme Method

The extreme method is based on the conditions of static equilibrium of a sliding wedge, with the assumption that the inclined boundary of the sliding wedge is straight, or a circular or spiral curve.

In the extreme method, the active pressure is the maximum lateral pressure obtained from the many trials investigated for failing wedges involving different assumed failure surfaces as the wall yields; while the passive pressure is the minimum lateral pressure obtained similarly as the wall rotates toward the soil, attempting to displace it.

It is essential to note that the unknown stresses along the failure line do not enter into the moment equilibrium equation when assuming a spiral failure line because the lines of action of these stresses pass through the pole of the spiral and thus the number of unknowns is reduced to make the determination of lateral pressure

possible, Rendulic[15].

In the case of an infinitely distant pole, the spiral will tend to become a straight line; this condition is essentially that considered by Coulomb[1].

If the angle of apparent friction, φ, is equal to zero, Fellenius[16] postulated that the failure line will be a circular arc for which the instanteneous center is the center of that circle.

In the case where $\varphi \neq 0$, Krey[17] postulated that the failure line will be partly a circle and the lines of action of the resultant stresses arising from the normal and frictional components and acting on this circular failure line, will be tangent to a circle, called the friction circle, that has a common center with the circular line of failure, and a radius of R sin φ.

2.2. Theories of Plasticity

The principle is based on setting a criterion of failure in addition to the two equilibrium equations of a stressed earth element.

Rankine's[12] criterion of failure is based on a straight line of failure, Prandtl[7] assumed spiral and straight failure lines.

Kötter was able to derive from the two equilibrium equations and from Coulomb's[1] criterion of failure, a general equation expressing the variation of the stress at any given point on the failure line. The possibility of making use of this equation depends mainly on the boundary conditions at the ends of the failure line.

Jaky[4], Ohde[5] and Frontard[18] made use of Kötter's equation in solving some particular problems.

Drucker and Prager[11] proposed a special theory of plasticity where the actual stresses should fall within a certain interval, the limits of which can be determined by means of a stress field called a statically admissible stress field and a velocity field (strain rate field) called a kinematically admissible velocity field.

2.3. Empirical Methods

These are based on model testing, where the pressure on the wall could be measured and the shape of the rupture line could be observed under actual loading conditions. Also some charts for the calculation of earth pressure were suggested by Peck[20] having a partly theoretical, partly empirical basis.

2.4. Limitations of Known Methods

2.4.1. Extreme Method

The error introduced by using Coulomb's method, which assumes a straight line of failure, is small when calculating the active pressure; but the error becomes large and on the critical side when dealing with the passive pressure.* Moreover, Coulomb's method does not allow the location of the pressure center nor that of the instantaneous center to be determined.

The method proposed by Fellenius[16] is based on the assumption that the angle of apparent friction is zero and that the line of failure is a circle. The instantaneous center of the earth wedge is

---

*K. Terzaghi. Theoretical Soil Mechanics. (New York, 1956) p. 107.

the center of the circle whereas the center of rotation of the wall is assumed to be the projection of the instantaneous center on the plane of the wall. This method will allow the location of the pressure center but it is limited by the major assumption that $\varphi = 0$, and by the fact that the pressure distribution cannot be determined.

Rendulic's method differs from that of Fellenius in that Rendulic considered the case of $\varphi \neq 0$ and used a spiral curve for the line of failure. Thus, he was able to eliminate the moment of the resultant normal stress and frictional component; and the moment due to the cohesion along the spiral curve was determined to be:

$$M_c = \frac{c}{2 \tan \varphi} (r_1^2 - r_0^2)$$

where r_1 and r_0 are the radial distances from the pole to the two extreme points on the spiral.

The disadvantage of this method is that it does not establish any definite relation between the spiral failure line and the center of rotation of the wall. Also the pressure distribution on the wall is not well determined.

The three methods described above are trial methods in which the active pressure is determined from the maximum point of a curve formed by plotting the results of all trials, while the passive pressure is similarly determined from the minimum point of the curve derived from passive pressure trials. These procedures are reliable, but they are lengthy and time consuming.

2.4.2. Theories of Plasticity

The drawback in the theory of limit analysis presented by Drucker, Hodge and Prager[19] is that the result obtained does not agree at all with the actual pressure. This discrepancy is due to the fact that small movement of the earth wedge will cause the shear strains along the rupture line to be so large that the kinematically admissible velocity field condition cannot possibly be satisfied.

However, the solutions by means of Kötter's equation as treated by Prandtl, Jaky[4] and Ohde[5] are exact and valuable for certain problems under specific boundary conditions. But in general this method is so cumbersome that it is frequently impractical.

2.4.3. Empirical Methods

These methods are limited. They can be helpful in research, but the fact that a laboratory model should be built for every specific case, makes their use costly and impracticable.

It may be concluded that none of the present methods for the determination of earth pressure is perfectly satisfactory. Each has its advantages and disadvantages. In practice an engineer will generally prefer to use the Coulomb's method, the friction circle method or the logarithmic spiral method due to their simplicity.

CHAPTER III

NEW METHOD FOR A DIRECT SOLUTION FOR LOCATION OF CRITICAL SLIP SURFACES IN IDEAL SAND

3.1. General

In the calculation of active and passive earth pressures, the soils engineer has, in the past, adopted a trial and error procedure. This has been necessitated by the fact that the location of the critical surface of potential failure is not known. Thus, the procedure consists of determining the earth pressure associated with various assumed failure surfaces and determining from the value so obtained the maximum value indicated for the active pressure and the minimum value indicated for the passive pressure.

The purpose of this study is to provide simple procedures for establishing the most critical surface without resorting to trial and error procedures. The methods to be used in accomplishing this are theoretical in nature and based on certain simplifying assumptions; but the derivations are, in some instances, tempered by practical considerations. Once the configuration of the most critical surface has been established, the friction circle method may be applied in the customary manner to determine the magnitude of the active or passive earth pressure.

3.2. Basic Assumptions

The backfill is assumed to be homogeneous and isotropic, and the horizontal strain, ϵ, is assumed to be constant and independent of depth in a wedge of soil adjacent to the wall. This will be the case when a lateral support yields by tilting about its lower edge, allowing the sand to fail in every point of the sliding wedge.

3.3. Slip Line for Active Pressure Due to Backfill with Horizontal Surface

In the following investigations the case of a cohesionless backfill with a horizontal surface will be studied first. An element at the bottom of the wall will be considered, and the orientation of the failure plane will be determined at that point. From Rankine's theory it is known that the slip line makes an angle with the horizontal surface of the backfill equal to $45^\circ + \varphi/2$ in the case of active pressure. The stresses acting on a soil element adjacent to the bottom of the wall will be as shown in Fig. 3.1 b, where p_A is the active stress on that element, δ is the angle of friction between the wall and the soil, and γ is the unit weight of the soil.

If these stresses are plotted on a Mohr's circle, the orientation of the angle of failure at the bottom of the wall may be readily determined.

The equation of the line of rupture OM is given by:

$$\tau = \sigma \tan \varphi \qquad (3.1)$$

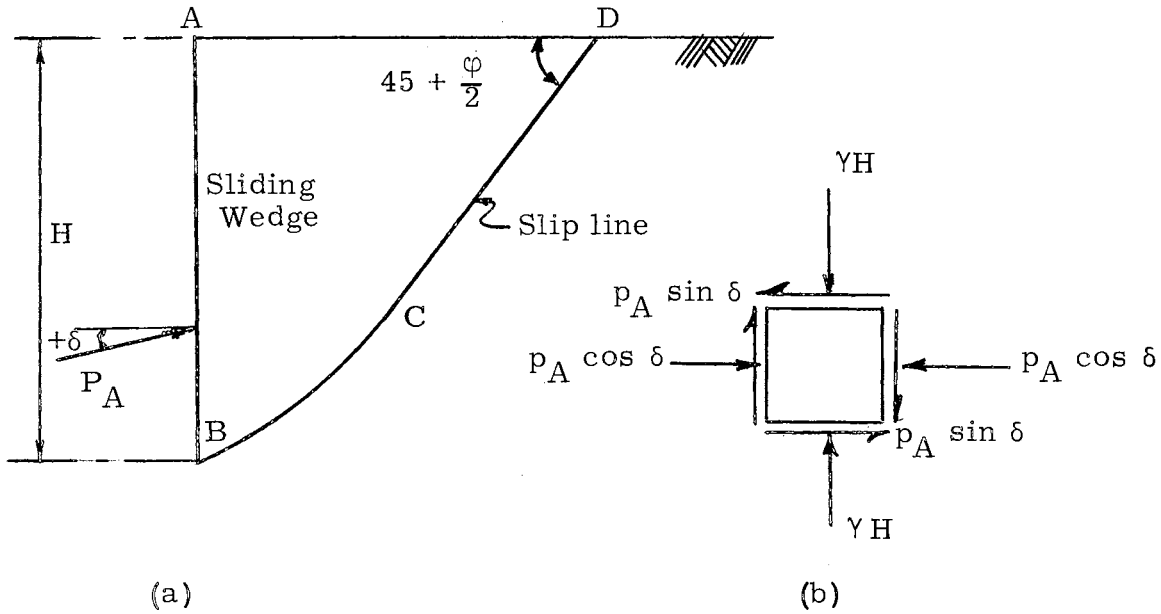

Fig. 3.1 - (a) Slip Line in Cohesionless Backfill Due to Active Case of Failure
(b) Stresses Acting on an Element of Soil at Point B

The following relations can be easily noted, Fig. 3.2:

$$OD = p_A \cos \delta$$

$$BD = p_A \sin \delta$$

$$AD = OD \tan \varphi = p_A \cos \delta \tan \varphi \qquad (3.2)$$

while

$$OA = \frac{AD}{\sin \varphi} = p_A \cos \delta \sec \varphi \qquad (3.3)$$

$$AB = AD - BD = p_A (\cos \delta \tan \varphi - \sin \delta) \qquad (3.4)$$

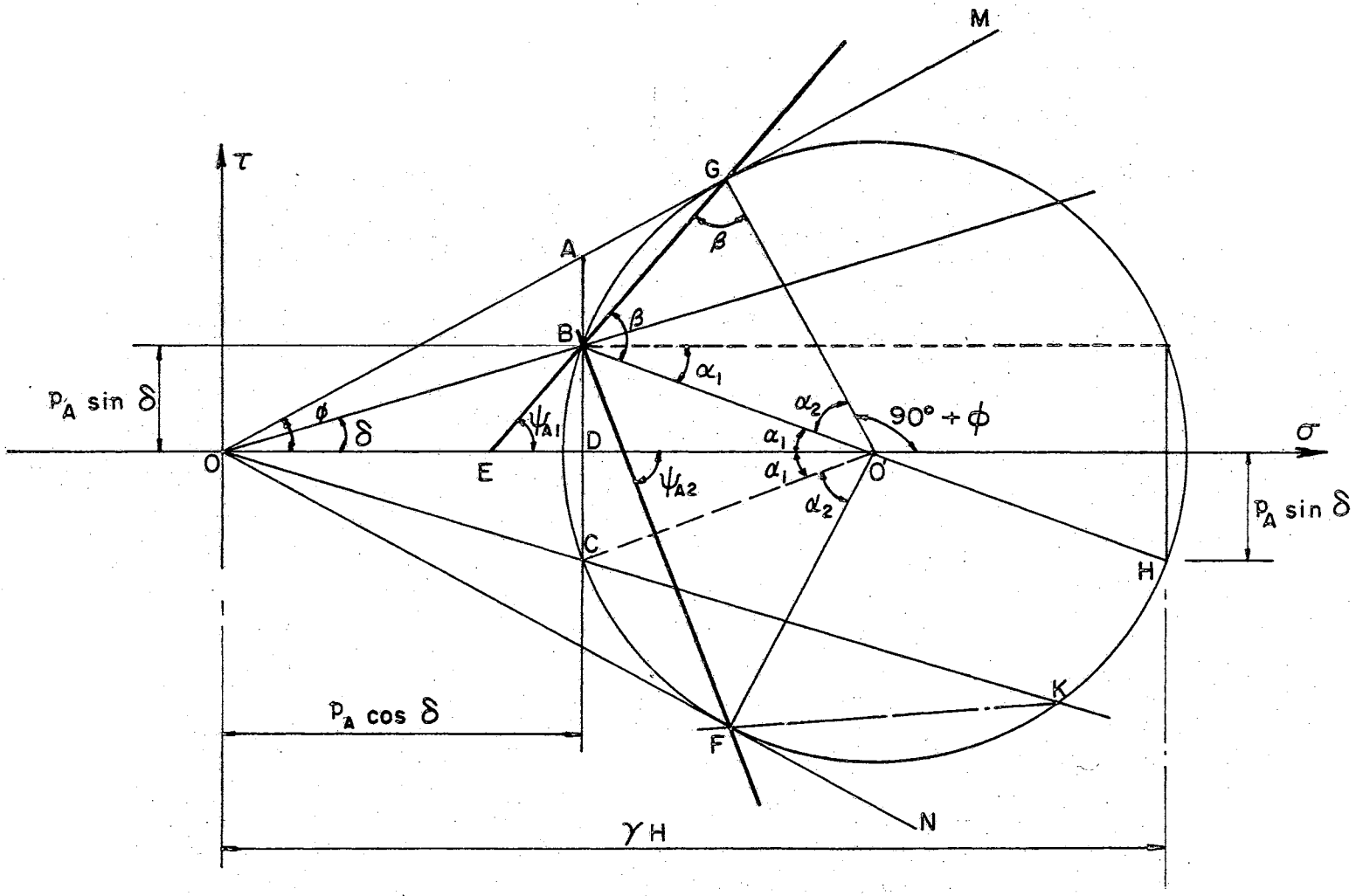

FIG. 3.2

COHESIONLESS SOIL: MOHR'S CIRCLE SOLUTION FOR ACTIVE RESISTANCE AT THE BOTTOM OF THE WALL.

since a tangent AG and a secant AC are drawn to the Mohr's circle from the same point A, it is known that the tangent is the mean proportional between the whole secant and its external segment. Thus:

$$AG^2 = AB \times AC$$

$$AC = AD + DC = AD + BD$$

$$= p_A(\cos \delta \tan \varphi + \sin \delta)$$

Therefore,

$$AG = p_A \sqrt{\cos^2 \delta \tan^2 \varphi - \sin^2 \delta} \qquad (3.5)$$

Now,

$$OG = OA + AG = p_A(\cos \delta \sec \varphi + \sqrt{\cos^2 \delta \tan^2 \varphi - \sin^2 \delta}),$$

and the radius of the circle, O'G, becomes after simplification:

$$O'G = OG \tan \varphi$$

$$= p_A \tan \varphi \sec \varphi (\cos \delta + \sqrt{\cos^2 \delta - \cos^2 \varphi}) \qquad (3.6)$$

Since point B is the active pole the direction of the slip line at the bottom of the wall is given by the slope of line BG.

Considering triangle O'BE, it can be said that ψ_{A1}, the angle of inclination of the failure plane at the bottom of the wall, is equal to:

$$\psi_{A1} = \beta - \alpha_1 \qquad (3.7)$$

But

$$\beta = 90 - \frac{\alpha_2}{2} \tag{3.8}$$

and

$$\sin \alpha_1 = \frac{BD}{O'B} = \frac{p_A \sin \delta}{p_A \tan \varphi \sec \varphi (\cos \delta + \sqrt{\cos^2 \delta - \cos^2 \varphi})}$$

Therefore,

$$\alpha_1 = \sin^{-1} \frac{\sin \delta \cos \varphi}{\tan \varphi (\cos \delta + \sqrt{\cos^2 \delta - \cos^2 \varphi})} \tag{3.9}$$

But

$$\alpha_1 + \alpha_2 = 90 - \varphi$$

then

$$\alpha_2 = 90 - \varphi - \sin^{-1} \frac{\sin \delta \cos \varphi}{\tan \varphi (\cos \delta + \sqrt{\cos^2 \delta - \cos^2 \varphi})} \tag{3.10}$$

Substituting α_2 from (3.10) in Eq. (3.8) and substituting the value obtained for β into Eq. (3.7) and solving for ψ_{A1}:

$$\psi_{A1} = (45 + \varphi/2) - \frac{1}{2} \sin^{-1} \frac{\sin \delta \cos \varphi}{\tan \varphi (\cos \delta + \sqrt{\cos^2 \delta - \cos^2 \varphi})} \tag{3.7a}$$

Let:

$$\omega = \frac{1}{2} \sin^{-1} \frac{\sin \delta \cos \varphi}{\tan \varphi (\cos \delta + \sqrt{\cos^2 \delta - \cos^2 \varphi})} \tag{3.11}$$

then

$$\psi_{A1} = (45 + \varphi/2) - \omega \qquad (3.7b)$$

A few important conclusions can be drawn from Eq. (3.7a):

1. If the angle of wall friction, δ, is equal to zero, the angle ψ_{A1} is equal to $45 + \varphi/2$ which means that the slip line is a straight line and the Rankine value of the earth pressure becomes identical with the Coulomb value.

2. If $\delta \neq 0$, then ψ_{A1} is less than $45 + \varphi/2$ and the slip line can no longer be a straight line. It is actually composed of a straight portion CD, and a circular portion BC as shown in Fig. 3.1a

3. Referring to the graphs in Fig. I,* it can be observed that the relation between ω and δ is approximately linear for values of $\delta \leq \varphi/2$. Beyond that, the relation becomes nonlinear, indicating that the rate of change of ω increases when δ increases. Therefore, when δ exceeds about $\frac{1}{3}\varphi$, ψ_{A1} begins to decrease rapidly. Terzaghi** has called attention to the fact that when δ gets large the failure surface cannot be approximated by a straight line. If Coulomb's method is used to determine the active earth pressure when δ is large, the results will be inaccurate. According to Terzaghi, the results will be on the unsafe side and the error may exceed five percent.

4. It can be observed for cohesionless soil that the slope of the slip line at the bottom of the wall is independent of the depth of

---

*All figures with Roman numerals are presented at the end of of the thesis.

**K. Terzaghi., Theoretical Soil Mechanics. (New York, 1956) p. 107

the wall. This invariant property will allow the pressure distribution on the wall to be accurately determined.

Method for Constructing the Slip Line

Referring to Fig. 3.3, the known properties of the slip line are as follows:

1. The angle that the slip line DC makes with the horizontal is equal to $45 + \frac{\varphi}{2}$, and the conjugate of the slip line, AC, makes the same angle with the horizontal.

2. The portion of the slip line above AC is always straight since the zone of plastic equilibrium includes an active Rankine Zone whose inclined boundaries rise at an angle of $45^\circ + \frac{\varphi}{2}$ to the horizontal.

3. The angle ψ_{A1}, that the slip line makes with the horizontal at the bottom of the wall is known irrespective of the height of the wall.

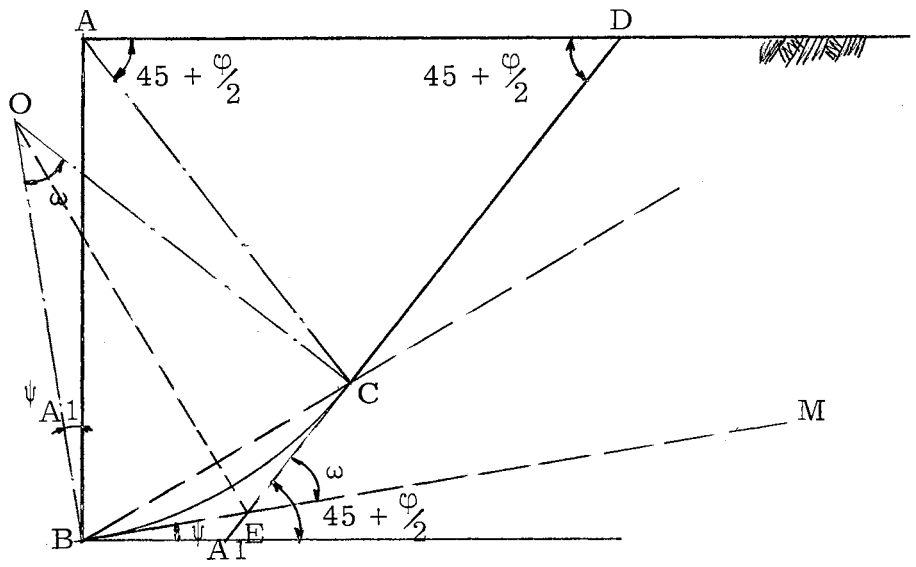

Fig. 3.3 - Method of Constructing the Slip Line for the Case of Active Pressure on a Retaining Wall with Cohesionless Backfill

Thus, the problem is to find a slip line that fulfills these specific requirements:

1. The straight portion DC should be tangent to the curve BC at point C.

2. Point C should be on the conjugate of the slip line, where AC is a unique line of a constant slope because A is a fixed point.

3. The curved portion of the slip line will have BM for a tangent at point B, where the inclination ψ_{A1} of BM is already determined.

For the curved portion of the slip surface, there will be only one circle that satisfies the above conditions. Even though an infinite number of circles may be passed through two points, there will be only one for which the tangents at B and C, respectively, have the slope angles ψ_{A1} and $45^\circ + \varphi/2$.

The location of point C can be determined quite easily from the geometry of the problem.

$$\angle DEM = 45 + \varphi/2 - \psi_{A1}$$

substituting for ψ_{A1} from (3.7b):

$$\angle DEM = 45 + \varphi/2 - 45 - \varphi/2 + \omega = \omega$$

Since EC and EB are tangents to the circle they are equal in length; thus, triangle EBC is isosceles and the two angles EBC and ECB are equal.

Then, since

$$\angle CBE = \angle BCE = \frac{\omega}{2}, \qquad (3.12)$$

point C can be located on AC by drawing line BC that makes an angle $\frac{\omega}{2}$ with the tangent BM.

The center of the unique circle can be located by finding graphically the point of intersection of the bisector of chord BC and the perpendicular to the tangent at point B.

Mathematically, the value of the radius of the circle can be determined from triangle OBC, Fig. 3.3:

$$R = \frac{BC}{2 \sin \frac{\omega}{2}} \tag{3.13a}$$

But it can be proved that

$$BC = h \frac{\sin (45 - \frac{\varphi}{2})}{\cos (\varphi - \frac{\omega}{2})}$$

Therefore:

$$R = \frac{h}{2} \frac{\sin (45 - \frac{\varphi}{2})}{\cos (\varphi - \frac{\omega}{2}) \sin \frac{\omega}{2}} \tag{3.13b}$$

3.4. Slip Line for Passive Pressure Due to Backfill with Horizontal Surface

The case of a cohesionless backfill with a horizontal surface will be first investigated. From Rankine's theory it is known that the slip line makes an angle with the horizontal equal to $45 - \frac{\varphi}{2}$ in the case of passive pressure.

If a soil element adjacent to the bottom of the wall (Fig. 3.4a) is taken, the stresses acting on it are as shown in (Fig. 3.4b), where

p_p is the passive stress and δ is the positive angle of friction between the wall and the soil.

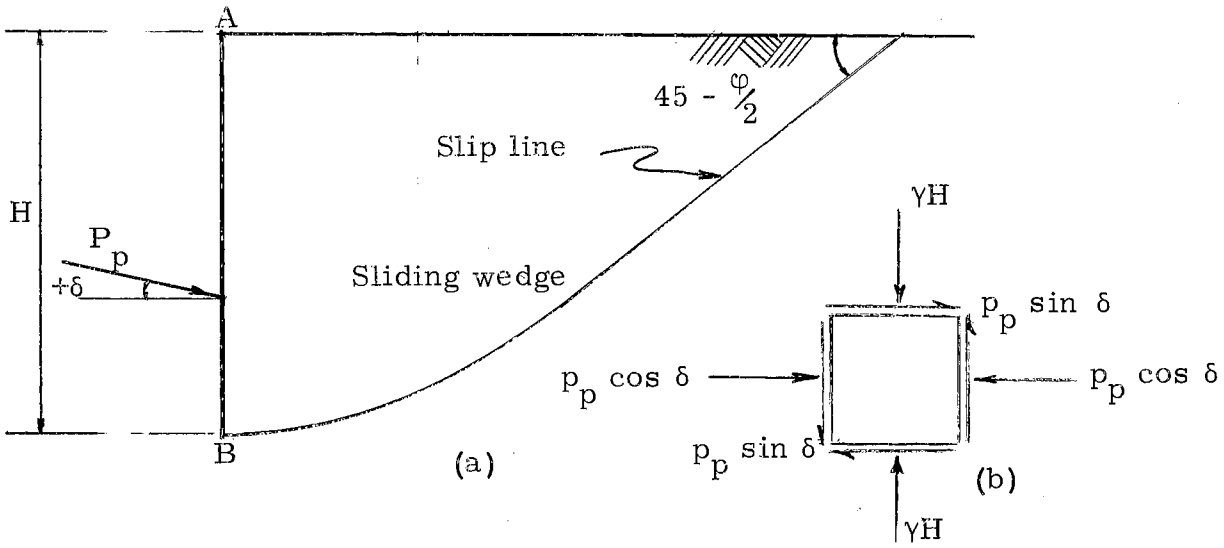

Fig. 3.4 - (a) Slip Line in Cohesionless Backfill Due to Passive Case of Failure
(b) Stresses Acting on an Element of Soil at Point B

If the stresses are plotted on a Mohr's circle, as shown in (Fig. 3.5), the orientation of the angle of failure at the bottom of the wall may be determined.

From Equations (3.9) and (3.10), it can be noted that α_1 and α_2 are independent of the depth z, and they are only dependent on φ and δ.

Point P_p is the pole of the circle and thus P_pF is the tangent to the slip curve at the bottom of the wall, and, indeed, at every point along the wall for which $z > 0$. From the geometry of the Mohr's circle, it can be stated that:

$$\angle C P_p F = \frac{\alpha_2}{2}$$

whereas $\angle C P_p D = \delta$.

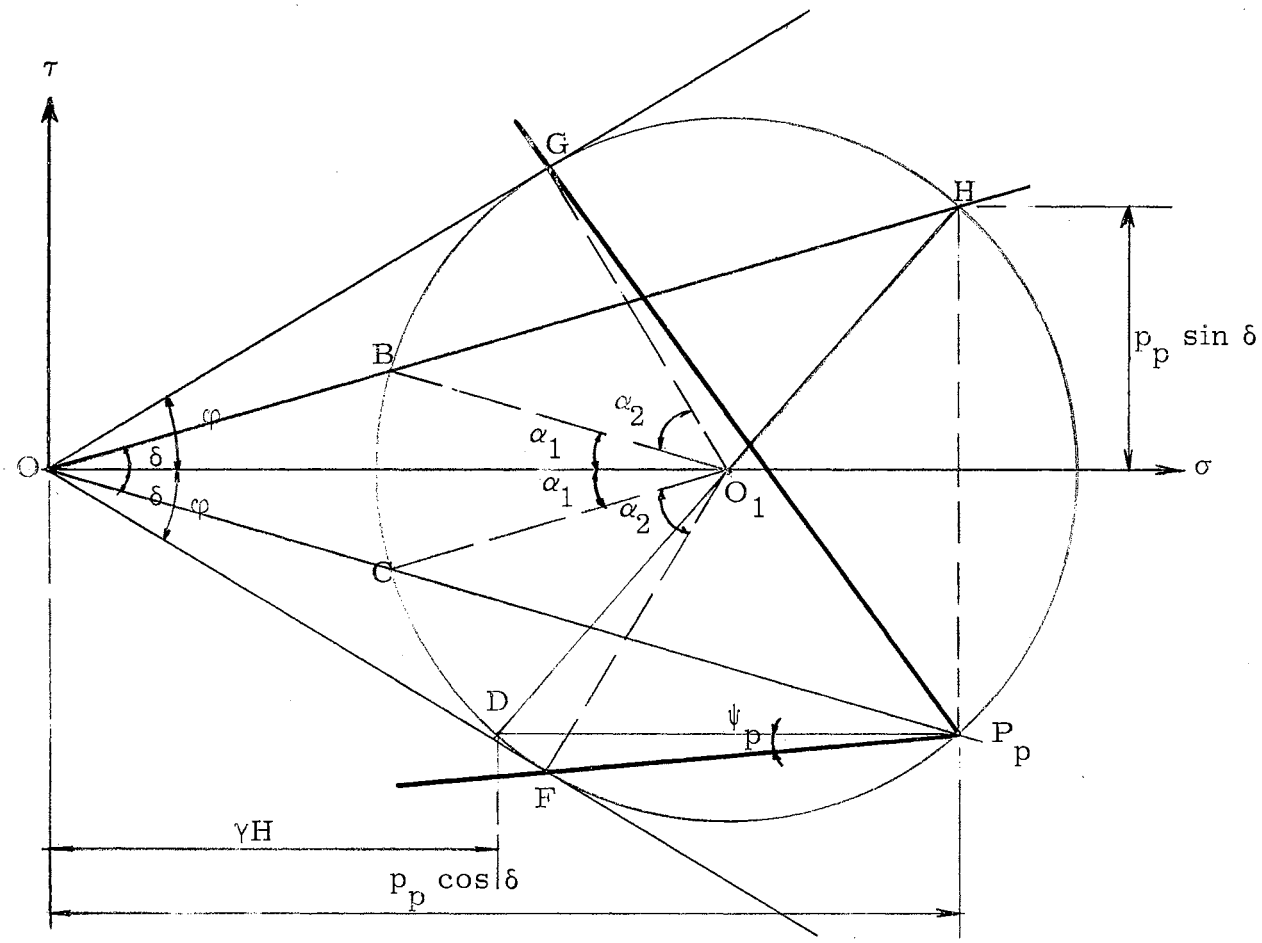

Fig. 3.5 - Cohesionless Soil: Mohr's Circle Solution for Passive Resistance at the Bottom of the Wall

Therefore, $\psi_p = \frac{\alpha_2}{2} - \delta$

Substituting for α_2 from Equation (3.10), it follows that

$$\psi_p = (45 - \frac{\varphi}{2}) - \delta - \omega \qquad (3.14)$$

where ψ_p is the inclination of the tangent to the slip line at the bottom of the wall for the state of passive pressure, and ω is the angle obtained from Eq. (3.11). From Eq. (3.14), it may be observed

that ψ_p can have either a positive value (i.e. the slip line is above the horizontal) when $45 - \varphi/2 > \delta + \omega$, or a negative value (i.e., the slip line at the bottom of the wall swings below the horizontal) when $45 - \varphi/2 < \delta + \omega$.

When $45 - \varphi/2 = \delta + \omega$, $\psi_p = 0$, and the slip line has a zero slope at the bottom of the wall. If ψ_p, equation (3.14), is plotted versus δ, for every φ, as in Fig. III, it may be seen that the curve is a straight line when δ is less than about $\varphi/3$ and then the curve becomes nonlinear. This may explain why Coulomb's method in the case of passive pressure yields result having increasingly excessive error on the critical side, when δ is larger than $\varphi/3$. According to Terzaghi, the percentage of error may become as great as thirty percent.

Method for Constructing the Slip Line

The general procedure used in Article 3.3.1 for the state of active pressure will be followed, except that ψ_p replaces ψ_{A_1}, and the inclination of the slip line with the horizontal surface is $45° - \varphi/2$. Figures 3.6, 3.7 and 3.8 illustrate the procedure.

Case 1: ψ_p Positive

$$\angle \text{MED} = 45 - \frac{\varphi}{2} - \psi_p = \delta + \omega$$

Therefore:

$$\angle \text{EBC} = \frac{1}{2}(\delta + \omega)$$

Angle ψ_p can be obtained from Fig. III and point C can be located on AN by measuring from BM an angle equal to $\frac{1}{2}(\delta + \omega)$.

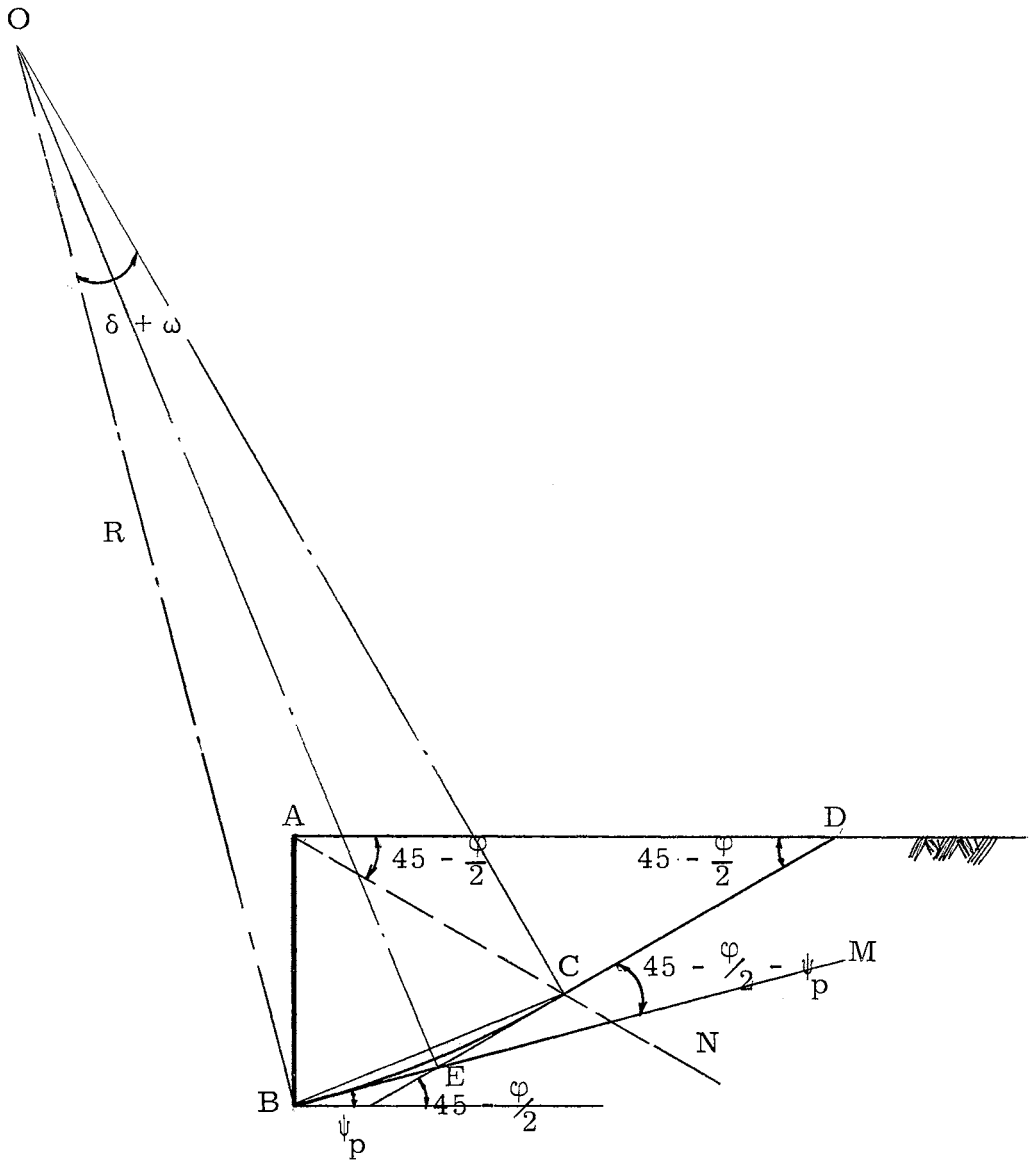

Fig. 3.6 - Method of Constructing the Slip Line for the Case of Passive Pressure on a Retaining Wall with Cohesionless Horizontal Backfill, Where ψ_p Is Positive

The radius of the circular curve is

$$R = \frac{BC}{2 \sin \left(\frac{\delta + \omega}{2}\right)} \qquad (3.15)$$

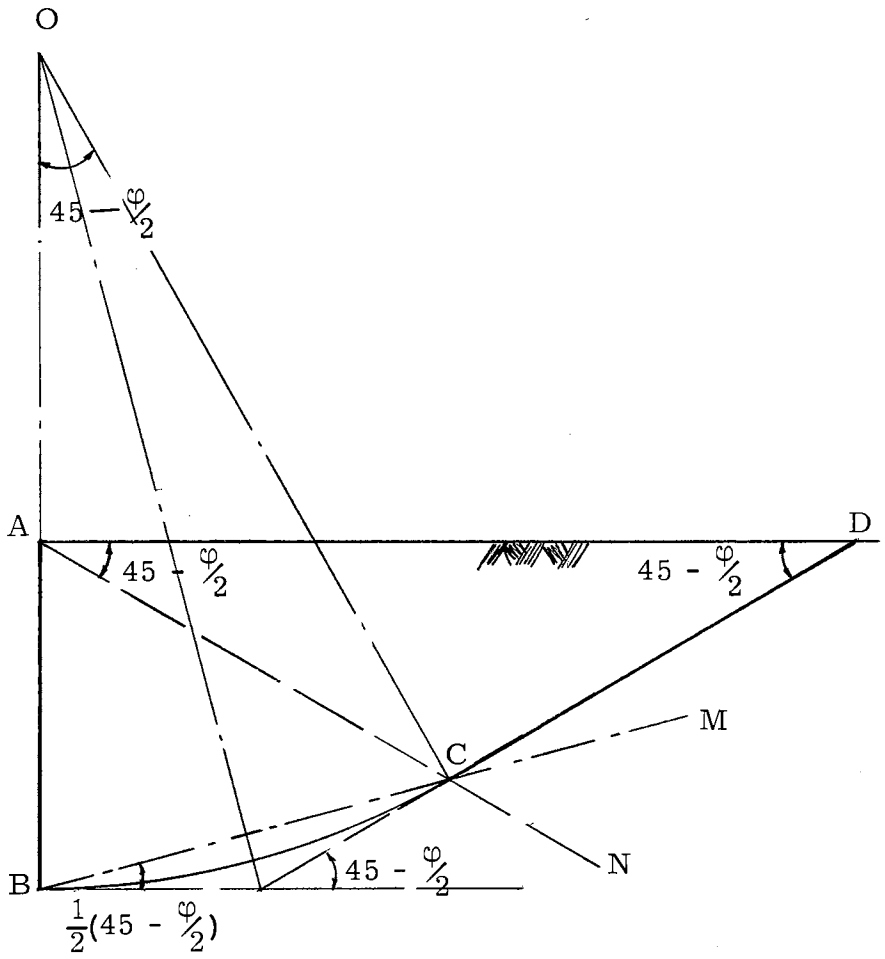

Fig. 3.7 - Method of Constructing the Slip Line for the Case of Passive Pressure on a Retaining Wall with Cohesionless Horizontal Backfill, Where $\psi_p = 0$

Case 2: ψ_p Equal to Zero

$$R = \frac{BC}{2 \sin \frac{1}{2}(45 - \frac{\varphi}{2})} \qquad (3.16)$$

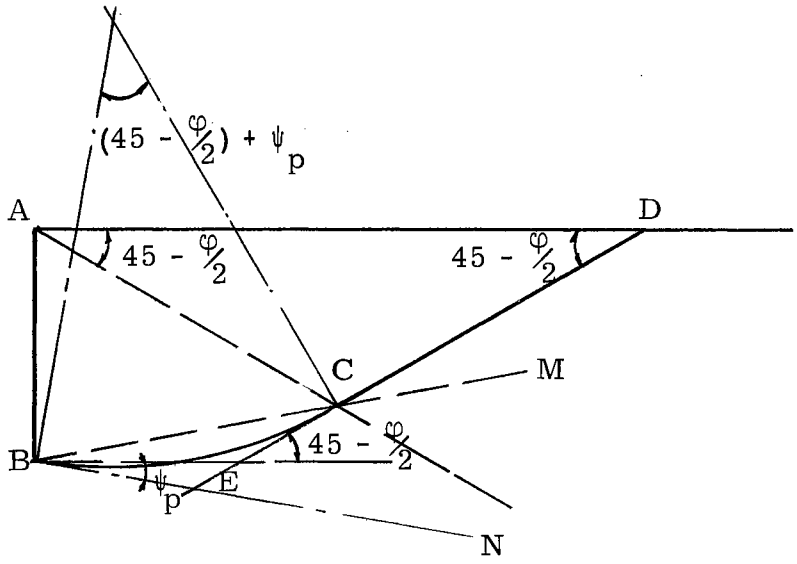

Fig. 3.8 - Method of Constructing the Slip Line for the Case of Passive Pressure on a Retaining Wall with Cohesionless Horizontal Backfill, Where ψ_p Is Negative

Case 3: ψ_p Negative

$$\angle CEN = 45 - \frac{\varphi}{2} + \psi_p$$

$$= (90 - \varphi) - (\delta + \omega) \qquad \text{(See Fig. 3.8)}$$

Therefore:

$$\angle CBE = \frac{1}{2}\angle CEN = (45 - \frac{\varphi}{2}) - \frac{1}{2}(\delta + \omega)$$

The radius of the circular curve is

$$R = \frac{BC}{2 \sin \left[(45 - \frac{\varphi}{2}) - \frac{1}{2}(\delta + \omega)\right]} \qquad (3.17$$

3.5. Slip Lines in Semi-Infinite Inclined Cohesionless Masses

To investigate the Rankine states in an inclined semi-infinite cohesionless mass where $\beta < \varphi$, the conditions for equilibrium of the prismatic element shown in Fig. 3.9a should be examined.

The total vertical force acting on the base of the element is equal to $\gamma z \cos \beta$ and its normal and tangential stress components are respectively equal to $\gamma z \cos^2 \beta$ and $\gamma z \sin \beta \cos \beta$.

In Mohr's diagram (Fig. 3.9b), the lines OM and OM' represent the lines of rupture. The state of stress on the base of the element at a depth z below the surface is represented by the point C where $OB = \gamma z \cos^2 \beta$ and $CB = \gamma z \sin \beta \cos \beta$, then line OC will make with the horizontal axis an angle equal to β.

There are only two circles that can pass through C and be tangent to the rupture lines.

The circle with center O_1 will represent the state of stress at the instant of active failure, while the circle with center O_2 will represent the state of stress at the instant of passive failure.

Point P_A will be the active pole, while P_p will be the passive one.

For the active case the surfaces of shear will be parallel to $P_A E$ and $P_A G$, while for the passive case they will be parallel to $P_p F$ and $P_p H$.

The analytical solutions which follow yield expressions for the angles α_1^A, α_2^A, α_1^P and α_2^P, between the slope surface and the slip surfaces, independently of z.

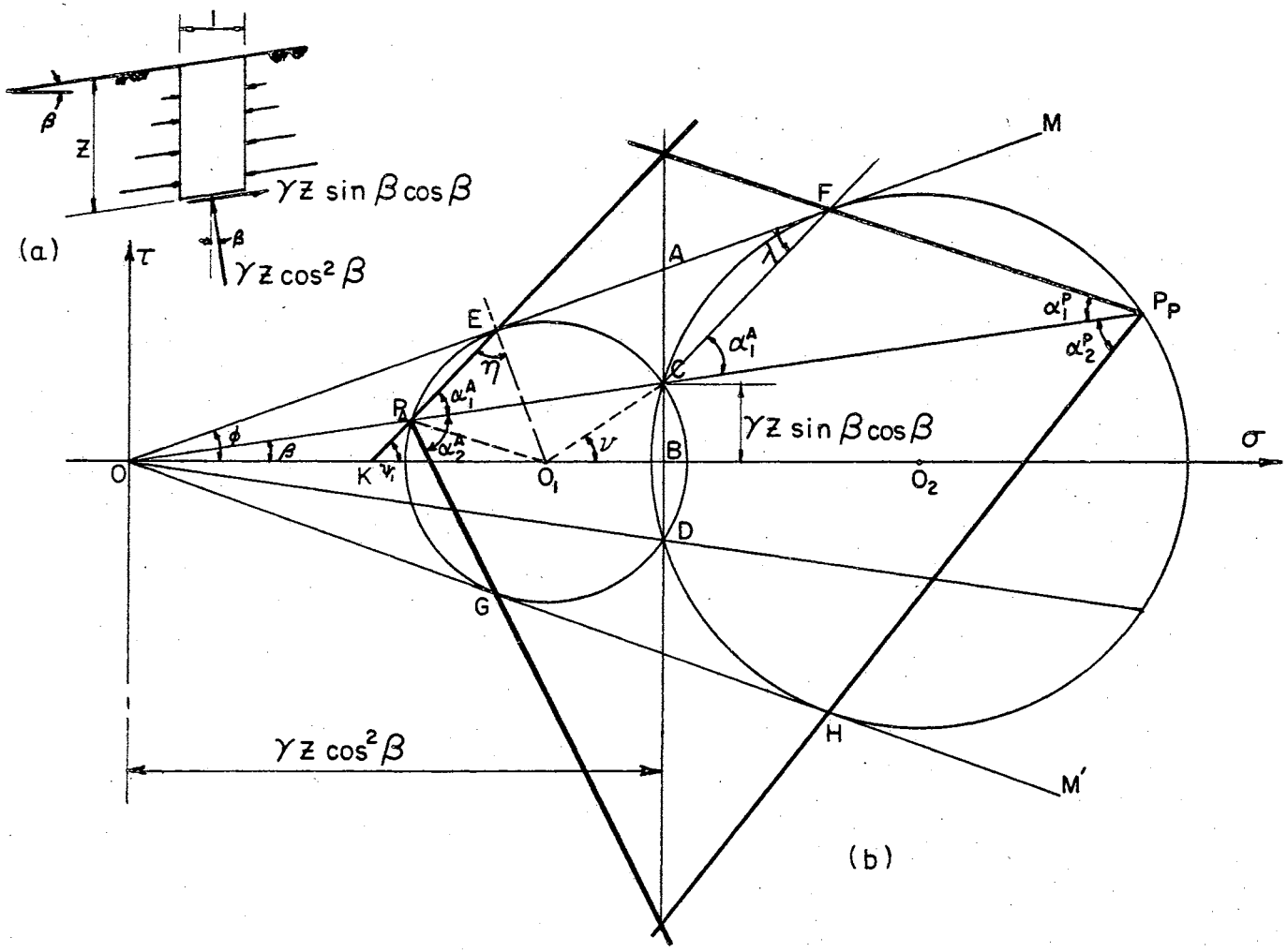

FIG. 3.9

SEMI-INFINITE COHESIONLESS MASS WITH INCLINED SURFACE. (a) STRESSES AT BOUNDARIES OF PRISMATIC ELEMENT. (b) GRAPHIC REPRESENTATION OF STATE OF STRESS AT FAILURE.

The lines AE and AF are tangent, respectively, to circle O_1 and O_2, and they are equal, since each is equal to $\sqrt{AC \times AD}$.

$$AC = \gamma z \cos\beta(\cos\beta \tan\varphi - \sin\beta)$$

$$AD = \gamma z \cos\beta(\cos\beta \tan\varphi + \sin\beta)$$

Therefore,

$$AE = AF = \sqrt{(\gamma z \cos\beta)^2 (\cos^2\beta \tan^2\varphi - \sin^2\beta)}$$

$$= \gamma z \cos^2\beta \sqrt{\tan^2\varphi - \tan^2\beta} \qquad (3.18)$$

But:

$$OA = \gamma z \frac{\cos^2\beta}{\cos\varphi}$$

Then, $OE = OA - AE$

$$= \gamma z \frac{\cos^2\beta}{\cos\varphi} - \gamma z \cos^2\beta \sqrt{\tan^2\varphi - \tan^2\beta}$$

$$= \gamma z \cos^2\beta \left[\sec\varphi - \sqrt{\tan^2\varphi - \tan^2\beta}\right] \qquad (3.19)$$

and

$$O_1E = OE \tan\varphi = \gamma z \cos^2\beta \tan\varphi \left[\sec\varphi - \sqrt{\tan^2\varphi - \tan^2\beta}\right]$$

$$\alpha_1^A = \frac{1}{2}\overset{\frown}{EC} = \frac{1}{2}(\angle EO_1B - \angle BO_1C)$$

Let $\angle BO_1C = \nu$, it follows from triangles O_1CB and OEO_1 that:

$$\nu = \sin^{-1} \frac{\gamma z \sin\beta \cos\beta}{\gamma z \cos^2\beta \tan\varphi \left[\sec\varphi - \sqrt{\tan^2\varphi - \tan^2\beta}\right]}$$

$$= \sin^{-1} \frac{\tan\beta}{\tan\varphi \left[\sec\varphi - \sqrt{\tan^2\varphi - \tan^2\beta}\right]} \qquad (3.20)$$

and $\angle EO_1B = 90 + \varphi$

Therefore:

$$\alpha_1^A = \frac{1}{2}\left(90 + \varphi - \sin^{-1} \frac{\tan\beta}{\tan\varphi \left[\sec\varphi - \sqrt{\tan^2\varphi - \tan^2\beta}\right]}\right)$$

$$\alpha_1^A = \left(45 + \frac{\varphi}{2}\right) - \frac{1}{2}\sin^{-1} \frac{\tan\beta}{\tan\varphi \left[\sec\varphi - \sqrt{\tan^2\varphi - \tan^2\beta}\right]} \qquad (3.21a)$$

But:

$$\alpha_1^A + \alpha_2^A = 90 + \varphi$$

Therefore:

$$\alpha_2^A = 45 + \frac{\varphi}{2} + \frac{1}{2}\sin^{-1} \frac{\tan\beta}{\tan\varphi \left[\sec\varphi - \sqrt{\tan^2\varphi - \tan^2\beta}\right]} \qquad (3.22a)$$

since both α_1^A and α_2^A are independent of z, it is obvious that CF makes with OP_p an angle equal to α_1^A. Therefore, it is easy to proceed to consideration of the passive case.

$$\angle OFC = \lambda = \alpha_1^P$$

because in the same circle, if inscribed angles have the same arc, they are equal. Also,

$$\lambda = \alpha_1^A + \beta - \varphi$$

Therefore:

$$\alpha_1^P = (45 - \tfrac{\varphi}{2}) + \beta - \tfrac{1}{2}\sin^{-1}\frac{\tan\beta}{\tan\varphi\left[\sec\varphi - \sqrt{\tan^2\varphi - \tan^2\beta}\right]} \quad (3.23a)$$

and

$$\alpha_2^P = (45 - \tfrac{\varphi}{2}) - \beta + \tfrac{1}{2}\sin^{-1}\frac{\tan\beta}{\tan\varphi\left[\sec\varphi - \sqrt{\tan^2\varphi - \tan^2\beta}\right]} \quad (3.24a)$$

Referring to Fig. 3.9b it may be seen that the angle ψ_1 that P_AE makes with the horizontal is constant, being independent of the location of P_A on line OC. By reasoning identical to that which led to the expression in Eq. (3.7b), except that β replaces δ, it is found that

$$\psi_1 = (45 + \tfrac{\varphi}{2}) - \tfrac{1}{2}\sin^{-1}\frac{\sin\beta\cos\varphi}{\tan\varphi(\cos\beta + \sqrt{\cos^2\beta - \cos^2\varphi})} \quad (3.25)$$

Referring to triangle OP_AK, ψ_1 is an external angle, and thus it is equal to the sum of non-adjacent internal angles

$$\alpha_1^A = \psi_1 - \beta \quad (3.21b)$$

$$\alpha_2^A = 90 + \varphi - \alpha_1^A \quad (3.22b)$$

Equation (3.23a) may be written in the following form:

$$\alpha_1^P + \frac{\varphi}{2} = (45 + \frac{\varphi}{2}) - \frac{1}{2}\sin^{-1}\frac{\tan\beta}{\tan\varphi\left[\sec\varphi - \sqrt{\tan^2\varphi - \tan^2\beta}\right]} + \beta - \frac{\varphi}{2}$$

in which the first three terms on the right side represent the expression for α_1^A as shown in expression (3.21a).

Therefore:

$$\alpha_1^P = \alpha_1^A + \beta - \varphi,$$

and substituting for α_1^A from (3.21b)

$$\alpha_1^P = \psi_1 - \beta + \beta - \varphi = \psi_1 - \varphi \qquad (3.23b)$$

Also, from Fig. 3.9b

$$\alpha_2^P = 90 - \varphi - \alpha_1^P,$$

from which (using Eq. 3.23b)

$$\alpha_2^P = 90 - \varphi - \psi_1 + \varphi = 90 - \psi_1 \qquad (3.24b)$$

Studying Fig. IV to VII, one can observe that the angles of failure are linearly related to β up to about $\beta = \varphi/3$, whereas beyond that limit the relation becomes nonlinear.

3.5.1. Application to the Slip Lines for Backfills Behind Retaining Walls in the Active Case

The procedure used previously will be followed, with only two modifications:

(1) The angle that the slip line makes with the sloping surface of the backfill should be equal to α_1^A which can be obtained from Fig. IV.

(2) The angle that the conjugate of the slip line makes with the sloping surface should be equal to α_2^A which can be obtained from Fig. V.

The procedure used to plot the slip line is illustrated in Fig. 3.10.

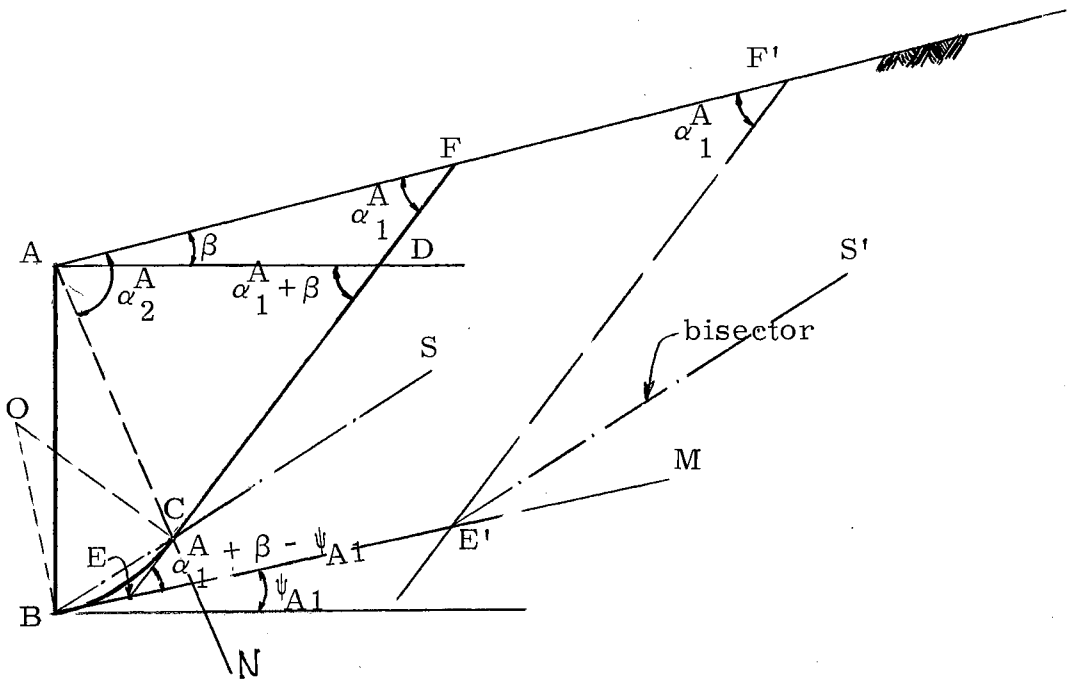

Fig. 3.10 - Method of Constructing the Slip Line for the Case of Active Pressure on a Retaining Wall with Cohesionless Sloping Backfill

$$\angle F'E'M = \alpha_1^A + \beta - \psi_{A1}$$

Through point E' draw the bisector E'S', and then through B draw BS parallel to E'S'. The point of intersection of BS with AN is C which is located at the juncture of the straight portion of the slip line with the circular curved portion.

$$R = \frac{BC}{2 \sin \frac{1}{2}\left[\alpha_1^A + \beta - \psi_{A1}\right]} \tag{3.26}$$

3.5.2. Application to the Slip Lines For Backfill Behind Retaining Walls in the Passive Case

In Article 3.5, expressions for α_2^P (3.24a, b) and its conjugate α_1^P (3.23a, b) were developed. These above angles can be obtained respectively from Fig. VI* and VII.*

The procedure for drawing the slip line is similar to that discussed for the case of a horizontal backfill surface. Since ψ_P may be either positive, zero, or negative, the expression for R varies accordingly as follows:

$$R = \frac{BC}{2 \sin \frac{1}{2}(\alpha_2^P + \beta - \psi_P)} \qquad \text{when } \psi_P > 0 \tag{3.27a}$$

$$R = \frac{BC}{2 \sin \frac{1}{2}(\alpha_2^P + \beta)} \qquad \text{when } \psi_P = 0 \tag{3.27b}$$

$$R = \frac{BC}{2 \sin \frac{1}{2}\left[\alpha_2^P + \beta + |\psi_P|\right]} \qquad \text{when } \psi_P < 0 \tag{3.27c}$$

* All figures in Roman numerals are presented at the end of the thesis.

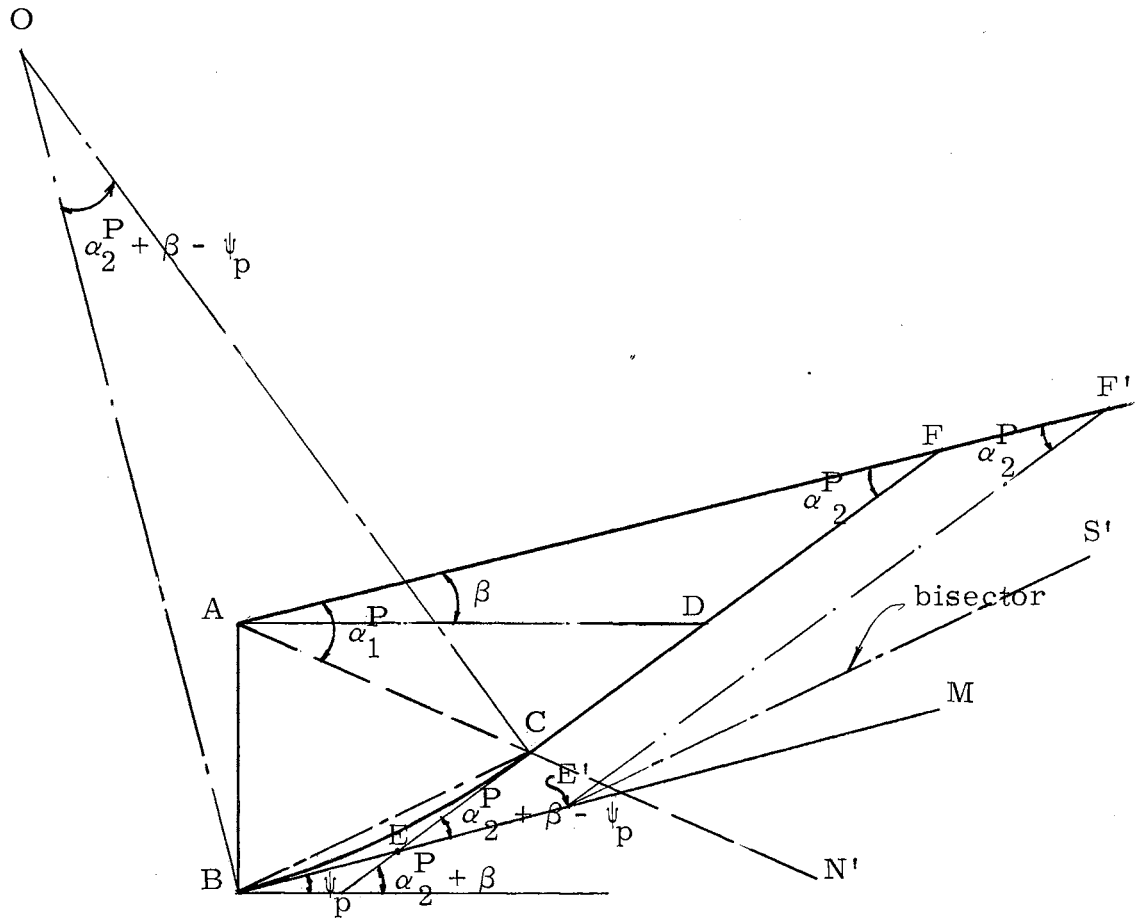

Fig. 3.11 - Method of Constructing the Slip Line for the Case of Passive Pressure on a Retaining Wall with Cohesionless Sloping Backfill

CHAPTER IV

NEW METHOD FOR A DIRECT SOLUTION FOR LOCATION OF CRITICAL SLIP SURFACES IN COHESIVE SOILS

4.1. Basic Assumptions

The cohesive backfill is assumed to be homogeneous and isotropic, and the horizontal strain, ϵ, is assumed to be constant and independent of depth in a wedge of soil adjacent to the wall. This will be the case when a lateral support yields by tilting about its lower edge, allowing the clay to fail in every point of the sliding wedge. Also, it is assumed that the adhesion between the back of the wall and the soil is equal to the cohesion of clay. In case the cohesion is larger than 1000 psf, it would be reasonable to limit the adhesion to 1000 psf, as suggested by the British Civil Engineering Code of Practice No. 2; this could be explained as a result of less intimate adhesion between the wall and the clay as the clay gets stiffer. Also, according to Terzaghi*, in the case of active pressure, the maximum stable height of an unsupported vertical bank which has been weakened by tension cracks is $2.67 \frac{c}{\gamma} \tan (45 + \frac{\varphi}{2})$.

4.2. Slip Line for Active Pressure Due to Backfill with Horizontal Surface

A soil element taken at the bottom of the wall is considered to

---

* K. Terzaghi. Theoretical Soil Mechanics. (New York, 1956), p. 154.

be in equilibrium, see Fig. 4.1a, b, and the stresses are plotted on a Mohr's circle diagram as shown in Fig. 4.2. The orientation of the failure surface at the bottom of the wall will be determined mathematically, but in practical problems a graphical solution is recommended for reasons that will be mentioned later.

c_a is the adhesion between the clay and the back of the wall and it is equal to c, p_A is the active stress, and δ is the angle of friction between the wall and the soil.

The equation of the line of rupture MN is given by:

$$\tau = c + \sigma \tan \varphi \qquad (4.1)$$

The following relations can be easily noted:

$$ED = p_A \sin \delta$$

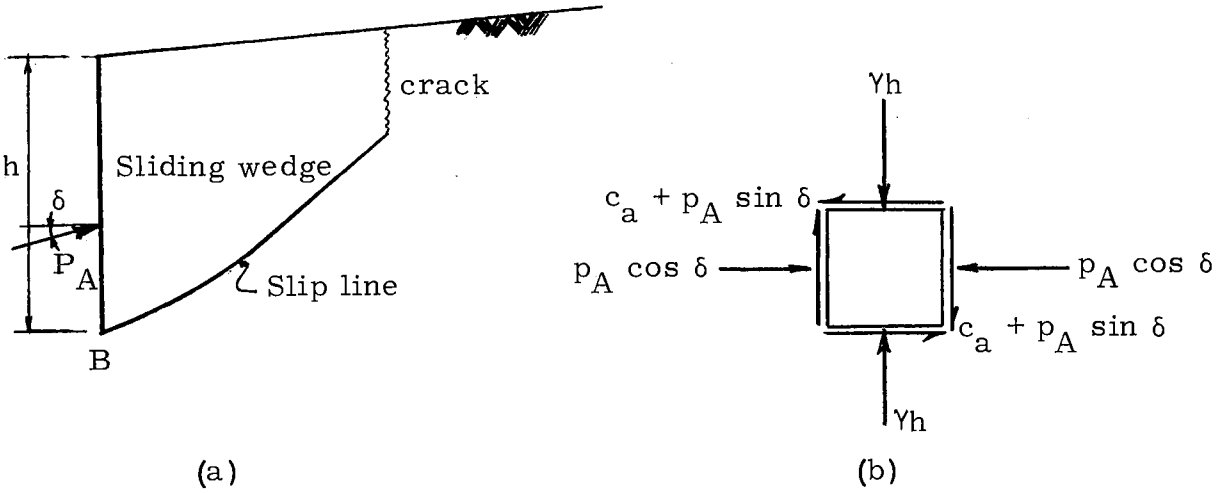

Fig. 4.1 - (a) Slip Line in Cohesive Backfill Due to Active Case of Failure
(b) Stresses Acting on an Element of Soil at Point B

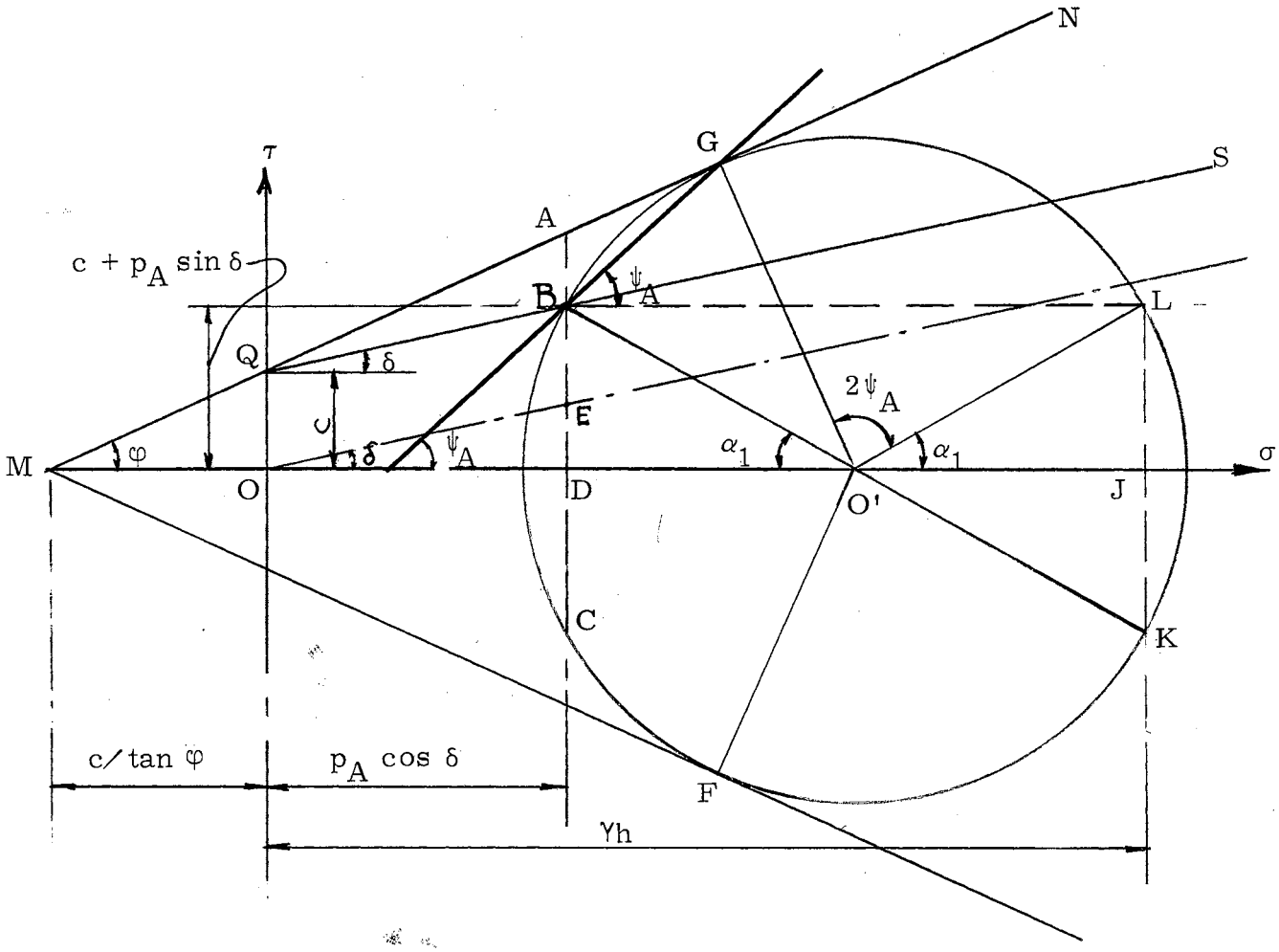

Fig. 4.2 - Cohesive Soil: Mohr's Circle Solution for Active Resistance at the Bottom of the Wall

$$EB = c$$

Therefore:

$$BD = c + p_A \sin \delta$$

$$AD = \left(\frac{c}{\tan \varphi} + p_A \cos \delta\right) \tan \varphi$$

whereas:

$$AB = AD - BD$$

$$= p_A (\cos \delta \tan \varphi - \sin \delta)$$

and

$$MA = \left(\frac{c}{\tan \varphi} + p_A \cos \delta\right) \frac{1}{\cos \varphi}$$

If a tangent and a secant are drawn to a circle from the same point, the tangent is the mean proportional between the whole secant and its external segment. Thus:

$$AG^2 = AB \times AC$$

where

$$AC = c + p_A \cos \delta \tan \varphi + c + p_A \sin \delta$$

$$= 2c + p_A (\cos \delta \tan \varphi + \sin \delta)$$

Then

$$AG = \sqrt{2 p_A c(\cos \delta \tan \varphi - \sin \delta) + p_A^2(\cos^2 \delta \tan^2 \varphi - \sin^2 \delta)}$$

After simplifying:

$$AG = \sec \varphi \sqrt{p_A c(\sin 2\varphi \cos \delta - 2 \cos^2 \varphi \sin \delta) + p_A^2(\cos^2 \delta - \cos^2 \varphi)} \qquad (4.2)$$

$$MG = MA + AG$$

$$= \frac{c}{\sin\varphi} + p_A \frac{\cos\delta}{\cos\varphi}$$

$$+ \frac{1}{\cos\varphi}\sqrt{p_A c(\sin 2\varphi \cos\delta - 2\cos^2\varphi \sin\delta) + p_A^2(\cos^2\delta - \cos^2\varphi)} \tag{4.3}$$

Let

$$B = \sqrt{p_A c(\sin 2\varphi \cos\delta - 2\cos^2\varphi \sin\delta) + p_A^2(\cos^2\delta - \cos^2\varphi)} \tag{4.4a}$$

Then:

$$O'G = MG \tan\varphi$$

$$= \frac{c}{\cos\varphi} + p_A \frac{\cos\delta \sin\varphi}{\cos^2\varphi} + \frac{\sin\varphi}{\cos^2\varphi} B \tag{4.5}$$

$$\sin\alpha_1 = \frac{BD}{O'B}$$

$$= \frac{(c + p_A \sin\delta)\cos^2\varphi}{c\cos\varphi + p_A \cos\delta \sin\varphi + B\sin\varphi}$$

Therefore:

$$\alpha_1 = \sin^{-1}\frac{(c + p_A \sin\delta)\cos^2\varphi}{c\cos\varphi + p_A \cos\delta \sin\varphi + B\sin\varphi} \tag{4.6a}$$

From Fig. 4.2 it is observed that:

$$90 + \varphi = 2\psi_A + \alpha_1$$

Therefore:

$$\psi_A = 45 + \frac{\varphi}{2} - \frac{1}{2}\alpha_1 \tag{4.7}$$

But

$$O'M = \frac{c}{\tan\varphi} + \frac{1}{2}(p_A \cos\delta + \gamma h) = \frac{MG}{\cos\varphi}$$

Substituting for MG from Equation (4.3):

$$\frac{c}{\tan\varphi} + \frac{1}{2}(p_A \cos\delta + \gamma h) = \frac{c}{\sin\varphi\cos\varphi} + \frac{\cos\delta}{\cos^2\varphi}\, p_A$$

$$+ \frac{1}{\cos^2\varphi}\sqrt{p_A c(\sin 2\varphi\cos\delta - 2\cos^2\varphi\sin\delta) + p_A^2(\cos^2\delta - \cos^2\varphi)}$$

Rearrange terms, and write the above equation in the following form:

$$p_A^2\left[\frac{\cos^2\delta}{4}(3 + \sin^2\varphi)(1 - \sin^2\varphi) - \cos^2\varphi\right]$$

$$+ p_A c\left[\sin(2\varphi - \delta) - \sin\delta - \frac{\cos\delta\sin 2\varphi}{2}(1 + \sin^2\varphi) + \frac{\gamma h}{2c}\cos\delta(1 - \sin^4\varphi)\right]$$

$$- \left[\frac{\gamma h}{2}\cos^2\varphi - \frac{c}{2}\sin 2\varphi\right]^2 = 0 \tag{4.8a}$$

Denoting:

$$\left.\begin{aligned} a &= \frac{\cos^2\delta}{4}(3 + \sin^2\varphi)(1 - \sin^2\varphi) - \cos^2\varphi \\ b &= \sin(2\varphi - \delta) - \sin\delta - \frac{\cos\delta\sin 2\varphi}{2}(1 + \sin^2\varphi) + \frac{\gamma h}{2c}\cos\delta(1 - \sin^4\varphi) \\ d &= \left(\frac{\gamma h}{2}\cos^2\varphi - \frac{c}{2}\sin 2\varphi\right)^2 \end{aligned}\right\} \tag{4.9a}$$

Equation (4.8a) may be presented in the following form:

$$a\, p_A^2 + cb\, p_A - d = 0$$

Solving for p_A:

$$p_A = \frac{-cb \mp \sqrt{(cb)^2 + 4ad}}{2a} \tag{4.10a}$$

For physical reasons the positive root should be used. Therefore:

$$p_A = \frac{-cb + \sqrt{(cb)^2 + 4ad}}{2a} \tag{4.10b}$$

p_A calculated from (4.10b) may be substituted in Equation 4.6a to determine α_1. Then the problem of getting ψ_A can be easily handled by Equation (4.7).

Equations (4.9a) may be expanded in series form; neglecting terms of the third power and above since in cohesive soils, the angles φ and δ are small, usually less than 30°. Thus:

$$\left.\begin{aligned} a &= \frac{1}{4}(2\varphi^2 - 3\delta^2 - 1) \\ b &= \varphi - 2\delta + \frac{\gamma h}{2c} \\ d &= \frac{(\gamma h)^2}{4}(1 - 2\varphi^2) - \gamma hc\,(1 - \varphi^2) + c^2 \end{aligned}\right\} \tag{4.9b}$$

Also, Equation (4.4a) may be expanded in series form:

$$B = \sqrt{2\, p_A\, c\,(\varphi - \delta) + p_A^2(\varphi^2 - \delta^2)} \tag{4.4b}$$

Then, from (4.6a), α_1 can be written in the following form:

$$\alpha 1 = \sin^{-1} \frac{(c + p_A \delta)(1 - \varphi^2)}{c\,(1 - \frac{\varphi^2}{2}) + (p_A + B)\varphi} \qquad (4.6b)$$

Note that φ and δ should be expressed in radians.

It is apparent that the numerical calculation for ψ_A are tedious and cumbersome, but with the use of the computer a solution may be obtained quite easily. Another mathematical solution for ψ_A is presented in the Appendix.

A graphical solution for ψ_A will be discussed, as a background for the method followed to tabulate values of ψ_A. The problem encountered is that, starting from the stresses acting on the particle shown in Fig. 4.1b, the equivalent Mohr's circle cannot be drawn directly to satisfy the failure conditions. This is due to the fact that p_A is unknown. The stress γh is known, and it can be located on the horizontal axis, while $c + p_A \sin \delta$ is unknown but must correspond to the ordinate at the intersection of Mohr's circle and line QS which makes an angle δ with the horizontal, see Fig. 4.2. Point L, which represents the state of stress on the horizontal faces of the particle, Fig. 4.1b, is antisymmetrical to point C, which represents the state of stress on the vertical faces of the particle. Point B, which is the image of points L and C, is the active pole and has to be simultaneously on the Mohr's circle and on line QS.

There will be an infinite number of Mohr's circles that satisfy the following conditions:

(a) Their centers are located on the horizontal σ-axis.

(b) They are all tangent to the rupture lines.

(c) Point J falls within the circles.

From all of these circles there is one and only one Mohr's circle satisfying the above conditions which also fulfills the condition that point B is the image of point L. Point B, as previously stated, has to lie on the line QS.

However, in spite of the fact that there exists a unique Mohr's circle that represents the state of failure for the known stress γh, this circle cannot be readily drawn.

A general method will be presented to illustrate the construction of the circle for any value of γh.

Through point M, Fig. 4.3, draw the two rupture lines MN and MN' making angle φ with the horizontal, and draw three circles far apart and tangent to the rupture lines. The center of the smallest of the three circles should be chosen such that this circle does not intersect the τ-axis. The reason of this condition will be clarified in the Appendix. Through point A (where OA = c) draw line AD such that it makes angle δ with the horizontal; this line cuts the three circles respectively at B, C and D. The respective images of these three points on the circles will be point E, F and G.

The line joining E, F and G is extremely close to a straight line. An analytical proof with a numerical illustration are presented in the Appendix. This locus of the images of the points of intersection of the δ-line with the Mohr's circles deviates negligibly from a straight line when it gets very close to the τ-axis.

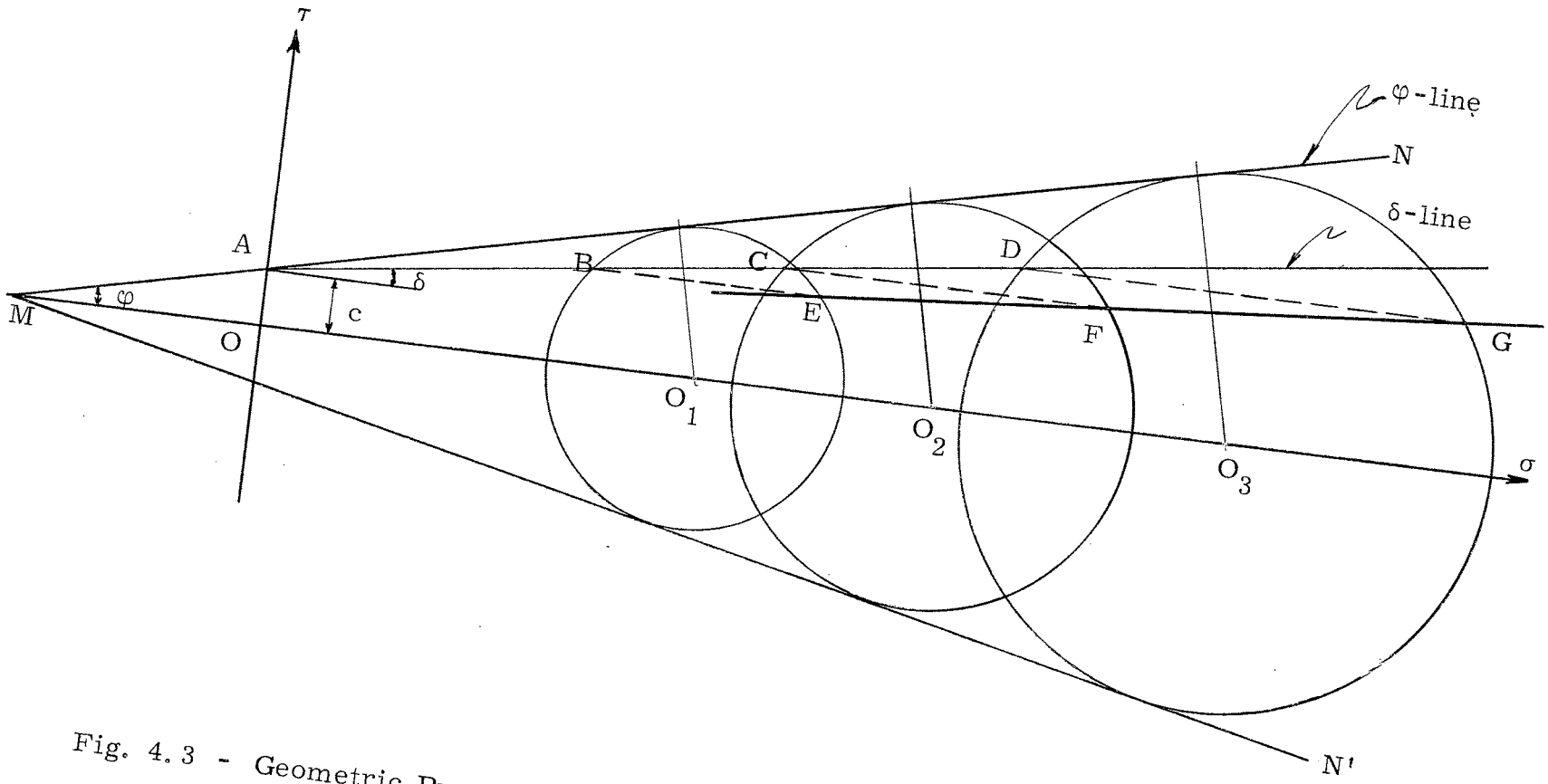

Fig. 4.3 - Geometric Properties of the Horizontal Projections of the Points of Intersection of the δ-Line with Mohr's Circles, (Active Case).

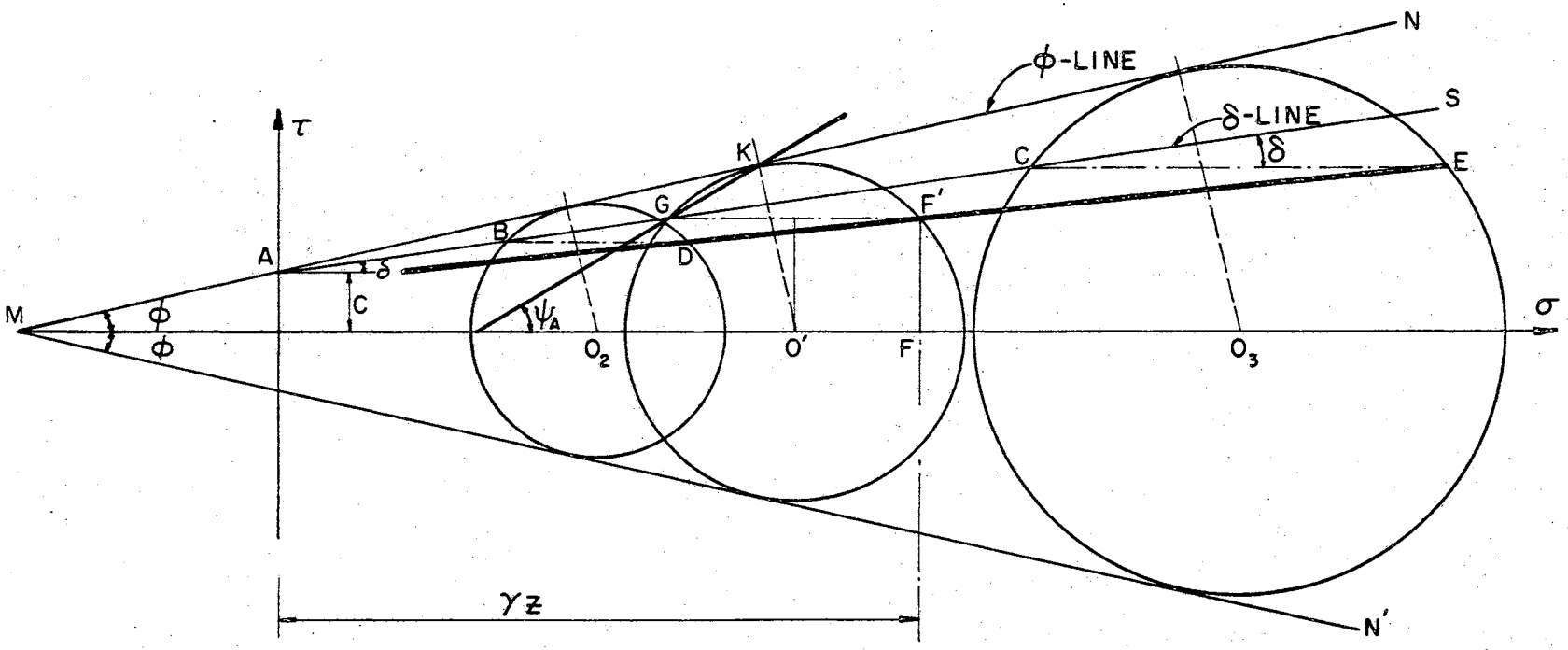

FIG. 4.4

METHOD OF DRAWING THE UNIQUE MOHR'S CIRCLE REPRESENTING THE STATE OF ACTIVE FAILURE AT THE BOTTOM OF THE WALL.

If, for given soil properties, the rupture lines MN and MN', and the line AS, are drawn as shown in Fig. 4.4, it will be enough to draw two circles far apart, tangent to the rupture lines. On these two circles locate the images of B and C, which are points D and E. The line connecting D to E is the locus of all the images of γz on the corresponding circles.

Let a certain stress γz be given, locate that value on the horizontal axis, e.g., point F. Then the vertical projection of F on line DE will be point F' and the horizontal projection of F' on line AS is point G.

Now, the unique Mohr's circle that passes through G and F' and is tangent to the rupture line may be drawn. This circle is constructed by extending the bisector of line GF' until it intersects the horizontal axis at point O'. Point O' will be the center of the required circle whose radius is O'G. The angle ψ_A that the tangent to the slip line makes at the bottom of the wall in the active case can be measured directly from the sketch, as shown.

Referring to Fig. VIII to XII, it may be observed that ψ_A is affected directly by the height of the wall and the adhesion of clay. The effect of these two variables becomes negligible if the height of the wall exceeds about twenty-five feet. Also, in the case of large δ the ψ_A-curve becomes quite flat and the rate of change of ψ_A with respect to the height becomes almost zero.

Once ψ_A is obtained from the graph, the method of plotting the slip line is as explained previously in section 3.3, except that the slip line should start from the bottom of the tension crack, see Section 5.4.2.

4.3. Slip Line for Passive Pressure Due to Backfill with Horizontal Surface

A mathematical derivation for ψ_P, where ψ_P is the inclination of the failure surfaces adjacent to the wall for the passive condition, can be accomplished in a manner similar to that used for the active case. However, the resulting expression is so complex that it is of no practical use; and a graphical solution for the problem may be made as simply as for the active case.

To get the angle of failure at the bottom of a retaining wall subjected to passive pressure, an element of soil adjacent to point B can be isolated. The stresses acting on the element are shown in Fig. 4.5b.

A Mohr's circle representing the state of stress cannot be drawn directly because p_p is unknown. However, the problem may

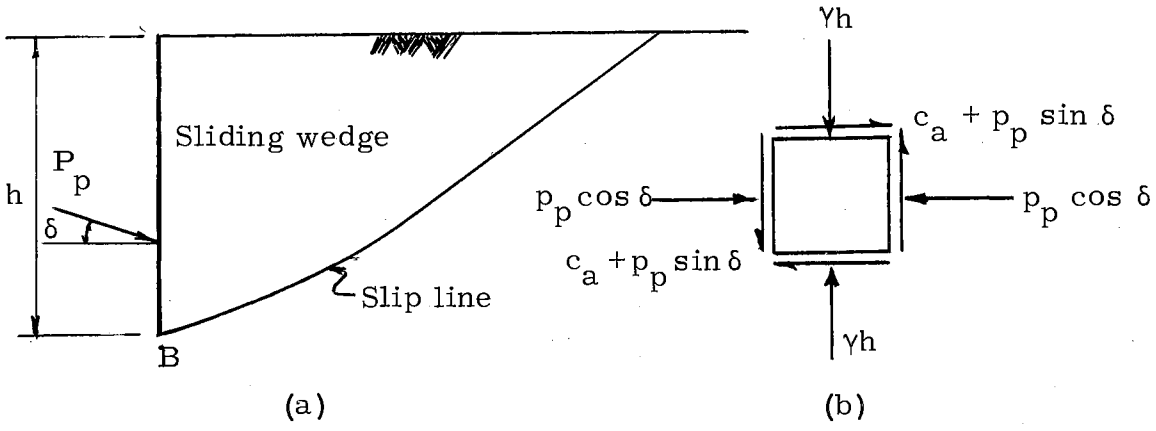

Fig. 4.5 - (a) Slip Line in Cohesive Backfill Due to Passive Case of Failure;
(b) Stresses Acting on an Element of Soil at Point B.

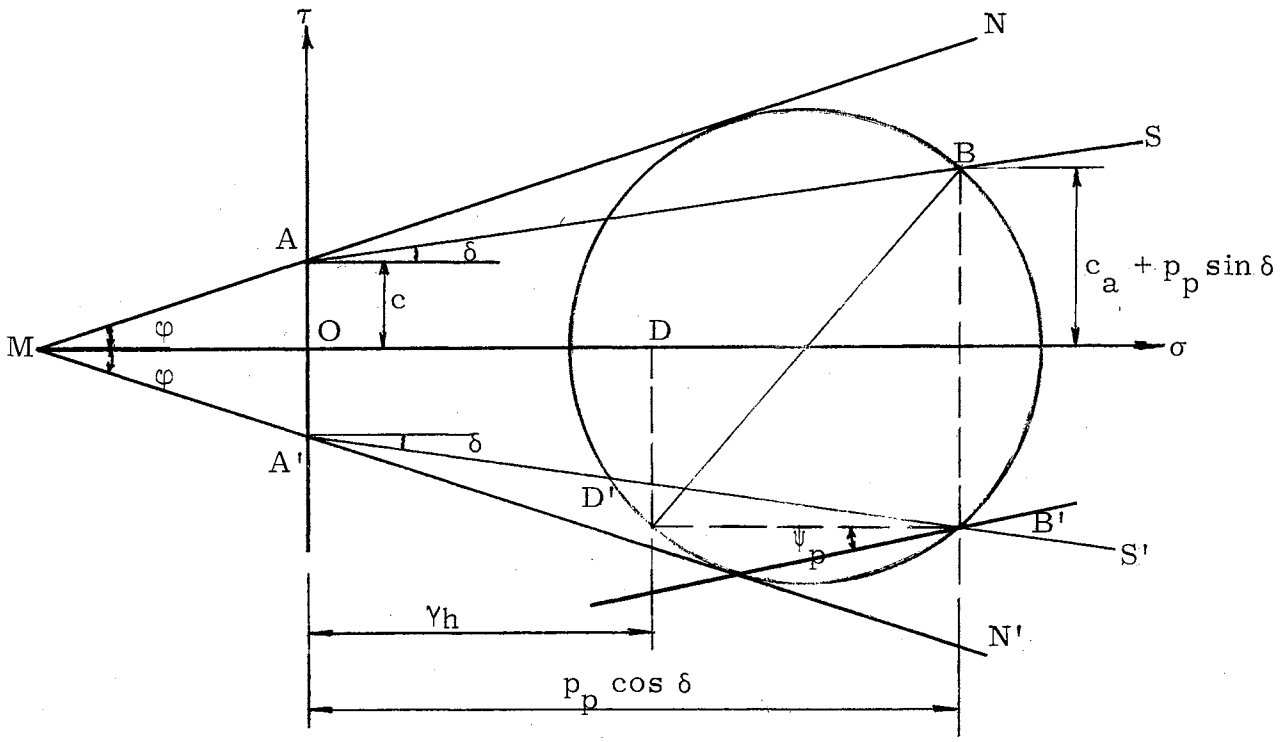

Fig. 4.6 - Cohesive Soil: Mohr's Circle Solution for Passive Resistance at the Bottom of the Wall

be solved in a manner similar to that used for the active pressure.

Let MN and MN' be the rupture lines and let AS be the line on which the shearing stress $c_a + p_p \sin\delta$ falls, see Fig. 4.6. The line AS has an inclination δ with the horizontal. The point on the horizontal axis representing γh has to fall within the respective Mohr's circle. There exists an infinite number of Mohr's circles that satisfy the following conditions:

(a) Their centers are located on the horizontal σ-axis.

(b) They are all tangent to the rupture lines.

(c) Point D falls within these circles.

But there will be one and only one Mohr's circle that satisfies, in addition to the above conditions, the property that the projection of D on the Mohr's circle, that is D', is the image of B' with respect to a vertical passing through the center of the circle. Point B', the reflection of point B, is located on line A'S'. This additional requirement is necessitated by the fact that equal shearing stresses must act on the vertical and horizontal planes, corresponding to D' and B.

Though the Mohr's circle for a specific state of stress is unique, its analytical construction is difficult. Therefore, a graphical method similar to the one described for the active case will be developed.

Through point M, Fig. 4.7, the two rupture lines MN and MN' are drawn making angle φ with the horizontal. Then two widely spaced arbitrary circles (i.e. circles O_2 and O_3) are drawn tangent to MN and MN'. The smallest of the two, circle O_3, should be drawn such that it does not intersect the τ-axis. It can be found, as shown in the Appendix, that if, through the points of intersection of the δ-line and the right side of the Mohr's circles, horizontal lines are drawn to intersect the left side of these circles, the line joining these left points is very closely a straight line. In the Appendix, an illustration for the deviation of the locus from a straight line is shown near the τ-axis. Since in the passive case, any Mohr's circle representing the state of stresses at the toe of a medium wall, does not intersect the τ-axis, the assumption of a straight line locus, as explained above, will hold then without any noticeable error. Thus, line ED, Fig. 4.7, is the locus of points representing the state of

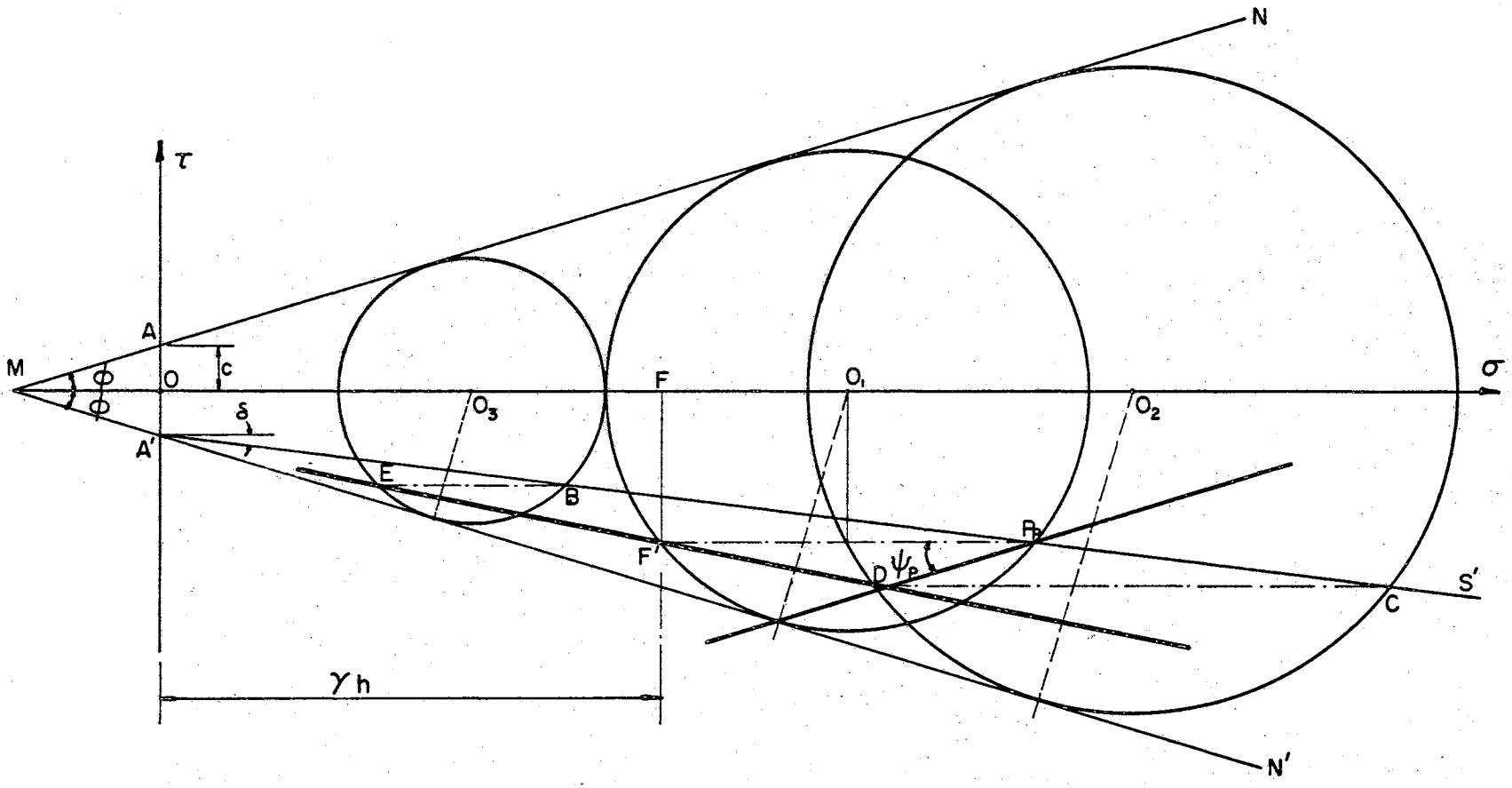

FIG. 4.7

METHOD OF DRAWING THE UNIQUE MOHR'S CIRCLE REPRESENTING THE STATE OF PASSIVE FAILURE AT THE BOTTOM OF THE WALL.

stress on the horizontal faces of particles at every depth.

If a wall having a height h is subjected to the passive pressure of the earth, the Mohr's circle representing the failure condition can be drawn in the following manner: Point F lies at a distance γh from the origin O. Through F a perpendicular is drawn to intersect ED at F'; then, a horizontal through F' is drawn to meet A'S' at P_P which is the passive pole of the Mohr's circle. The bisector of $F'P_P$ intersects the σ-axis at O_1 which is the center of the required Mohr's circle.

The angle that the tangent to the slip line makes with the horizontal at the base of the wall is equal to ψ_P, shown in Fig. 4.7.

The dependency of ψ_P upon certain variables is shown in Figs. XIII to XVII. It may be seen that ψ_P decreases when δ increases. Also ψ_P increases with increasing height of the wall; but the rate of increase becomes negligible when the depth exceeds about 20 ft. It is also worthy of note that ψ_P decreases when the cohesion of the soil increases.

4.4. Slip Lines in Semi-Infinite Inclined Cohesive Masses

Fig. 4.8 illustrates the graphical method of determining the state of stress in a cohesive inclined mass on the verge of active failure. Let β be the inclination of the surface of the cohesive mass with respect to the horizontal. As a practical measure, this study will be limited to the case of $\beta \leq \varphi$.

An element of depth z is isolated as shown in Fig. 4.8a. All the points on the Mohr's circles which represent the states of stress on sections parallel to the surface at every depth z are located on

line OS which rises at an angle β to the horizontal axis.

There exists a case for which the active pressure is zero, corresponding to $z_o = \frac{2c}{\gamma} \tan (45 + \frac{\varphi}{2})$, (for explanation refer to Terzaghi*). For depths less than z_o, the active Rankine state requires the existence of tensile stresses on the vertical plane, whereas for depths greater than z_o, the principal stresses are compressive.

The active pole P_A is located along OS, and the lines of failure P_AB and P_AD make, respectively, the angles α_1^A and α_2^A with the surface of the slope. The angles α_1^A and α_2^A vary with respect to z, as illustrated in Fig. 4.9.

However, in the Rankine zone the curvature of the slip lines, as well as their conjugates, is slight; and there appears to be little practical value in obtaining their exact configuration, in so far as applications to retaining wall problems are concerned. The negligible effect of the curvature is illustrated in Fig. 4.10. To facilitate solution, the slip lines in the active Rankine zone, OAGED, are approximated by a set of chords.

It was found that the change in slope of the slip line becomes especially slight when z exceeds about 20 feet. Hence, it can be assumed that since the total change in slope is small, no significant error is introduced by replacing the curved line by an equivalent straight line to facilitate the handling of the problem.

---

* Karl Terzaghi. Theoretical Soil Mechanics. (New York, 1956), p. 38.

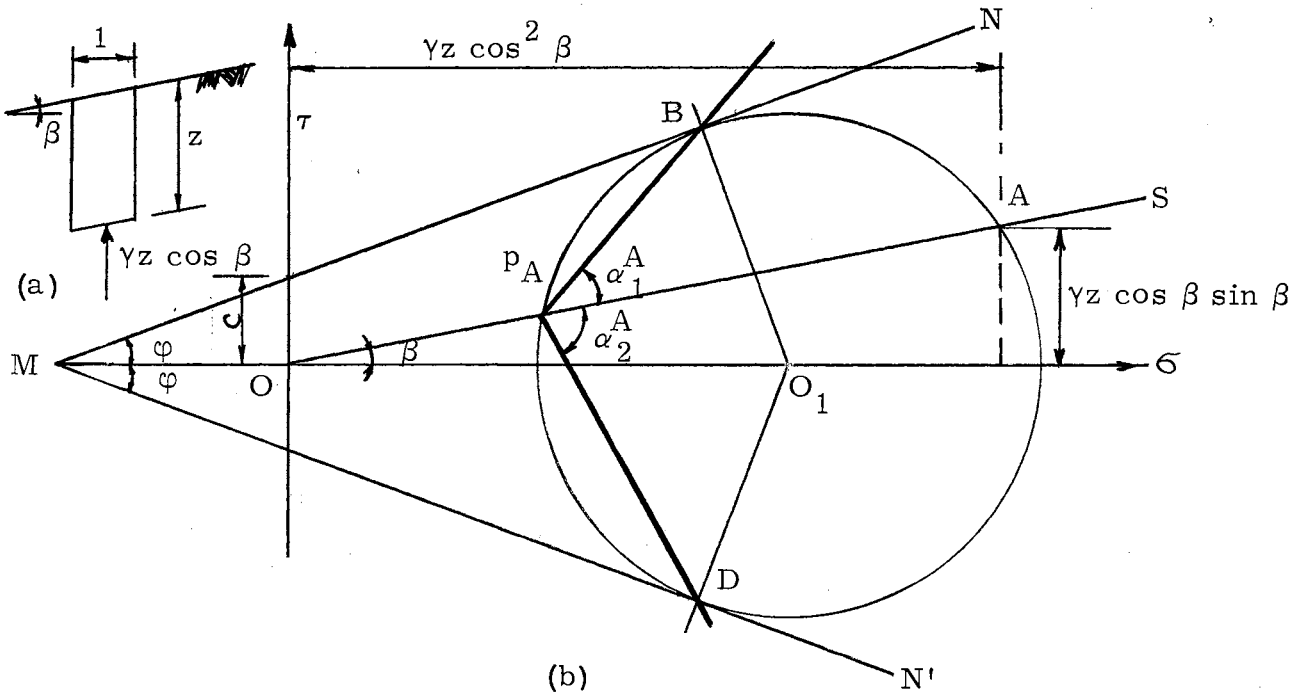

Fig. 4.8 - (a) Stresses at Boundaries of Prismatic Element
(b) Graphic Representation of Active State of Stress at Failure

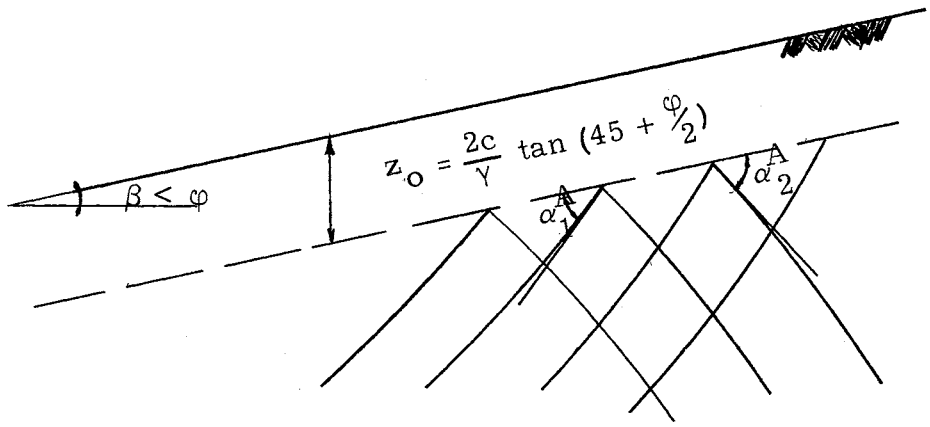

Fig. 4.9 - Shear Pattern for Active State in a Sloping Semi-Infinite Cohesive Mass

The remaining part of the technique for drawing the final slip line follows the procedure explained previously for retaining walls with horizontal backfill.

To illustrate the reasonableness of using a linear approximation for a portion of the curved slip surface, a retaining wall 20 feet in height is considered, having a backfill of clay that has the following properties: $\varphi = 15^\circ$, $\delta = 10^\circ$, $\beta = 10^\circ$, $c = 300$ lb/ft^2 and $\gamma = 110$ lb/ft^3. The depth of the crack, as suggested by Terzaghi*, is taken as

$$H'_c = 2.67 \times \frac{c}{\gamma} \tan (45 + \tfrac{\varphi}{2}) .$$

Thus,

$$H'_c = 2.67 \times \frac{300}{110} \times \tan (45 + 7.5) = 9.5'$$

The inclination of the slip line and its conjugate will be determined graphically at $z = 9.5$ ft. and $z = 15$ ft., as shown in Fig. 4.10.

$$\sigma_n = \gamma z \cos^2 \beta = 110 \times 9.5 \times (0.985)^2 \qquad \text{at } z = 9.5'$$
$$= 1010 \text{ lb/ft}^2$$

$$\sigma_n = \gamma z \cos^2 \beta = 110 \times 15 \times (0.985)^2 \qquad \text{at } z = 15'$$
$$= 1596 \text{ lb/ft}^2$$

From Fig. X, it is found that the slope of the slip line at the toe of the wall is $\psi_A = 31.2^\circ$, whereas the slope of the line at depths of 9.5'

---

*K. Terzaghi. Theoretical Soil Mechanics. (New York, 1956) p. 97 and 154.

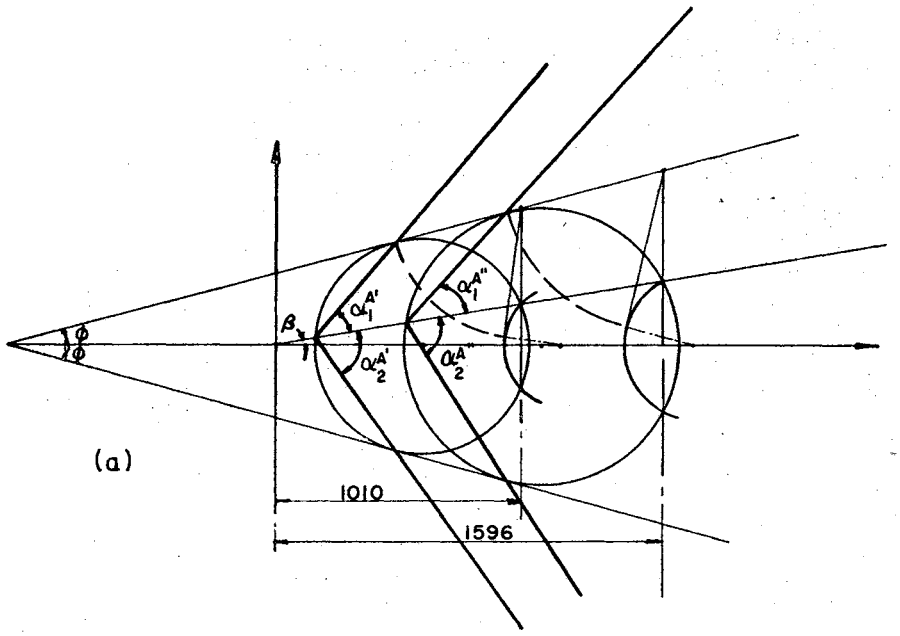

THE FOLLOWING VALUES OF THE SLOPES OF THE SLIP LINE AND ITS CONJUGATE AT DEPTHS 9.5' AND 15' ARE MEASURED OFF FIG. 4.10a.

$\alpha_1^{A'} = 41°$ $\alpha_2^{A'} = 64°$

$\alpha_1^{A''} = 38.5°$ $\alpha_2^{A''} = 66.5°$

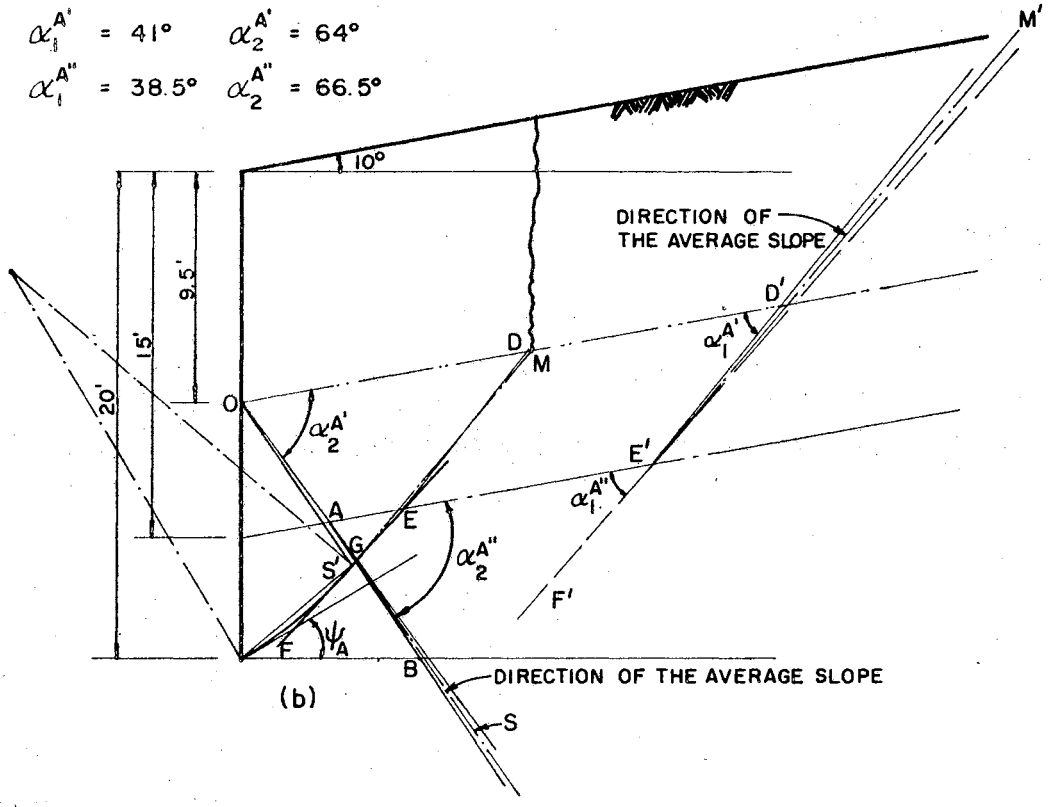

FIG. 4.10

(a) GRAPHICAL DETERMINATION OF THE SLOPE OF THE SLIP LINE AT POINTS D AND E; (b) METHOD OF CONSTRUCTING THE SLIP LINE FOR THE CASE OF ACTIVE PRESSURE ON A RETAINING WALL WITH COHESIVE SLOPING BACKFILL.

and 15' may be obtained graphically, as is illustrated in Fig. 4.10a.

Fig. 4.10b illustrates that the real curved slip line may be rather closely approximated in the Rankine zone by means of a straight line. Line OS' is parallel to AS which has the mean slope of OA and AB. Also, line S'D is parallel to E'M', where the latter has the mean slope of E'D' and E'F'.

For the state of passive pressure, an approach similar to that used for the active case will be followed, with required differences being noted.

The Mohr's circle for the state of passive stress at depth z is shown in Fig. 4.11b. It is apparent that all the points which represent stresses on sections parallel to the surface are located on line OS which rises at an angle β to the horizontal axis. The stresses acting on the vertical faces must be larger than those acting on the inclined faces of the element.

The passive pole, P_p, is located on OS, and the lines of failure P_pD and P_pB make, respectively, the angles α_1^P and α_2^P with OS. These two angles vary with respect to z as shown in Fig. 4.12.

From the preceding discussion, it may be concluded that in the case of a retaining wall problem that portion of the slip line and its conjugate which defines the passive Rankine zone will be slightly curved, as is indicated in Fig. 4.12. An approximation similar to the one used in the active case will be presented in order to simplify the calculation of the passive pressure acting on a retaining wall with a sloping cohesive backfill.

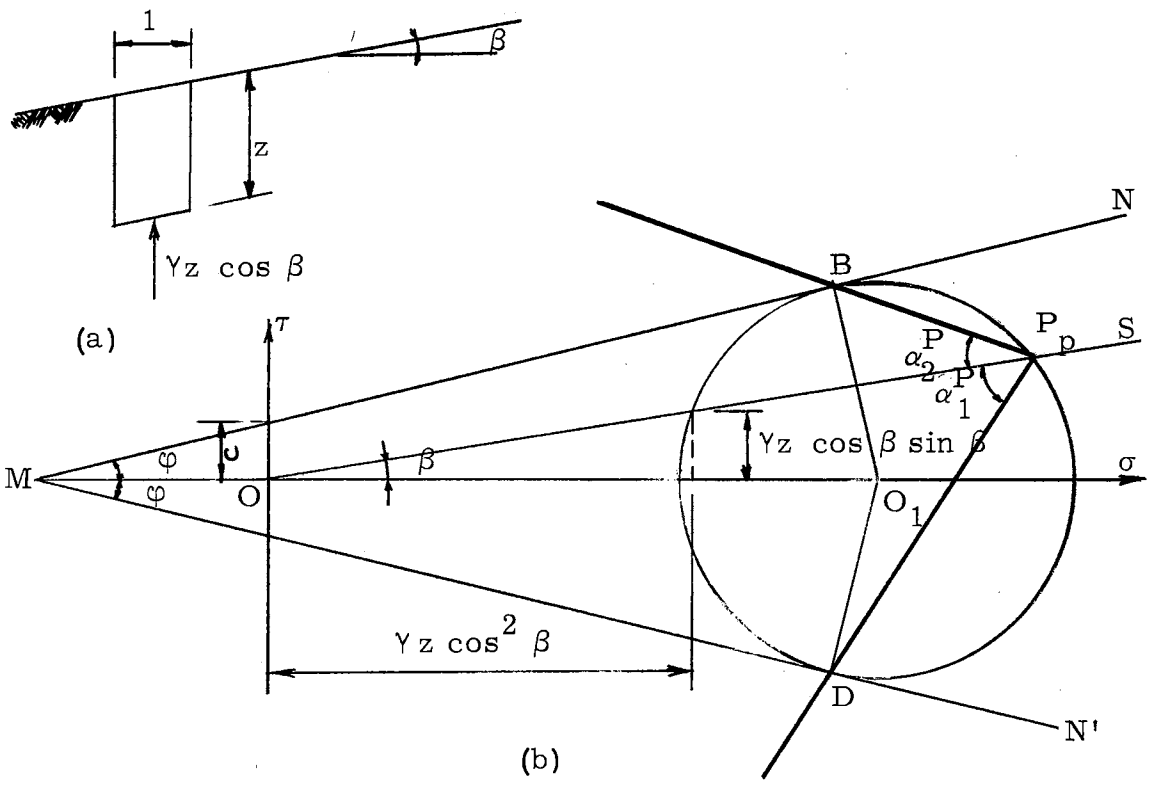

Fig. 4.11 - Semi-Infinite Cohesive Mass with Inclined Surface

(a) Stresses at Boundaries of Prismatic Element

(b) Graphic Representation of Passive State of Stress at Failure

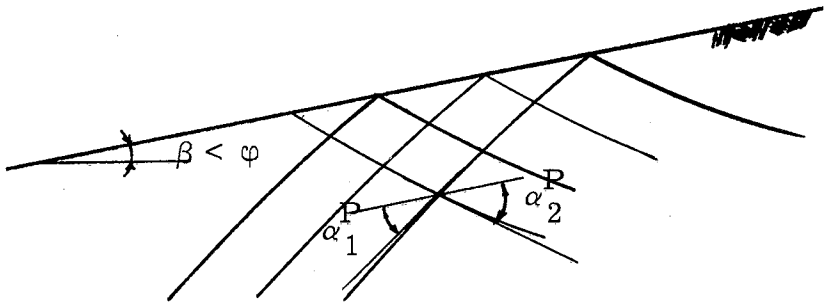

Fig. 4.12 - Shear Pattern for Passive State in a Sloping Semi-Infinite Cohesive Mass

Because of the complexity of the mathematical solutions of the equations of these curves, the rise of the curve with respect to the inclined surface will be determined graphically at different depths, then the curved slip line will be replaced by broken segments as shown in Fig. 4.13b. This procedure illustrates that the curvature in the Rankine zone is very small. Therefore, the curve represented by the broken segments may be replaced by a straight line without introducing too much error.

The technique for drawing the curved portion of the slip line is the same as that explained previously for retaining walls subjected to the passive pressure of backfill having a horizontal surface.

To illustrate the method a retaining wall 20 feet high is considered, with a backfill of clay that has the following properties: $\varphi = 25^\circ$, $\delta = 10^\circ$, $\beta = 10^\circ$, $c = 300 \text{lb/ft}^2$, $\gamma = 110 \text{ lb/ft}^3$.

The inclination of the slip line and its conjugate will be determined graphically at: $z_o = 0$, $z_1 = 10'$, and $z_2 = 15'$, as shown in Fig. 4.13.

$\sigma_{n0} = \gamma z_0 \cos^2 \beta = 0$ $\qquad$ $\psi_p = 12.4^\circ$ from Fig. XVII

$\sigma_{n1} = \gamma z_1 \cos^2 \beta = 110 \times 10 \times \cos^2 10 = 1065 \text{ lb/ft}^2$

$\sigma_{n2} = \gamma z_2 \cos^2 \beta = 110 \times 15 \times \cos^2 15 = 1600 \text{ lb/ft}^2$

It can be seen in Fig. 4.13b that the approximate slip line is very close to the real one; and because of the advantage of the simple calculations involved in working with straight surfaces, the approximate representation is recommended.

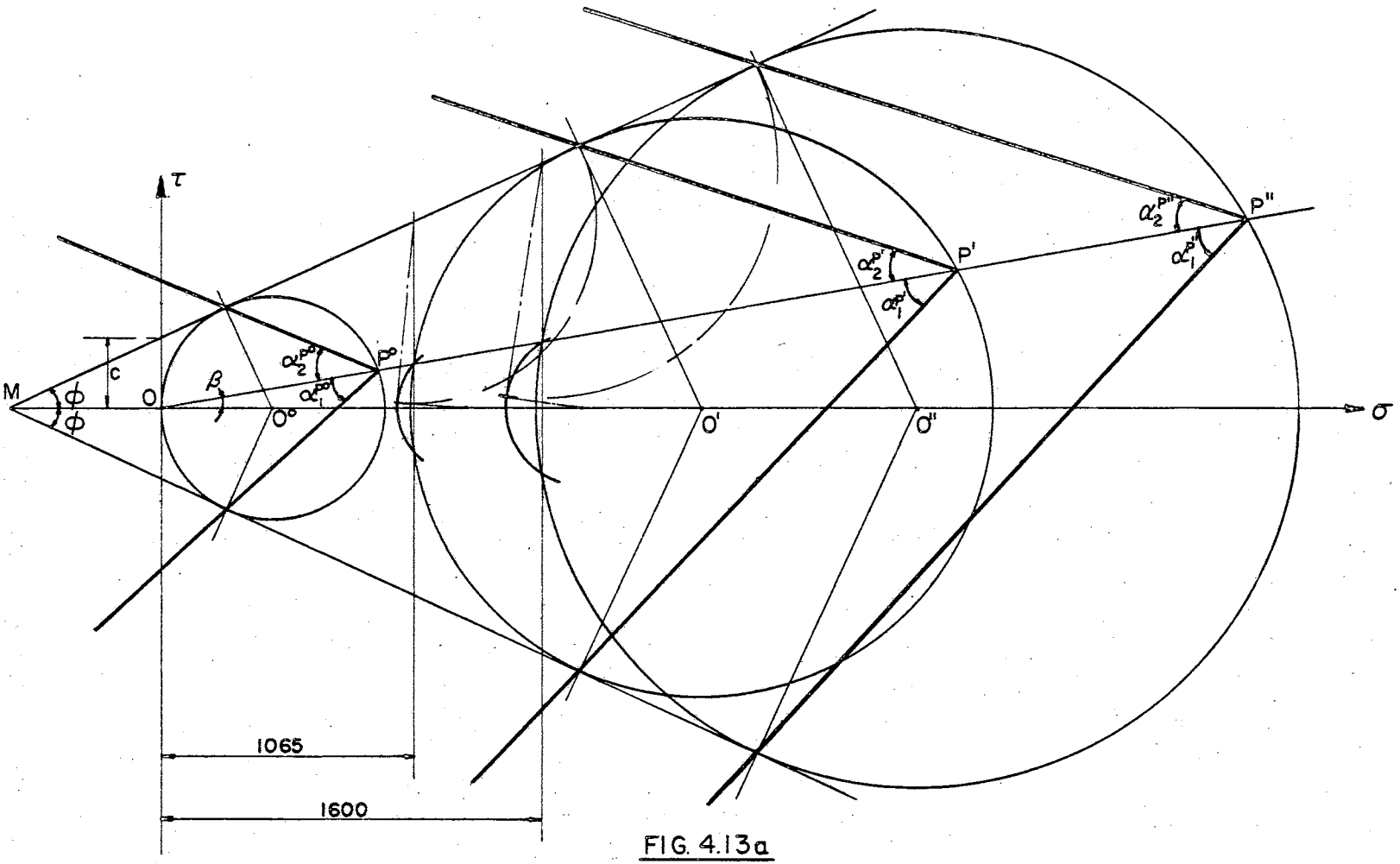

FIG. 4.13a

GRAPHICAL DETERMINATION OF THE SLOPE OF THE SLIP LINE AT POINTS A', B' AND C'. (SEE FIG. 4.13b)

THE FOLLOWING VALUES OF THE SLOPES OF THE SLIP LINE AND ITS CONJUGATE AT DEPTHS 0', 10' AND 15' ARE MEASURED OFF FIG. 4.13a.

@ z = 0	$\alpha_1^{P^o}$ = 32.5°	$\alpha_2^{P^o}$ = 32.5°
@ z = 10'	$\alpha_1^{P'}$ = 37.0°	$\alpha_2^{P'}$ = 28.2°
@ z = 15'	$\alpha_1^{P''}$ = 37.75°	$\alpha_2^{P''}$ = 27.75°

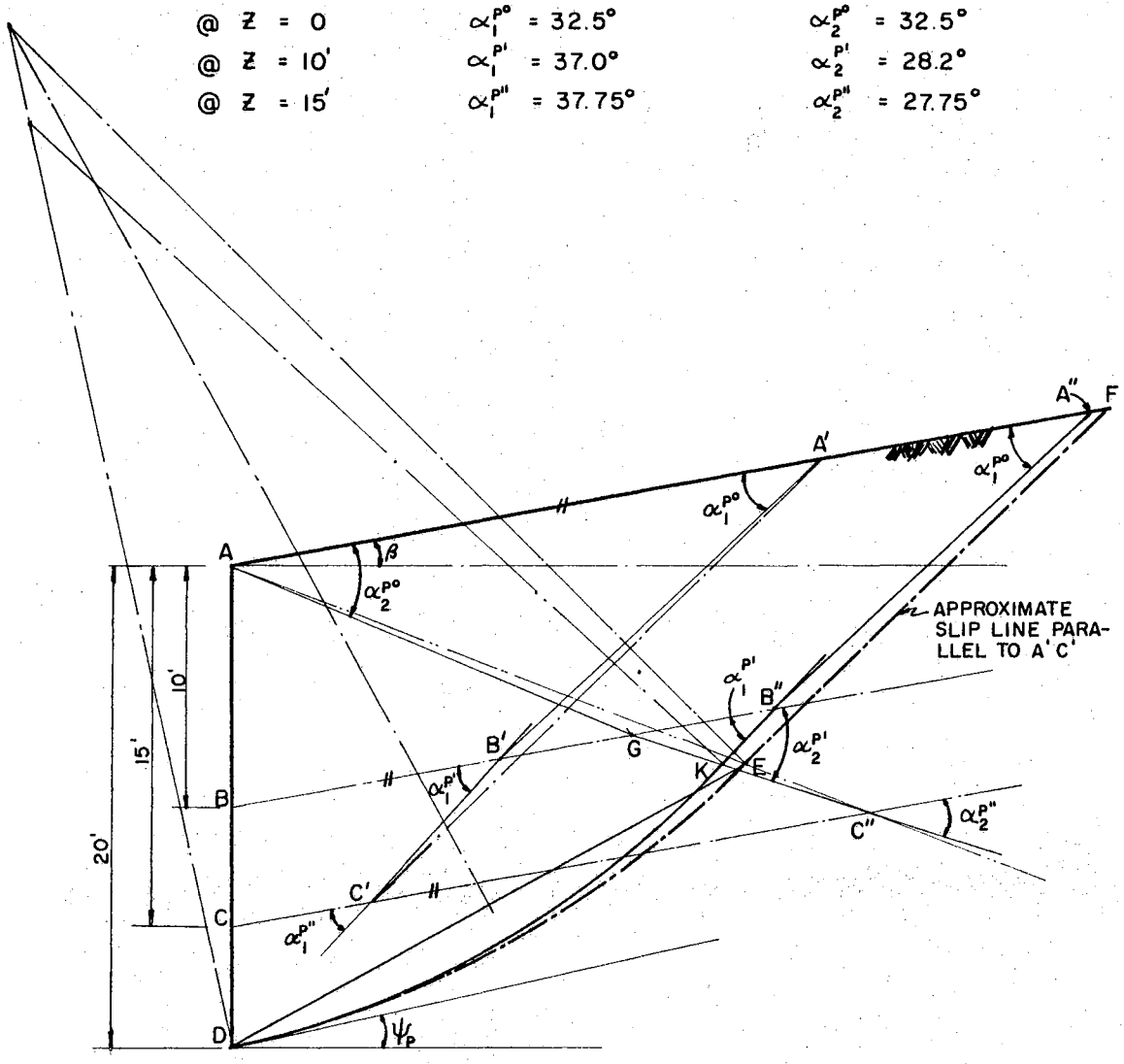

FIG. 4.13b

METHOD OF CONSTRUCTING THE SLIP LINE FOR THE CASE OF PASSIVE PRESSURE ON A RETAINING WALL WITH COHESIVE SLOPING BACKFILL.

CHAPTER V

NUMERICAL EXAMPLES

5.1. Problem No. 1 - Calculation of Active Earth Pressure Exerted by a Cohesionless Levelled Backfill on Retaining Walls

Given: wall height = 16'

horizontal backfill surface

soil properties:

$\gamma = 110$ lb/ft^3

$\varphi = 35^\circ$

angle of wall friction

$\delta = 26^\circ$

5.1.1. Coulomb's Method

$$P_A^* = \frac{1}{2} \gamma H^2 \frac{K_A}{\sin \alpha \cos \delta}$$

where α is the angle that the wall makes with the horizontal (in this problem $\alpha = 90^\circ$) and K_A^* is a coefficient obtained from graphs, and H is the height of the wall.

---

* Karl Terzaghi. Theoretical Soil Mechanics. (New York, 1956), p. 80, formula (1a) and (1b).

Thus:

$$P_A = \frac{1}{2} \times 0.11 \times (16)^2 \times \frac{0.22}{0.899} = 3.45 \text{ k/l. ft.}$$

5.1.2. Slip Line Method

To be able to draw the slip line, it will be necessary to obtain ω and ψ_{A1} for $\varphi = 35^\circ$ and $\delta = 26^\circ$.

From Fig. I and Fig. II it was found that:

$$\psi_{A1} = 50.57^\circ \qquad \text{and} \qquad \omega = 11.92^\circ$$

The slip line was drawn according to the steps explained in Article 3.3. The friction circle method will be used to determine the active earth pressure as shown in Fig. 5.1.

The effect of the portion def may be represented by Rankine's active pressure:

$$E_A = \frac{1}{2} \gamma (ed)^2 \tan^2 (45 - \varphi/2)$$

The problem thus resolves itself into a study of the equilibrium of the portion of the wedge acde.

At the point of failure the full frictional resistance of the sand has been mobilized, and the resisting force at any point on cdf must act at φ to the normal. On the cd portion of the slip line the resisting forces must thus all be tangent to the friction circle whose radius is R sin φ

It will be assumed that the resultant of all the resisting forces is also tangent to the φ-circle. This is not strictly true but is

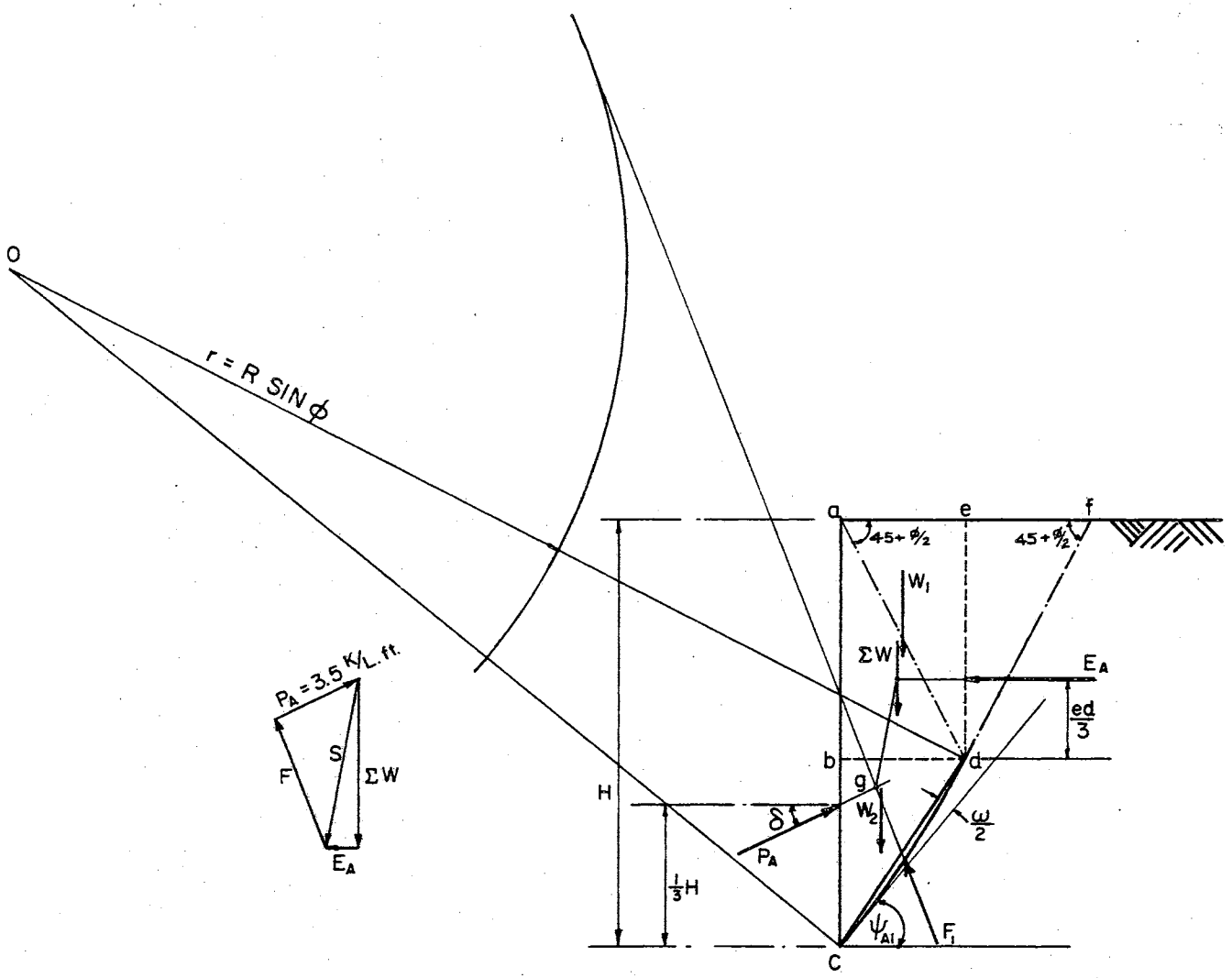

FIG. 5.1

CALCULATION OF LATERAL EARTH PRESSURE OF COHESIONLESS BACKFILL BY THE SLIP LINE APPROACH.

sufficiently close to the truth to justify its acceptance.

To be able to determine the active earth force, P_A, on the retaining wall it will be necessary first to find the magnitude of E_A and the weight of the area acde.

$$E_A = \frac{1}{2} \times 0.11 \times (9)^2 \times (0.52)^2 = 1.21 \text{ k/l. ft.}$$

W_1 = weight of area abde

$$= 0.11 \times 4.65 \times 9 = 4.6 \text{ k/l. ft.}$$

W_2 = weight of area bcd

$$= \frac{1}{2} \times 0.11 \times 4.65 \times 7 = 1.79 \text{ k/l. ft.}$$

W_3, the weight of segment cd, can be neglected in this problem. The locations of the following forces are known: E_A is at $\frac{1}{3}$ of ed from e. The resultant ΣW of force W_1 and W_2 is located at $\bar{X}$ from the face of the wall where:

$$\bar{X} = (4.6 \times 2.32 + 1.79 \times \frac{4.65}{3}) \div 6.39 = 2.11 \text{ ft.}$$

The resultant, S, of ΣW and E_A can be obtained graphically and its line of action can be drawn through the point of intersection of force E_A and ΣW.

Since the direction and location of P_A is known, let g be the point of intersection of the line of action of P_A with that of S. Thus the direction of the resultant resisting force, F_1, will be along the line passing through g and tangent to the friction circle. As the

direction of F_1 is established, it becomes very simple to draw to scale the polygon of forces as shown and scale the force P_A.

In this problem P_A was found equal to 3.5^K. It can be observed that this answer is very close to that obtained by Coulomb's method, and the error is less than 1.5%. Terzaghi* stated that the difference between the exact value of the earth pressure on a retaining wall, in the active case, and Coulomb's value is smaller than 5%; and in connection with practical problems this error is insignificant, and with decreasing values of δ the error decreases further.

5.2. Problem No. 2 - Calculation of Active Earth Pressure Exerted by a Cohesionless Sloping Backfill on Retaining Walls

Given: wall height = 15'

sloping backfill surface

soil properties:

$\gamma = 110$ lb/ft^3

$\varphi = 30^\circ$

Angle of wall friction

$\delta = 16^\circ$

5.2.1. Coulomb's Method

$$P_A = \frac{1}{2} \gamma H^2 \frac{K_A}{\sin \alpha \cos \delta}$$

$$K_A = \frac{\sin^2 (\alpha + \varphi) \cos \delta}{\sin \alpha \sin (\alpha - \delta) \left[1 + \sqrt{\frac{\sin (\varphi + \delta) \sin (\varphi - \beta)}{\sin (\alpha - \delta) \sin (\alpha + \beta)}} \right]^2}$$

*K. Terzaghi. Theoretical Soil Mechanics. (New York, 1956), p. 80.

Calculating K_A, it is found that:

$$K_A = 0.329$$

Therefore,

$$P_A = \frac{1}{2} \times 0.11 \times (15)^2 \times \frac{0.329}{0.961} = 4.23 \text{ k/l. ft.}$$

5.2.2. Slip Line Method

To be able to draw the slip line, the angles ψ_{A1}, ω, α_1^A and α_2^A should be obtained from Fig. I, II, IV, and V.

It was found that:

$$\psi_{A1} = 51.27^\circ \qquad \omega = 8.72^\circ$$

$$\alpha_1^A = 44.83^\circ \qquad \alpha_2^A = 75.17^\circ$$

The method followed in determining the slip line is as was explained in Article 3.5.1. It was found in this specific problem that dc is almost collinear with bc, see Fig. 5.2; therefore, the slip line was considered to be bd. By following the same reasoning as in Problem No. 1, the force P_A can be calculated very easily from the equilibrium force polygon. Since in this problem the slip line came out to be a straight line, the resultant of all resisting forces will make an angle φ with the normal to line bd.

The weight W of the wedge abd is:

$$W = \frac{1}{2} \times 0.11 \times 12 \times 15 = 9.9 \text{ k/l. ft.}$$

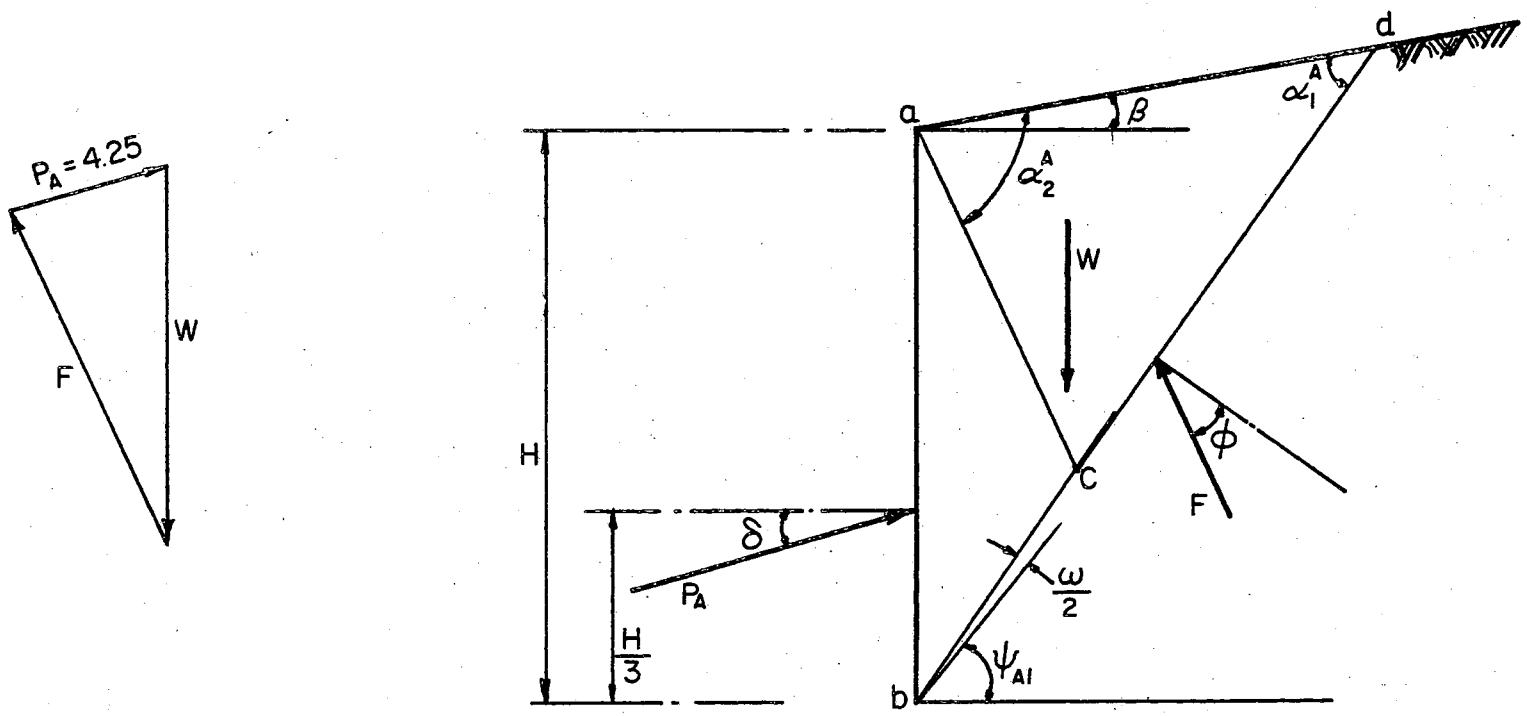

FIG. 5.2

CALCULATION OF LATERAL EARTH PRESSURE OF SLOPING COHESIONLESS BACKFILL BY THE SLIP LINE APPROACH.

Drawing the equilibrium force polygon, the force P_A can be scaled.

It was found that $P_A = 4.25$ k/l.ft. agrees very closely with that found by Coulomb's formula.

5.3. Problem No. 3 - Calculation of Passive Earth Pressure Exerted by a Cohesionless Levelled Backfill on Retaining Walls

Given: wall height = 20'

horizontal backfill surface

soil properties:

$\gamma = 112$ lb/ft^3

$\varphi = 36^\circ$

Angle of wall friction

$\delta = 20^\circ$

5.3.1. Friction Circle Method

Since $\delta > \varphi/3$ Coulomb's assumption that the slip surface under passive resistance is a plane introduces excessive error. The lower portion of the slip surface is definitely curved and it can be approximated by an arc of a circle.

The upper part of the wedge is assumed to fail as indicated by Rankine's theory, at an angle of $45^\circ - \varphi/2$ with the direction of maximum principal stress, which is horizontal. If a line AC is drawn at $45^\circ - \varphi/2$ to the horizontal, and a vertical CD drawn from C, the effect of the portion CDE may be represented by Rankine's passive pressure:

$$E_p = \frac{1}{2} \gamma (CD)^2 \tan^2 (45 + \varphi/2)$$

Then the problem is to consider the equilibrium of the portion ABCD where CE must be tangent to the circular arc BC.

At the point of failure, the resisting force at any point on the assumed slip line must act at φ to the normal. Along the curved portion the normals pass through the center of the circle, and the resisting forces must thus all be tangent to the friction circle whose radius is R sin φ.

The procedure to determine the passive pressure is as follows (Fig. 5.3):

(a) Measure the height of CD and calculate the force E_p from $E_p = \frac{1}{2} \gamma (CD)^2 \tan^2 (45 + \varphi/2)$. This force is located at one-third of CD from C.

(b) Determine the weight of the sections AGCD, GCB and BJC and call them, respectively, W_1, W_2 and W_3.

(c) Locate the mass center of the weight ABJCD and represent all the weight by one vector, ΣW, at the mass center.

(d) Combine graphically ΣW and E_p to give the resultant S.

(e) Draw the passive thrust, P_p, at one-third of the height of the wall from point B at an angle $+\delta$ with the horizontal. The intersection of the line of action of P_p with that of S determines the point Q through which the resisting force F must pass.

(f) Draw through Q a line tangent to the φ-circle. This is the direction of the resultant F.

(g) Draw P_p and F on the force diagram and scale off their magnitudes.

Trial No. 1 - AD = 29 ft.

From Fig. 5.3 the following dimensions can be scaled off:

CD = 14.8'

R = OC = 50.8'

CB = 48.7' $\qquad \angle COB = 34^\circ$

$W_1 = 0.112 \times 29 \times 14.8 = 48$ k/l. ft.

$W_2 = \frac{1}{2} \times 0.112 \times 29 \times 5.2 = 8.45$ k/l. ft.

$W_3 = \frac{1}{2} \times 0.112 \left[(50.8)^2 \times \frac{34\pi}{180} - 29.3 \times 48.7 \right] = 5.6$ k/l. ft.

Therefore,

$\Sigma W = 48 + 8.45 + 5.6 = 62.05$ k/l. ft.

The location of the mass center of ABCD can be obtained by summing moments around point B. Thus:

$$\bar{X} = \frac{\Sigma W_i a_i}{\Sigma W_i}$$

$$= \frac{48 \times 14.5 + 8.45 \times 9.67 + 5.6 \times 14.6}{62.05} = 13.85 \text{ ft.}$$

The radius of the friction circle is:

$r = R \sin \varphi = 50.8 \times 0.588 = 29.9$ ft.

and

$E_p = \frac{1}{2} \times 0.112 \, (14.8)^2 (1.9626)^2 = 47.3$ k/l. ft.

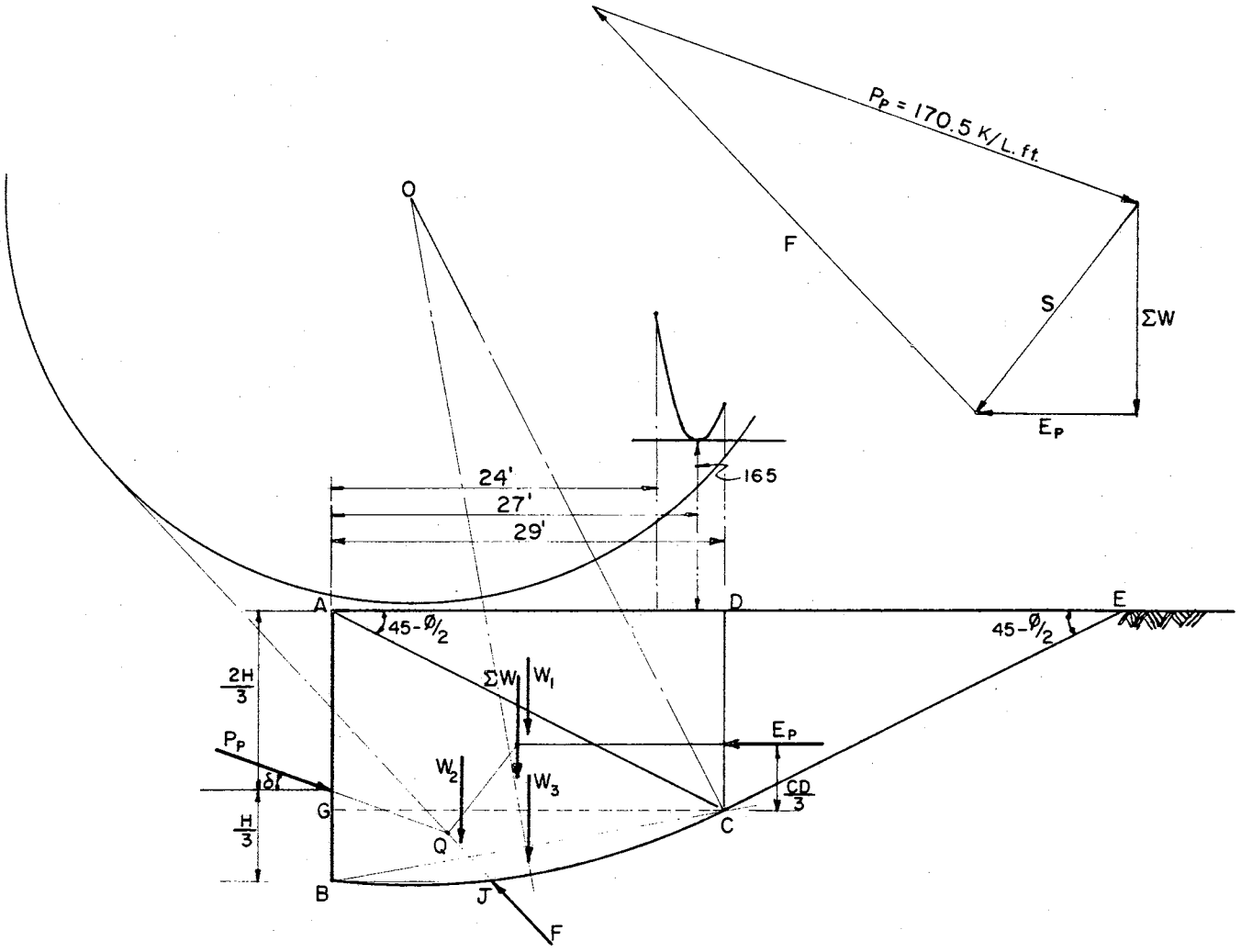

FIG. 5.3

FRICTION CIRCLE METHOD OF DETERMINING PASSIVE EARTH PRESSURE OF SAND. - (TRIAL NO. 1)

For trial No. 1 the magnitude of P_p is found from the force diagram to be:

$$P_p = 170.5 \text{ k/l. ft.}$$

Trial No. 2 - AD = 24 ft.

From Fig. 5.4 the following dimensions can be scaled off:

CD = 12.2 ft.

R = OC = 81.5 ft.

CB = 25.2 ft. $\qquad \angle COB = 18^\circ$

$W_1 = 0.112 \times 24 \times 12.2 = 32.8$ k/l. ft.

$W_2 = \frac{1}{2} \times 0.112 \times 24 \times 7.8 = 10.5$ k/l. ft.

$$W_3 = \frac{1}{2} \times 0.112 \left[(81.5)^2 \times \frac{18\pi}{180} - 80.5 \times 25.2 \right] = 3.36 \text{ k/l. ft.}$$

Therefore,

$$\Sigma W = 32.8 + 10.5 + 3.36 = 46.66 \text{ k/l. ft.}$$

$$\bar{X} = \frac{32.8 \times 12 + 10.5 \times 8 + 3.36 \times 12.2}{46.66} = 11.15'$$

$$r = 81.5 \times 0.588 = 48 \text{ ft.}$$

and

$$E_p = \frac{1}{2} \times 0.112 \times (12.2)^2 (1.9626)^2 = 32.1 \text{ k/l. ft.}$$

From trial No. 2 the magnitude of P_p is found from the force diagram to be:

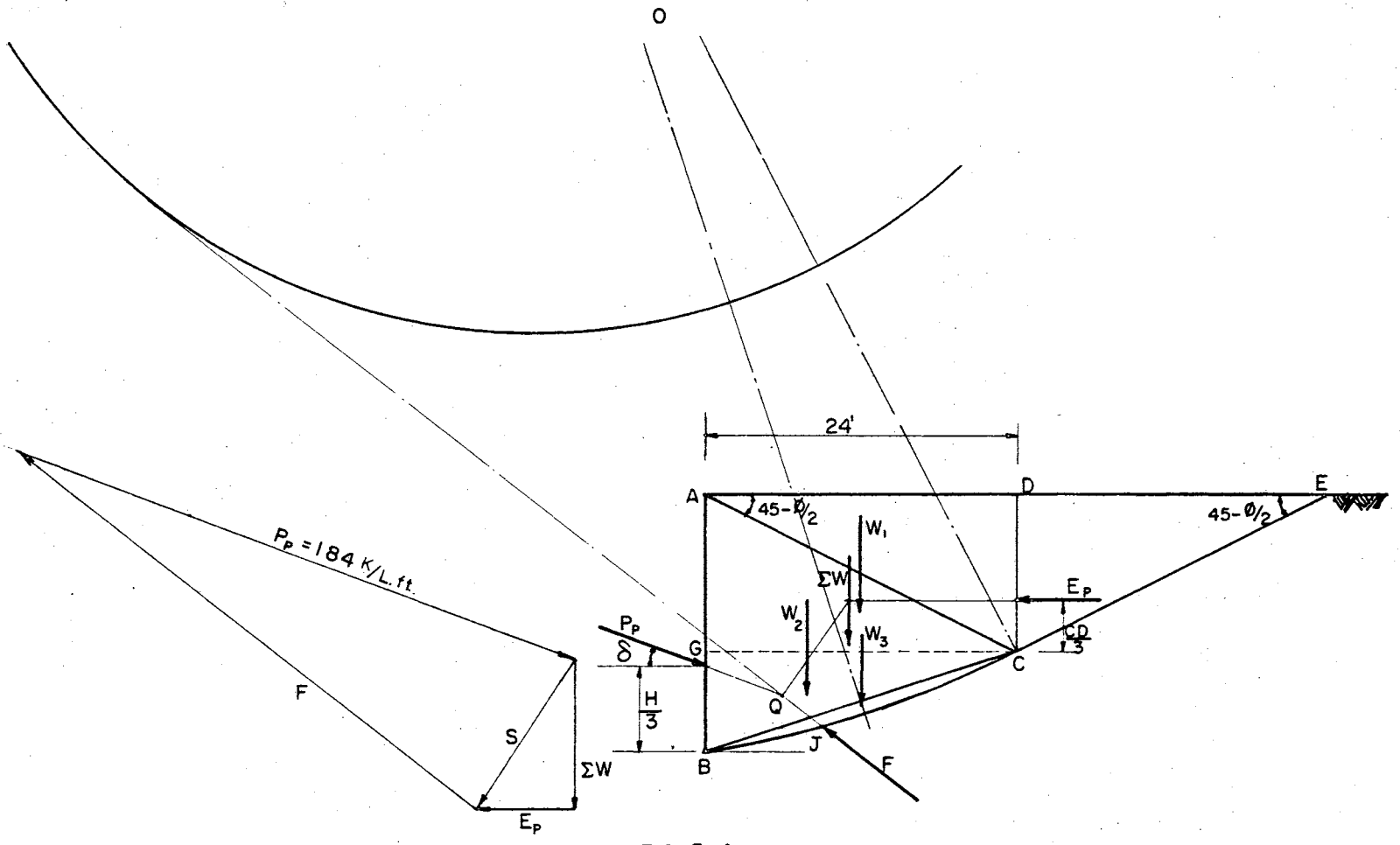

FIG. 5.4

FRICTION CIRCLE METHOD OF DETERMINING PASSIVE EARTH PRESSURE OF SAND. (TRIAL NO. 2)

$P_p = 184$ k/l. ft.

Trial No. 3 - AD = 27 ft.

From Fig. 5.5, the following dimensions can be scaled off:

CD = 14 ft.

R = 60 ft.

CB = 27.6 ft. $\quad \angle COB = 26.26^\circ$

$W_1 = 0.112 \times 27 \times 14 = 42.2$ k/l. ft.

$W_2 = \frac{1}{2} \times 0.112 \times 27 \times 6 = 9.06$ k/l. ft.

$$W_3 = \frac{1}{2} \times 0.112 \left[(60)^2 \times \frac{26.26\,\pi}{180} - 27.6 \times 58.3 \right] = 2.24 \text{ k/l. ft.}$$

Therefore,

$\Sigma W = 42.2 + 9.06 + 2.24 = 53.5$ k/l. ft.

$$\bar{X} = \frac{42.2 \times 13.5 + 9.06 \times 9 + 2.24 \times 13.8}{53.5} = 12.75 \text{ ft.}$$

$r = 60 \times 0.588 = 35.3$ ft.

$$E_p = \frac{1}{2} \times 0.112 \times (14)^2 \times (1.9626)^2 = 42.4 \text{ k/l. ft.}$$

From trial No. 3 the magnitude of P_p is found from the force diagram to be:

$P_p = 165$ k/l. ft.

Plotting the values of P_p above the corresponding positions of C, the least value of P_p which can be determined from the graph shown

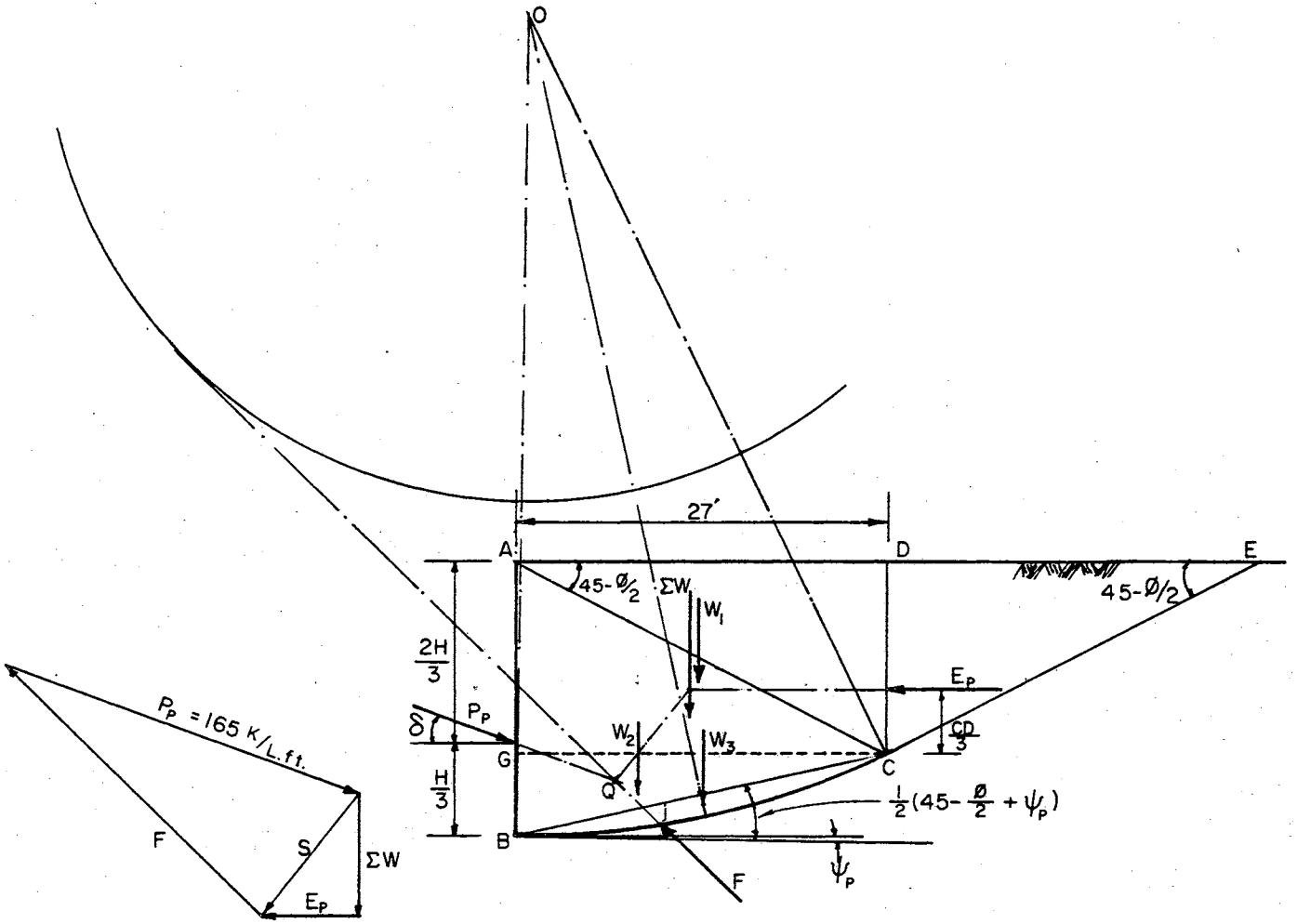

FIG. 5.5

FRICTION CIRCLE METHOD OF DETERMINING PASSIVE EARTH PRESSURE OF SAND - [(TRIAL NO. 3) AND THE SLIP LINE APPROACH]

in Fig. 5.3 is found to be:

$$P_{p\,(minimum)} = 165 \text{ k/l. ft.}$$

5.3.2. Calculation of Passive Earth Pressure by the Use of the Slip Line Method.

From Fig. I and III, the angles ω and ψ_p are found to be:

$\omega = 7.75^\circ$ and $\psi_p = -0.75^\circ$

Following the procedure for drawing the slip line as explained in Article 3.4, the shape of the line is that shown in Fig. 5.5.

It was found that AD is equal to 27 ft. which happens to coincide with trial No. 3 of the preceding section. Having located the critical slip line, the method followed in calculating P_p is the friction circle method previously explained. It follows that the value of P_p obtained by this method is the same as that of trial No. 3 which represented the minimum value of P_p.

The advantage of the use of the slip line method is quite obvious. The method is direct, accurate and fast.

5.4. Problem No. 4 - Calculation of Active Earth Pressure Exerted by a Cohesive Levelled Backfill on Retaining Walls

Given: wall height = 20'

horizontal backfill surface

soil properties:

$\gamma = 110$ lb/ft^3

$\varphi = 10^\circ$

$c = 0.3$ K/ft^2

angle of wall friction

$\delta = 7^\circ$

5.4.1. Wedge Method

In the case of cohesive backfill, the effect of cohesion must be taken into account. It is assumed that there is a neutral or ineffective zone of depth $H_c' = 2.67 \frac{c}{\gamma} \tan (45 + \frac{\varphi}{2})$, as suggested by Terzaghi*, within which there is no adhesion or friction along the back of the wall or along the slip surface.

There are five forces acting on the wedge ABDE, Fig. 5.6a:

(1) The weight of the whole wedge ABDE (ΣW_5).

(2) The reaction F_5 on the plane of rupture.

(3) The resultant of the normal and frictional forces (P_{A5}).

(4) The cohesion along the length BD (C_{S5}).

(5) The adhesion along the height of wall BG (C_a).

---

*K. Terzaghi. Theoretical Soil Mechanics. (New York, 1956), p. 154.

There are only two unknown forces, F_5 and P_{A5} whose directions are known, their magnitudes can be determined from the force polygon. The selection of a few trial planes of failure permits a curve to be drawn describing the variation of the magnitude of P_A. From this curve the maximum possible value for P_A may be determined. P_A is assumed, as is usual, to act at a height of one-third of the height of the wall.*

Trial No. 1:

$$H_c' = AB = 2.67 \times \frac{300}{110} \tan (45 + 5) = 8.7 \text{ ft.}$$

$$\Sigma W_1 = 0.11(24 \times 8.7 + \frac{24}{2} \times 11.3) = 37.92 \text{ k/l. ft.}$$

$$C_a = 0.3 \times 11.3 = 3.39 \text{ k/l. ft.}$$

$$C_{s1} = 0.3 \times 26.6 = 8 \text{ k/l. ft.}$$

From the force polygon diagram Fig. 5.6b, P_{A1} is found to be:

$$P_{A1} = 1.5 \text{ k/l. ft.}$$

Trial No. 2:

$$\Sigma W_2 = 0.11\left[19.3 \times 8.7 + \frac{19.3}{2} \times 11.3\right] = 30.45 \text{ k/l. ft.}$$

---

* P. L. Capper and W. F. Cassie. The Mechanics of Engineering Soils. (London, 1963), p. 111.

C_a = 3.39 k/l. ft. (it is constant)

C_{s2} = 0.3 x 22.4 = 6.73 k/l. ft.

P_{A2} = 3 k/l. ft. Scaled from the force polygon.

Trial No. 3:

$$\Sigma W_3 = 0.11\left[16 \times 8.7 + \frac{16}{2} \times 11.3\right] = 25.25 \text{ k/l. ft.}$$

C_a = 3.39 k/l. ft.

C_{s3} = 0.3 x 19.65 = 5.9 k/l. ft.

P_{A3} = 3.75 k/l. ft.

Trial No. 4:

$$\Sigma W_4 = 0.11\left[12.2 \times 8.7 + \frac{12.2}{2} \times 11.3\right] = 19.3 \text{ k/l. ft.}$$

C_a = 3.39 k/l. ft.

C_{s4} = 0.3 x 16.5 = 4.95 k/l. ft.

P_{A4} = 4.1 k/l. ft.

Trial No. 5:

$$\Sigma W_5 = 0.11\left[9 \times 8.7 + \frac{9}{2} \times 11.3\right] = 14.22 \text{ k/l. ft.}$$

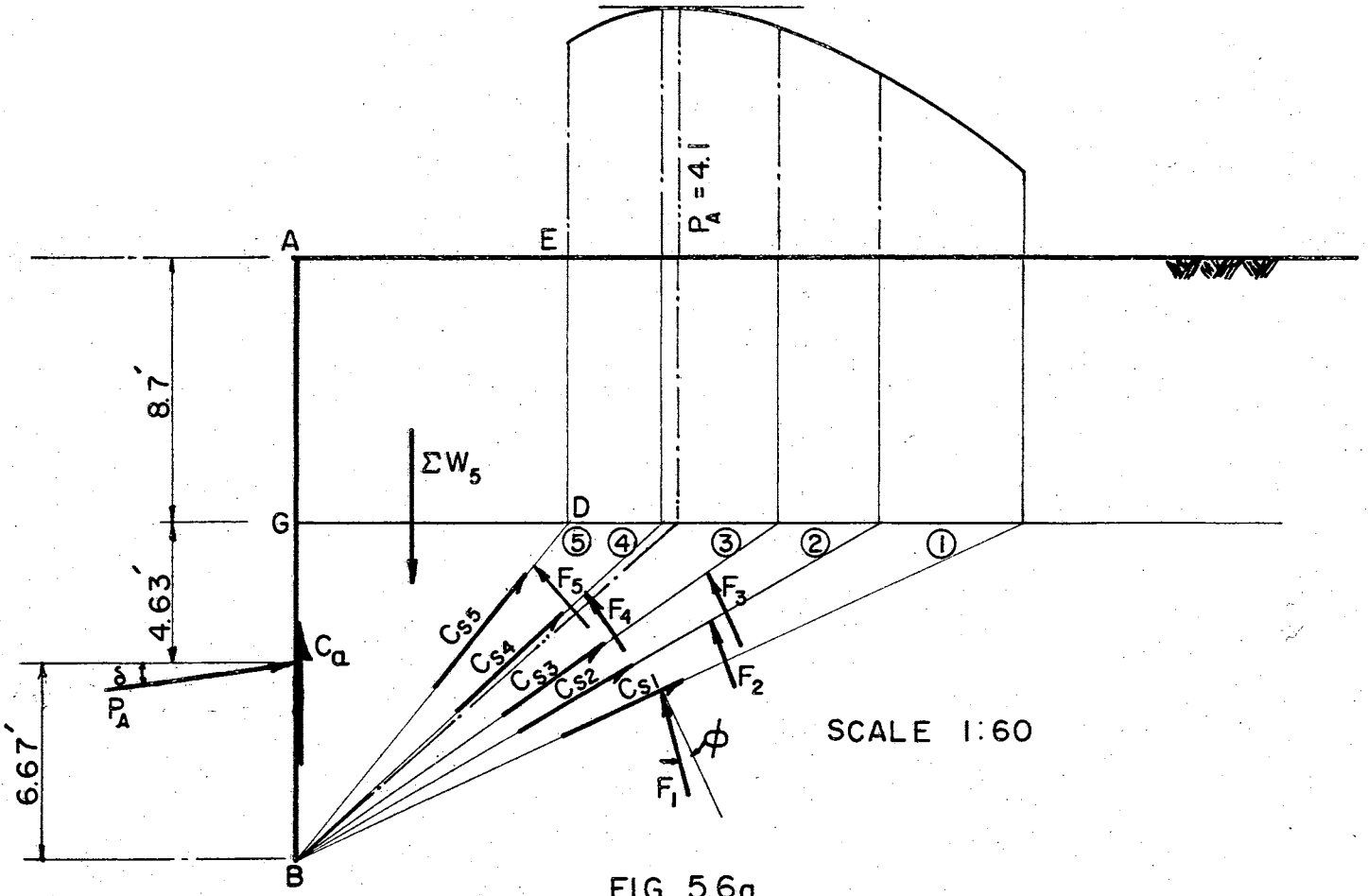

FIG. 5.6a

ACTIVE EARTH PRESSURE ON RETAINING WALL BACKFILLED WITH COHESIVE SOIL, BY THE WEDGE METHOD.

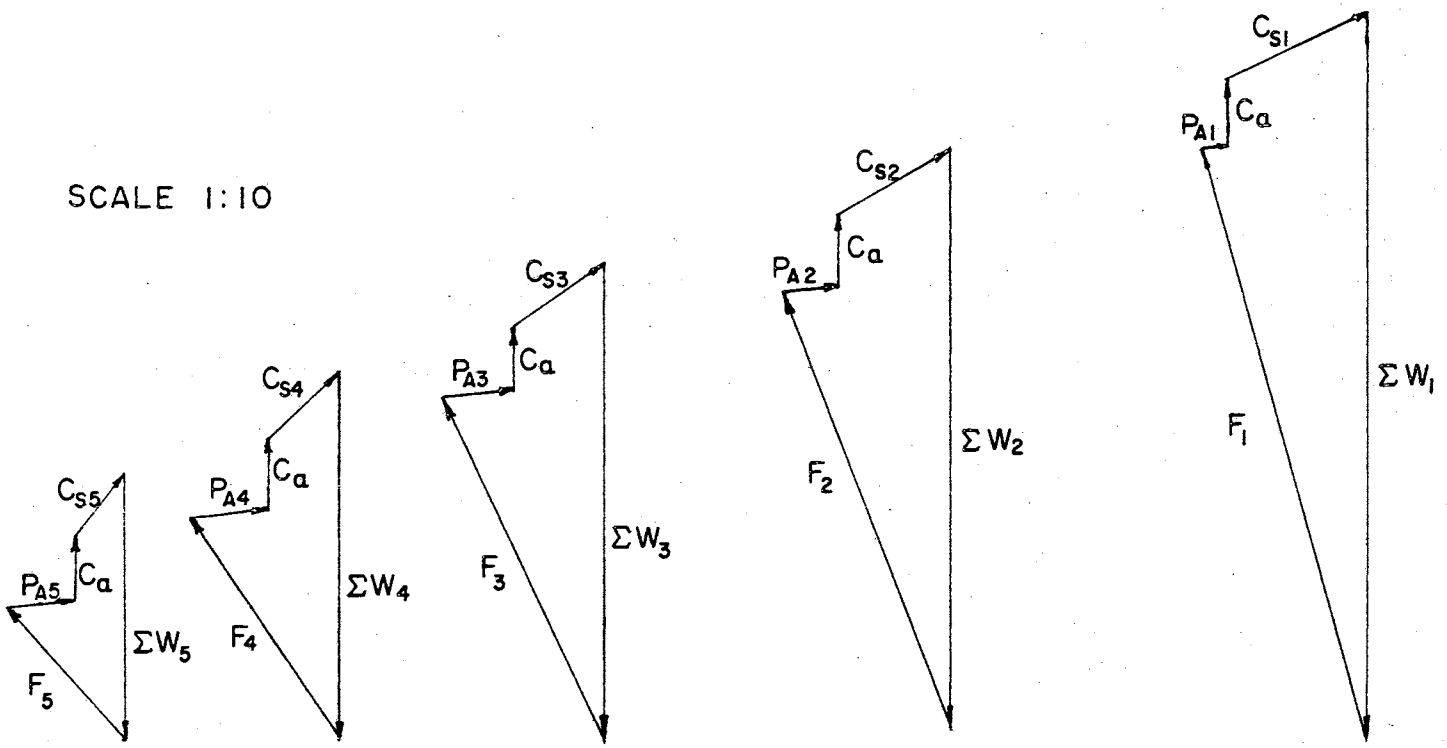

TRIAL NO. 5 TRIAL NO. 4 TRIAL NO. 3 TRIAL NO. 2 TRIAL NO. 1

$P_{A5} = 3.5$ $P_{A4} = 4.1$ $P_{A3} = 3.75$ $P_{A2} = 3$ $P_{A1} = 1.5$

FIG. 5.6b

FORCE POLYGON DIAGRAMS FOR THE VARIOUS TRIALS INVESTIGATED IN FIG. 5.6a.

C_a = 3.39 k/l. ft.

C_{s5} = 0.3 x 14.4 = 4.33 k/l. ft.

P_{A5} = 3.5 k/l. ft.

Plotting the values of P_A for the above trials as shown in Fig. 5.6a, it is found that the maximum value for P_A is 4.1 k/l. ft.

5.4.2. Slip Line Method

From Fig. IX, for $K = \frac{1}{3}$ (Note $K = \frac{c_o}{c} = \frac{100}{300}$), ψ_A is found to be 25°. Once the slip line is drawn according to the method described in Article 4.2, the friction circle method can be applied to find the active earth pressure.

It is convenient to consider the active resistance of cohesive soils in two parts, Fig. (5.7a):

(1) The frictional resistance developed along the slip line and the back of the wall when the backfill is mobilized;

(2) The cohesive resistance along the slip line combined with the adhesion resistance along the back of the wall.

The evaluation of part (1) is similar to the application of the friction circle method to cohesionless backfill except that the weight of area ABJL is considered as surcharge. The steps of the friction circle method were already outlined in Article 5.1.2. The effect of the portion JGH may be represented by Rankine's active pressure:

$$E_A'' = \frac{1}{2} \gamma (JG)^2 \tan^2 (45 - \varphi/2) \qquad (5.1)$$

The force P''_A is taken at one-third of the height BD from point D. The force polygon is drawn as shown in Fig. 5.7b and as explained in Article 5.1.2.

When cohesion alone is considered, the effect of the cohesive forces on GH can be replaced by the active resistance E'_A where:

$$E'^{*}_A = \left[-2c \tan (45 - \tfrac{\varphi}{2}) + q \tan^2 (45 - \tfrac{\varphi}{2})\right](JG) \qquad (5.2)$$

where q is the surcharge stress due to the fissured portion above line BH. The force E'_A acts at half the height JG. Similarly, P'_A, the active resistance on the wall due to cohesion alone acts at half the height BD. C_w, the cohesion on the wall, acts along the line of the back of the wall. The resultant of the cohesive forces on the curve DG is parallel to the chord DG, and the value C_s represents the sum of the components of the cohesion parallel to DG.

$$C_s = c \times \text{chord } DG .$$

The line of action of C_s is found by taking the moment of the cohesive force on curve DG around the center of the friction circle, and then equating this moment to that of force C_s acting at a distance L_1 from the center of the friction circle. Actually, C_s is the equipollent force for the cohesion force acting along the curve DG. Thus:

$$C_s L_1 = c \times \text{curve } DG \times R \qquad (5.3)$$

---

*K. Terzaghi. Theoretical Soil Mechanics. (New York, 1956), p. 38, formula (4).

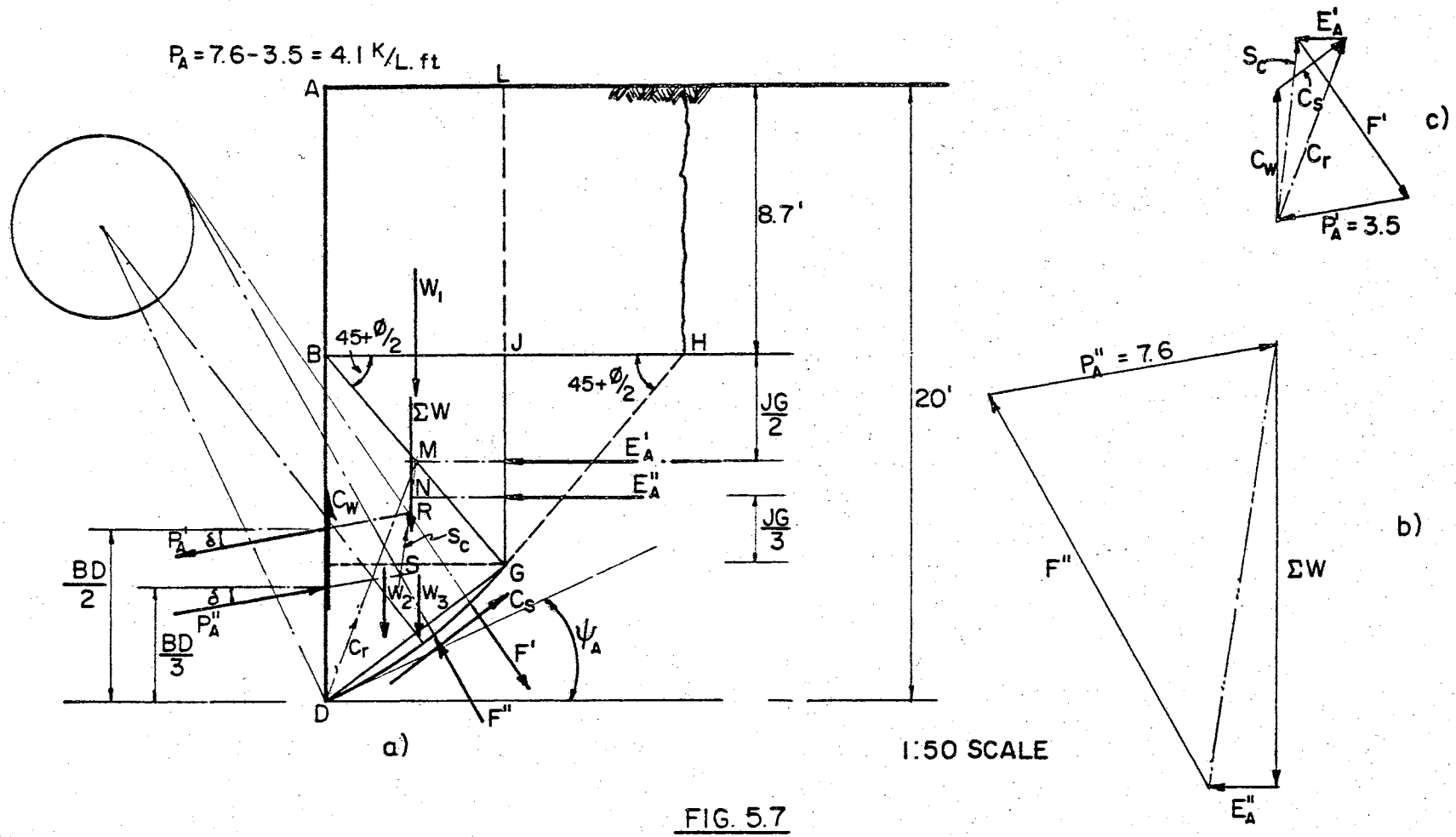

FIG. 5.7

ACTIVE EARTH PRESSURE ON RETAINING WALL BACKFILLED WITH COHESIVE SOIL, BY THE USE OF SLIP LINE METHOD. a) PROPER SLIP LINE, b, c) FORCE POLYGONS.

where R is the radius of the curve DG.

The steps to be taken to determine the active resistance due to cohesion are as follows:

(1) Obtain the values of C_w, C_s and E'_A by calculation.

(2) Draw the triangle of forces for C_w and C_s and mark the resultant C_r in its position on the wedge diagram.

(3) Determine the point M where E'_A meets the line of action of C_r and then draw through M the resultant S_c (see Fig. 5.7a and c).

(4) S_c meets P'_A at point R. Through R draw a line tangent to the friction circle. This is the line of action of force F'.

(5) Complete the force polygon and so determine P'_A. The total active force acting on the wall is the algebraic summation of P'_A and P''_A.

Numerical Calculations

The radius R of the curved portion DG was scaled off and found to be 17.1 ft., and the angle subtending are DG, equal to 25°. Thus:

$$L_1 = \frac{\text{arc DG}}{\text{chord DG}} \times R = (17.1)^2 \times \frac{25\pi}{180} \times \frac{1}{7.3} = 17.5 \text{ ft.}$$

The radius r of the friction circle is:

$$r = R \sin \varphi = 17.1 \times 0.1736 = 2.97 \text{ ft.}$$

Let W_1 be the weight of area AB'GL, W_2 the weight of area DB'G, and W_3 the weight of segment DG. Thus:

$$W_1 = 0.11 \times 5.85 \times 15.5 = 10 \text{ k/l. ft.}$$

$$W_2 = 0.11 \times \frac{5.85}{2} \times 4.5 = 1.45 \text{ k/l. ft.}$$

$$W_3 = \frac{0.11}{2}\left[(17.1)^2 \frac{25\pi}{180} - 7.3 \times 16.7\right] = 0.3 \text{ k/l. ft.}$$

$$C_s = c \times \text{chord DG} = 0.3 \times 7.3 = 2.19 \text{ k/l. ft.}$$

$$C_w = c \times BD = 0.3 \times 11.3 = 3.39 \text{ k/l. ft.}$$

From Eq. (5.1) and (5.2), E'_A and E''_A follow

$$E'_A = \left[-2 \times 0.3 \times \tan 40^\circ + 0.11 \times 8.7 \times \tan^2 40\right]6.85$$

$$= 1.22 \text{ k/l. ft.}$$

$$E''_A = \frac{1}{2} \gamma \ (JG)^2 \tan^2(45 - \varphi/2) = \frac{1}{2} \times 0.11 \times (6.85)^2 \tan^2 40^\circ$$

$$= 1.82 \text{ k/l. ft.}$$

From the force polygons (Fig. 5.7b and c) the values of P'_A and P''_A are

$$P'_A = 3.5 \text{ k/l. ft.}$$

$$P''_A = 7.6 \text{ k/l. ft.}$$

Their vectorial summation gives

$$P_A = P'_A + P''_A = -3.5 + 7.6 = 4.1 \text{ k/l. ft.}$$

This answer agrees exactly with that obtained by the wedge method.

5.5. Problem No. 5 - Calculation of Passive Earth Pressure Exerted by a Cohesive Levelled Backfill on Retaining Walls

Given: wall height = 20'

horizontal backfill surface

soil properties:

$\gamma = 110$ lb/ft^3

$\varphi = 15^\circ$

$c = 0.3$ k/ft^2

angle of wall friction

$\delta = 10^\circ$

5.5.1. Friction Circle Method

The passive resistance of cohesive soils can be considered in two parts:

(1) The frictional resistance developed along the slip line and the back of the wall.

(2) The cohesive resistance along the slip line combined with the adhesive resistance along the back of the wall.

The main difference between the active and passive cases when the friction circle method is applied is that in the passive case, since the soil is in compression, no tension cracks appear at the surface, and the cohesive forces are assumed to be distributed uniformly over the entire back of the wall and the curved surface DG.

The corresponding total pressures on the section JG, Fig. 5.8 are

$$E'_p = 2\,c\,(JG)\tan(45 + \varphi/2) \qquad (5.4)$$

and

$$E''_p = \frac{1}{2}\,\gamma\,(JG)^2 \tan^2(45 + \varphi/2) \qquad (5.5)$$

Once the passive resistances are calculated for each of the assumed slip surfaces and plotted to scale, the minimum value which can be found for the term $P'_p + P''_p$ is used in the design.

Trial No. 1: AJ = 16'

The following dimensions are scaled off Fig. 5.8:

R = 42.6 ft. JG = 12.3 ft.

DG = 17.7 ft. $\angle$ DOG = 24°

The radius of the friction circle is

$$r = R \sin\varphi = 42.6 \times 0.2588 = 11'$$

From Eq. (5.3), solve for L_1:

$$L_1 = (42.6)^2 \times \frac{24\pi}{180} \times \frac{1}{17.7} = 43'$$

From Eq's (5.4) and (5.5), solve for E'_p and E''_p:

$$E'_p = 2 \times 0.3 \times 12.3 \times \tan 52.5 = 9.6 \text{ k/l. ft.}$$

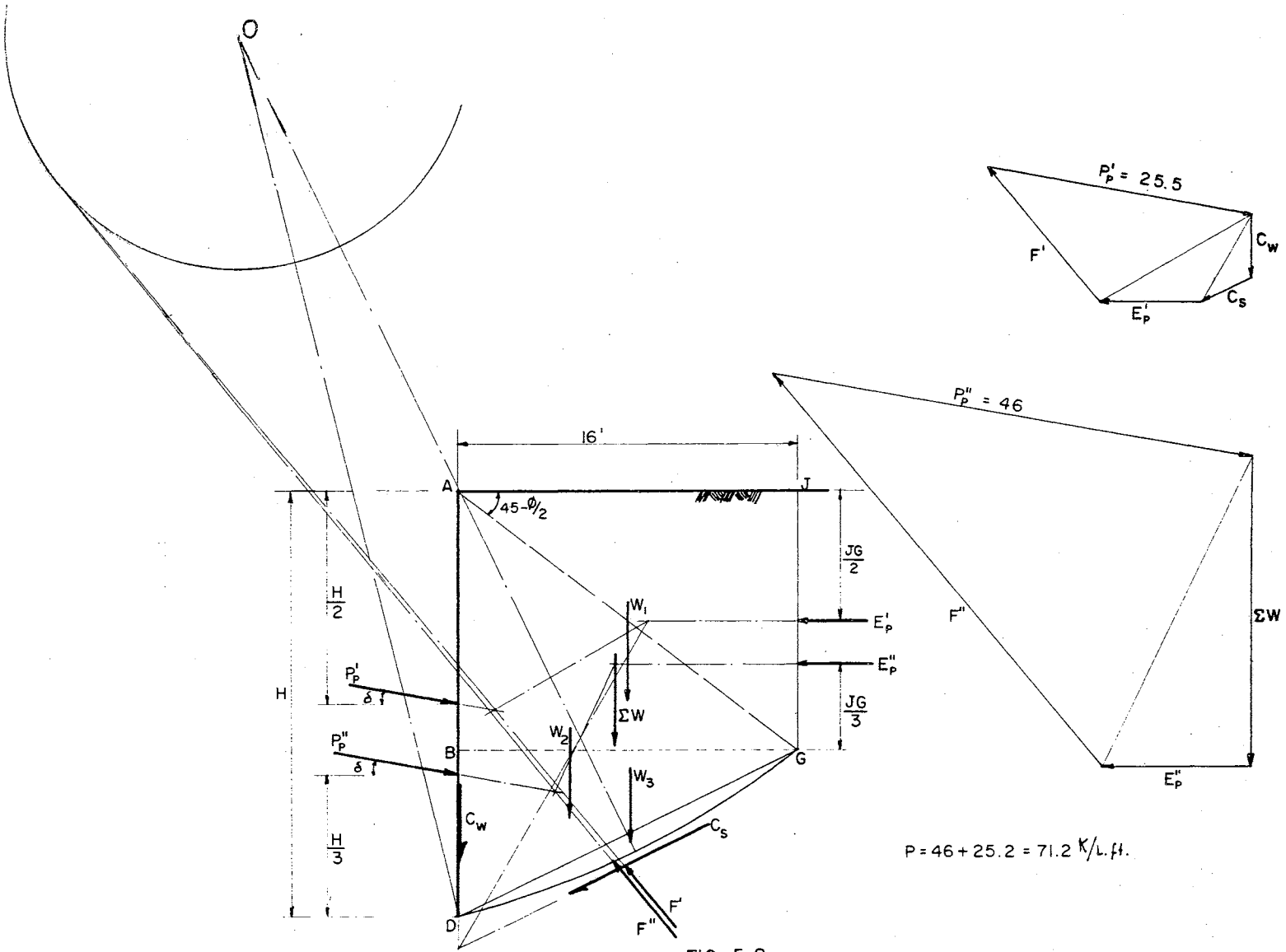

FIG. 5.8

PASSIVE EARTH PRESSURE ON RETAINING WALL WITH COHESIVE SOIL BY THE FRICTION CIRCLE METHOD. (TRIAL NO. 1)

and

$$E_p'' = \frac{1}{2} \times 0.11 \times (12.3)^2 \times \tan^2 52.5^\circ = 14.15 \text{ k/l. ft.}$$

$$C_w = c \times (AD) = 0.3 \times 20 = 6 \text{ k/l. ft.}$$

$$C_s = c \times \text{chord DG} = 0.3 \times 17.7 = 5.32 \text{ k/l. ft.}$$

W_1 = weight of area ABGJ

$$= 0.11 \times 16 \times 12.3 = 21.6 \text{ k/l. ft.}$$

W_2 = weight of area BDG

$$= \frac{1}{2} \times 0.11 \times 16 \times 7.7 = 6.76 \text{ k/l. ft.}$$

$$W_3 = \frac{1}{2}\, 0.11 \left[(42.6)^2 \frac{24\pi}{180} - 17.7 \times 41.7 \right] = 1.1 \text{ k/l. ft.}$$

The location of the equipollent force ΣW can be obtained by taking summation of moments of W_1, W_2 and W_3 with respect to D. Thus:

$$\bar{X} = \frac{21.6 \times 8 + 6.76 \times 5.35 + 1.1 \times 8.05}{29.46} = 7.4 \text{ ft.}$$

The resultant passive pressure on the back of the wall is equal to the vectorial summation of P_p' and P_p''.

$$P_p = P_p' + P_p'' = 25.2 + 46 = 71.2 \text{ k/l. ft.}$$

Trial No. 2: AJ = 18'

The following values are scaled off from Fig. 5.9:

R = 27.7 ft. JG = 14 ft.

DG = 19.1 ft. $\angle$DOG = 40.5°

The radius of the friction circle is:

$$r = 27.7 \times 0.2588 = 7.16 \text{ ft.}$$

$$L_1 = (27.7)^2 \times \frac{40.5\,\pi}{180} \times \frac{1}{19.1} = 28.4 \text{ ft.}$$

$$E'_p = 2 \times 0.3 \times 14 \times \tan 52.5 = 10.94 \text{ k/l. ft.}$$

$$E''_p = \frac{1}{2} \times 0.11 \times (14)^2 \tan^2 52.5 = 18.3 \text{ k/l. ft.}$$

$$C_w = 0.3 \times 20 = 6 \text{ k/l. ft.}$$

$$C_s = 0.3 \times 19.1 = 5.74 \text{ k/l. ft.}$$

$$W_1 = 0.11 \times 18 \times 14 = 27.7 \text{ k/l. ft.}$$

$$W_2 = \frac{1}{2} \times 0.11 \times 18 \times 6 = 5.95 \text{ k/l. ft.}$$

$$W_3 = \frac{1}{2} \times 0.11 \left[(27.7)^2 \frac{(40.5\,\pi)}{180} - 19.1 \times 26 \right] = 2.53 \text{ k/l. ft.}$$

$$\overline{X} = \frac{27.7 \times 9 + 5.95 \times 6 + 2.53 \times 9.2}{36.2} = 8.6 \text{ ft.}$$

$$P_p = P'_p + P''_p = 23.5 + 46.7 = 70.2 \text{ k/l. ft.}$$

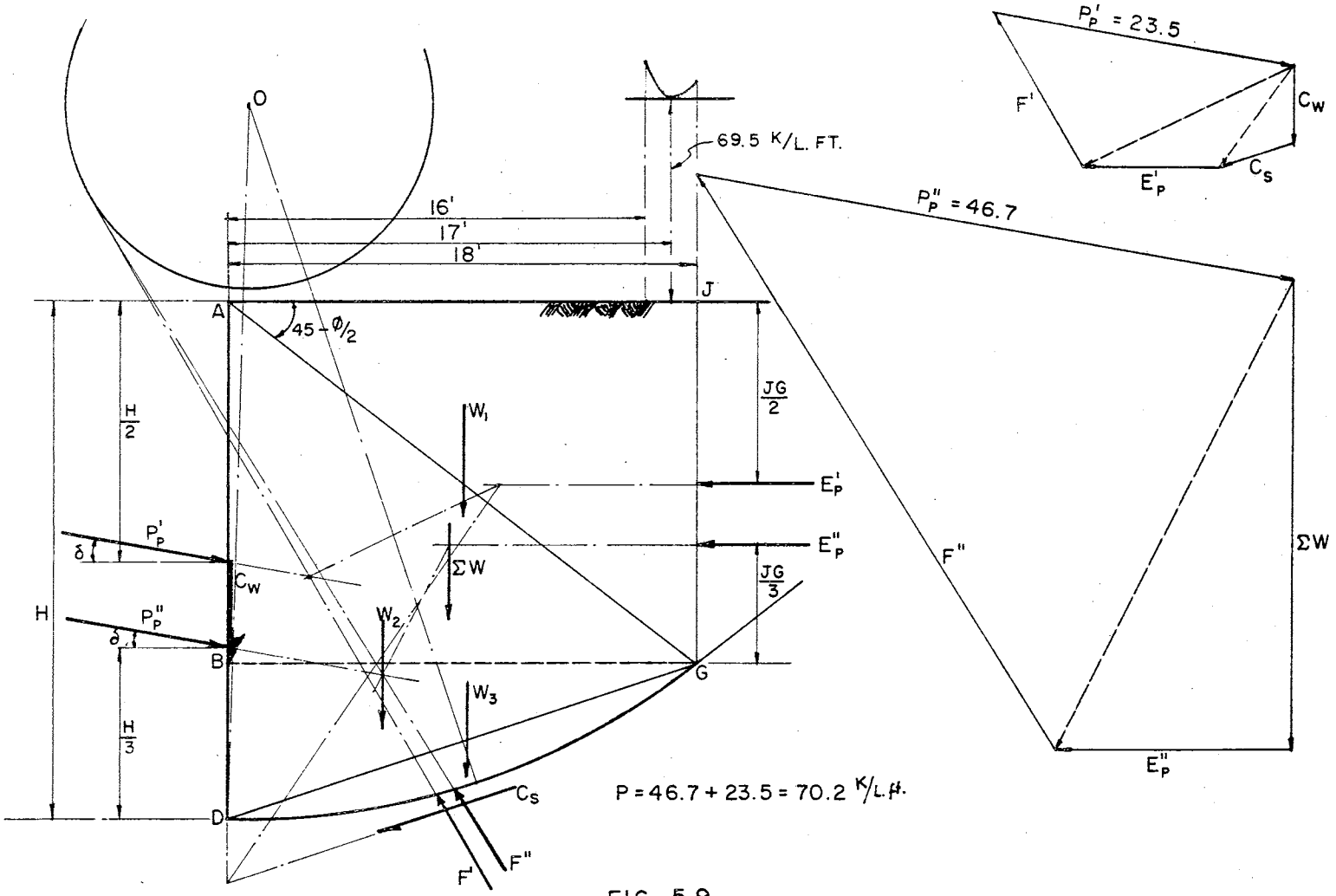

FIG. 5.9

PASSIVE EARTH PRESSURE ON RETAINING WALL WITH COHESIVE SOIL BY THE FRICTION CIRCLE METHOD. (TRIAL NO. 2)

Trial No. 3: AJ = 17 ft.

The following values are scaled off from Fig. 5.10:

R = 35.2 ft. JG = 13.2 ft.

DG = 18.4 ft. $\angle$ DOG = 30°

The radius of the friction circle is:

$$r = 35.2 \times 0.2588 = 9.12 \text{ ft.}$$

$$E'_p = 2 \times 0.3 \times 13.2 \times \tan 52.5^\circ = 10.3 \text{ k/l. ft.}$$

$$E''_p = \frac{1}{2} \times 0.11 \times (13.2)^2 \times \tan^2 52.5 = 16.3 \text{ k/l. ft.}$$

$$C_w = 0.3 \times 20 = 6 \text{ k/l. ft.}$$

$$C_s = 0.3 \times 18.4 = 5.53 \text{ k/l. ft.}$$

$$W_1 = 0.11 \times 17 \times 13.2 = 24.7 \text{ k/l. ft.}$$

$$W_2 = \frac{1}{2} \times 0.11 \times 17 \times 6.8 = 6.36 \text{ k/l. ft.}$$

$$W_3 = \frac{1}{2} \times 0.11 \left[(35.2)^2 \times \frac{30\pi}{180} - 18.4 \times 34 \right] = 1.21 \text{ k/l. ft.}$$

$$\bar{X} = \frac{24.7 \times 8.5 + 6.36 \times 5.65 + 1.21 \times 8.7}{32.27} = 7.95 \text{ ft.}$$

$$P_p = P'_p + P''_p = 24 + 45.5 = 69.5 \text{ k/l. ft.}$$

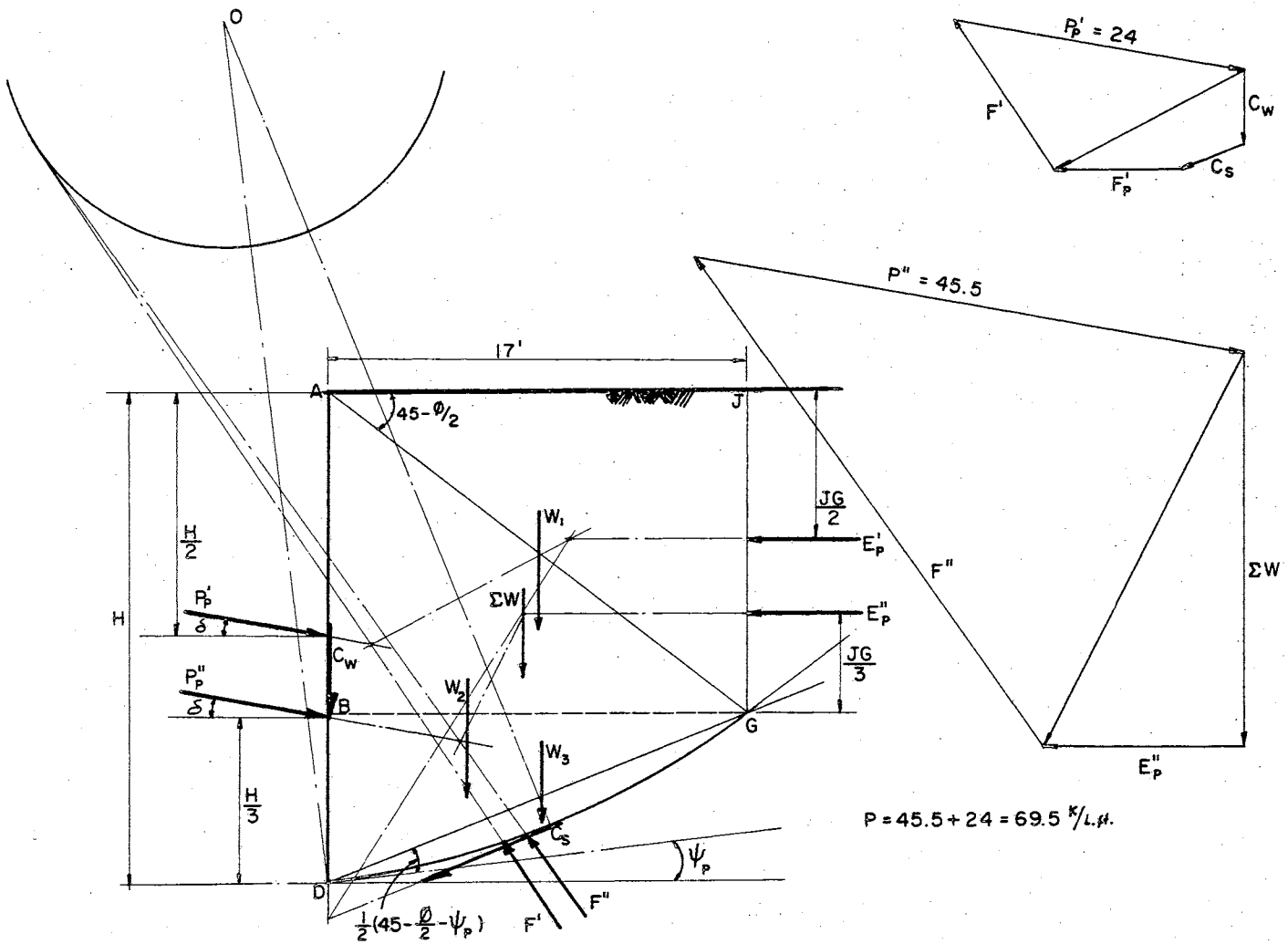

FIG. 5.10

PASSIVE EARTH PRESSURE ON RETAINING WALL WITH COHESIVE SOIL BY THE USE OF SLIP LINE METHOD. (ALSO TRIAL NO. 3)

From these three trials a graph representing the variation of P_p can be plotted and the minimum value is found to be 69.5 k/l. ft.

5.5.2. Slip Line Method

From Fig. XV, for $K = \frac{c_o}{c} = \frac{100}{300} = \frac{1}{3}$, the value of ψ_p is found to be 6.6°. Knowing ψ_p, the slip line can be drawn, Fig. 5.10, according to the steps explained in Article 4.3. Then, by the use of the friction circle method, the passive earth pressure can be obtained. In this problem it was found that the calculated slip line agrees with that assumed in Trial No. 3. Therefore, the passive pressure acting on the wall is equal to 69.5 k/l. ft. as was obtained from Trial No. 3, which proved to be the minimum value. Thus, the efficiency and convenience of the slip line method is well demonstrated.

CHAPTER VI

CONCLUSIONS

The new method developed in this study for finding the earth pressure on a retaining wall, by determining the critical slip surface, has proved to be simple, accurate and fast. It provides a direct solution for earth pressure without resorting to trial and error procedures. The method is particularly advantageous when applied to the calculation of passive earth pressure on retaining walls with either cohesive or cohesionless backfills.

Also, mathematical relations for the slope of the slip surfaces are provided which permit an evaluation of the effect of soil properties on the shape of the failure surfaces.

For retaining walls with cohesionless backfill, it was proved that (a) the shape of the slip surface is independent of the height of the wall, in both the active and passive cases and (b) the slope of the slip surface at the toe of the wall is linearly related to δ for $\delta \leq \varphi/3$, beyond which a nonlinear relation is found. The error involved in assuming the slip surface to be a plane becomes intolerably large when $\delta > \varphi/3$. It has been found that active earth pressures calculated by means of Coulomb's method, while on the unsafe side, are only a few percent smaller than the correct values; whereas in the passive case, the results obtained by Coulomb's method are on the unsafe side, and if $\delta > \varphi/3$, they may exceed by 30 percent the correct values.

For retaining walls with cohesive backfill, a graphical solution to determine the slope of the failure surface at the toe of the wall was developed. The method proved to be quite simple and accurate. For the active case it is concluded that ψ_A, the slope of the slip line at the toe of the wall, (a) increases when the height of the wall increases or when cohesion decreases; but the effects of these two variables become negligible when the height of the wall exceeds 25', (b) decreases when δ increases.

For the passive case it is concluded that ψ_p, the slope of the slip line at the toe of the wall, (a) decreases when δ increases, (b) increases when the height of the wall increases, but the rate of increase becomes negligible when the depth exceeds about 20 feet, and (c) decreases when the cohesion of the soil increases.

In summary, it can be said that the slip line approach presented in this thesis provides a direct solution for the earth pressure exerted on retaining walls without resorting to trial and error procedures. The charts which have been prepared to facilitate the solution of the problem clearly illustrate the manner in which the shape of the surface of failure is influenced by the various soil properties.

BIBLIOGRAPHY

1. Coulomb, C.A. "Essai Sur Une Application Des Règles Des Maximis et Minimis a Quelques Problèmes de Statique Relatifs a L'Architecture." Mémoires de L'Academic Royale Présentées Par Divers Savants, Vol. 7, Paris, 1776.

2. Rankine, W.J.M. "On the Stability of Loose Earth." Philosophical Transactions of the Royal Society of London, Vol. 147.

3. Kötter, F. "Die Entwicklung Der Lehre Vom Erddruck." Jahresber. Deut. Math. Ver., Vol. 2, 1892.

4. Jáky, J. "Stability of Earth Slopes." Proceedings of International Conference of Soil Mechanics, Cambridge, Mass., Vol. 2, 1936.

5. Ohde, J. "Zur Theorie Des Erddruckes Unter Besonderer Berücksichtigung Der Erddruck Verteilung." Die Bautechnik, Vol. 16, 1938.

6. Hansen, J.B. "Earth Pressure Calculation." The Danish Technical Press, Copenhagen, 1953.

7. Prandtl, L. "Über Die Härte Plastischer Körper." Nachricht Akademie Wissen, Göttingen, 1920.

8. Sokolvski, V.V. "Statics of Soil Media." Butterworths Scientific Publications, London, 1960.

9. Freudenthal, A.M. "The Inelastic Behaviour of Engineering Materials and Structures." Wiley, New York, 1950.

10. Nadai, A. "Theory of Flow and Fracture of Solids." McGraw-Hill, New York, 1950.

11. Drucker, D.C. and W. Prager. "Soil Mechanics and Plastic Analysis or Limit Design." Office of Naval Research, Technical Report No. 64, Providence, November, 1951.

12. Terzaghi, K. "Large Retaining-Wall Tests." Engineering News Record, 1934.

    Terzaghi, K. "Distribution of the Lateral Pressure of Sand on the Timbering of Cuts." Proceeding of First International Conference on Soil Mechanics, Vol. 1, Harvard, 1936.

13. Tschebotarioff, G. P. "Large-Scale Model Earth Pressure Tests on Flexible Bulkheads." Proceedings of the American Society of Civil Engineers, January, 1948.

Tschebotarioff, G. P. "Soil Mechanics, Foundations and Earth Structures." McGraw-Hill, New York, 1951.

14. Rowe, P. W. "Anchored Sheet-Pile Walls." Proceedings of the Institution of Civil Engineers, Vol. I, January and September, 1952.

15. Rendulic L. "Gleifflächen, Prüfflächen Und Erddruck." Die Bautechnik, Heft 13/14, 1940.

16. Fellenius W. "Erdstatische Berechnungen." W. Ernst U. Sohn, Berlin, 1939.

17. Krey, H. "Erddruck, Erdwiderstand Und Tragfähigkeit Des Baugrundes." W. Ernst U. Sohn, Berlin, 1936.

18. Fronfard, M. "Cycloides De Glissement Des Terres." Comptes Rendus Hebdomadères, Academie De Sciences, Paris, Vol. 174, 1922.

19. Prager, W. and P. G. Hodge. "Theory of Perfectly Plastic Solids." Wiley, New York, 1951.

20. Terzaghi, K. and R. Peck. "Soil Mechanics in Engineering Practice." Wiley, New York, 1948.

APPENDIX

DETERMINATION OF THE LOCUS OF THE SHEARING STRESSES ON VERTICAL AND HORIZONTAL PLANES OF COHESIVE ELEMENTS TAKEN AT THE TOE OF RETAINING WALLS OF DIFFERENT HEIGHTS

Case 1: Active Case of Failure

Referring to Fig. 4.1b and 4.2, the problem encountered in drawing the equivalent Mohr's circle for the state of stresses acting on the element is that the undetermined shearing stress, $c + p_A \sin \delta$, cannot be located directly to establish the circle. In Article 4.2, it was assumed that the locus of the shearing stresses on elements taken at the toe of retaining walls with cohesive backfill and of different heights, when plotted on Mohr's circles, is approximated by a straight line. The reliability of this assumption will be demonstrated analytically.

Let MM' be the rupture line, making angle φ with the horizontal, and cutting the τ-axis at A where $OA = c$. Through point A draw the line AS that makes an angle δ with the horizontal. This line cuts the various arbitrary Mohr's circles at A, F, G, H and K, Fig. A.1. The horizontal projections of these points on their respective circles are A', F', G', H' and K'. The problem then, is to investigate the linearity of these latter points. To do this, the coordinates of points A', F', G', H' and K' will be determined analytically, and the slope of the segments $A'F'$, $F'G'$, $G'H'$ and $H'K'$ will be compared.

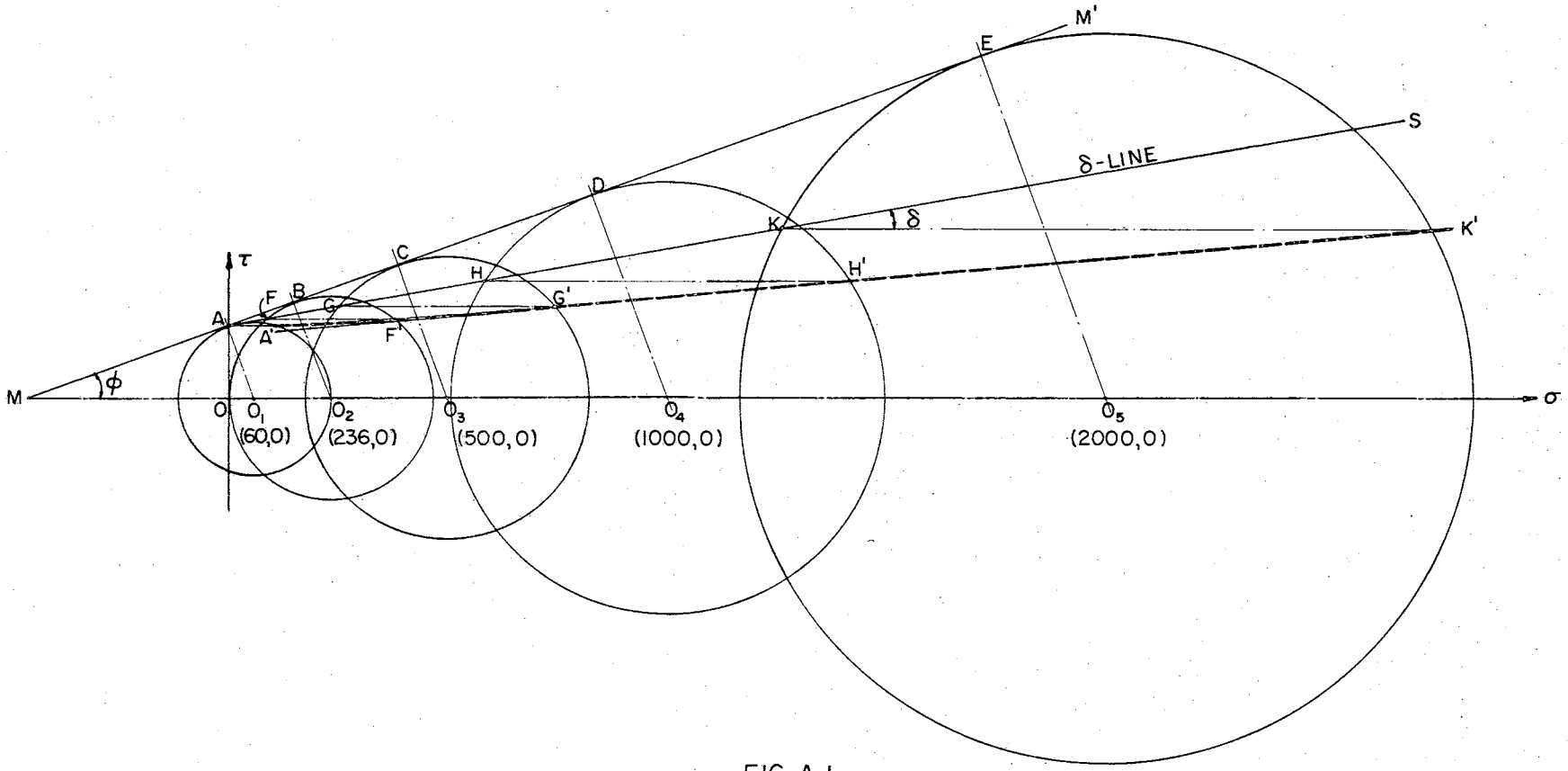

FIG. A.1

COHESIVE SOIL, ACTIVE CASE: GRAPHICAL DETERMINATION OF THE LOCUS OF THE SHEARING STRESSES ACTING ON THE VERTICAL AND HORIZONTAL PLANES OF ELEMENTS TAKEN AT THE TOES OF DIFFERENT HEIGHT RETAINING WALLS.

The equation of line MM' is

$$\tau = m\sigma + c \qquad (A.1)$$

where $m = \tan \varphi$.

The radius of any circle tangent to MM' and having its center at (σ_o, o) is, (Fig. A.2):

$$r = \left| \frac{\tau - m\sigma - c}{\sqrt{1 + m^2}} \right|_{@(\sigma_o, o)} = \left| \frac{-m\sigma_o - c}{\sqrt{1 + m^2}} \right| = \frac{m\sigma_o + c}{\sqrt{1 + m^2}} \qquad (A.2)$$

The general equation of any Mohr's circle becomes:

$$(\sigma - \sigma_o)^2 + \tau^2 = r^2$$

substituting for r from (A.2):

$$(\sigma - \sigma_o)^2 + \tau^2 = \frac{(m\sigma_o + c)^2}{1 + m^2} \qquad (A.3)$$

The equation of line AS is:

$$\tau = n\sigma + c \qquad (A.4)$$

where $n = \tan \delta$.

The points of intersection of line AS with the arbitrary Mohr's circle can be obtained by substituting for τ in Eq.(A.3) the value obtained from (A.4). Thus:

$$(\sigma - \sigma_o)^2 + (n\sigma + c)^2 = \frac{(m\sigma_o + c)^2}{1 + m^2}$$

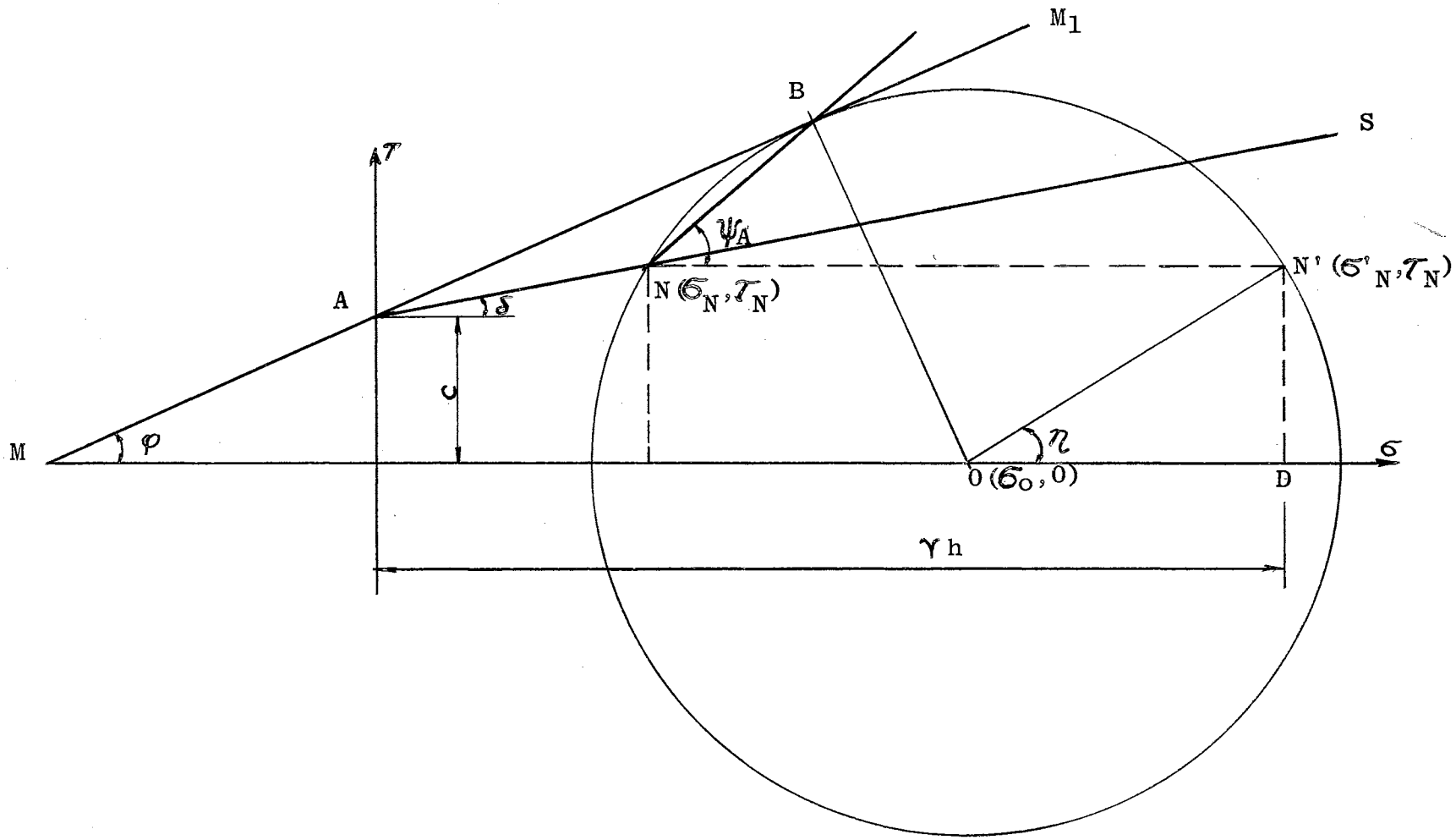

Fig. A.2 - Cohesive Soil: Mohr's Circle Representation for the Active State of Stress at the Toe of the Wall

Expanding the previous equation and collecting terms, it follows that:

$$\sigma^2(1+n^2) - 2\sigma(\sigma_o - nc) + \sigma_o^2 + c^2 - \frac{(m\sigma_o + c)^2}{1 + m^2} = 0 \qquad \text{(A.5a)}$$

Let:

$$1 + n^2 = A$$

$$\sigma_o - nc = B$$

and

$$\sigma_o^2 + c^2 - \frac{(m\sigma_o + c)^2}{1 + m^2} = D$$

Then (A.5a) can be written in the following form:

$$A\sigma^2 - 2B\sigma + D = 0 \qquad \text{(A.5b)}$$

Solve for σ:

$$\sigma = \frac{+B \mp \sqrt{B^2 - AD}}{A} \qquad \text{(A.6a)}$$

For the active case, the abscissa of point N is:

$$\sigma_N = \frac{+B - \sqrt{B^2 - AD}}{A} \qquad \text{(A.6b)}$$

Substitute for σ in (A.4) the value obtained in (A.6b), thus:

$$\tau_N = n\,\frac{(B - \sqrt{B^2 - AD})}{A} + c \qquad \text{(A.7)}$$

The coordinates of point N' can be determined by finding the intersection of line NN' with the circle O. Since line NN' is parallel to the σ-axis, its equation is as expressed in (A. 7).

Substitute for τ in Eq. (A. 3) the value obtained from (A. 7):

$$(\sigma - \sigma_o)^2 + \left[n \frac{(B - \sqrt{B^2 - AD})}{A} + c \right]^2 = \frac{(m\sigma_o + c)^2}{1 + m^2} \qquad \text{(A. 8a)}$$

Let:

$$\frac{n(B - \sqrt{B^2 - AD})}{A} + c = E$$

and

$$\frac{(m\sigma_o + c)^2}{1 + m^2} = F$$

Then (A. 8a) can be written in the following form:

$$(\sigma - \sigma_o)^2 + E^2 - F = 0$$

Expand this equation and collect the terms:

$$\sigma^2 - 2\sigma_o\sigma + \sigma_o^2 + E^2 - F = 0 \qquad \text{(A. 8b)}$$

The roots of (A. 8b) are:

$$\sigma = \sigma_o \mp \sqrt{F - E^2}$$

The abscissa of point N' is:

$$\sigma_{N'} = \sigma_o + \sqrt{F - E^2} \qquad (A.9)$$

Since in any practical problem the value of $\sigma_{N'}$ is given as γh (see Fig. 4.1b), it becomes possible, by the use of (A.9), to solve for σ_o and thus the center of the required Mohr's circle can be obtained. The value E in Eq. A.9 can be written in the following form, if one makes use of (A.6b):

$$E = n\sigma_N + c = \tau_N$$

But it is known from the properties of the Mohr's circle that:

$$\frac{\sigma_N + \gamma h}{2} = \sigma_o \qquad (A.10)$$

Therefore,

$$\sigma_N = 2\sigma_o - \gamma h$$

Thus:

$$E = n(2\sigma_o - \gamma h) + c \qquad (A.11)$$

Substitute (A.11) for E in Eq. A.9 to obtain:

$$\gamma h = \sigma_o + \sqrt{\frac{(m\sigma_o + c)^2}{1 + m^2} - \left[n(2\sigma_o - \gamma h) + c\right]^2}$$

After simplification, the above equation can be written in the following

form:

$$\sigma_o^2\left(\frac{1}{1+m^2} + 4n^2\right) - 2\sigma_o\left[\gamma h(1+2n^2) + \frac{mc}{1+m^2} - 2nc\right]$$

$$+ (n\gamma h - c)^2 + (\gamma h)^2 - \frac{c^2}{1+m^2} \qquad \text{(A.12)}$$

Let

$$\alpha = \frac{1}{1+m^2} + 4n^2$$

$$\beta = \left[\gamma h(1+2n^2) + \frac{mc}{1+m^2} - 2nc\right]$$

and

$$\lambda = (n\gamma h - c)^2 + (\gamma h)^2 - \frac{c^2}{1+m^2}$$

then Eq. (A.12) can be presented as:

$$\alpha\sigma_o^2 - 2\beta\sigma_o + \lambda = 0 \qquad \text{(A.13)}$$

Solving for σ_o and using the smallest root since σ_o has to be smaller than γh

$$\sigma_o = \frac{\beta - \sqrt{\beta^2 - \alpha\lambda}}{\alpha} \qquad \text{(A.14)}$$

Eq. (A.14) is an accurate solution for the position of the center of the Mohr's circle that satisfies the stresses on the element shown in Fig. 4.1b.

Using expressions (A.6b), (A.7) and (A.9), the coordinates of points N and N' can be determined. Since circle O is an arbitrary circle, the expression above can be used with respect to any specific circle if σ_o is replaced by the abscissa of the center of the proposed circle. The angle ψ_A which is represented approximately by Eq. (4.7) can now be derived accurately, see Fig. A.2. It is observed that

$$\psi_A = \frac{\widehat{BN'}}{2} = \frac{1}{2}(\angle BOD - \eta) \qquad (A.15)$$

$$\angle BOD = 90 + \varphi$$

and

$$\eta = \tan^{-1}\frac{\tau_n}{\gamma h - \sigma_o} \qquad (A.16)$$

Solve for σ_o in terms of γh, as shown in Eq. (A.14)and determine η. Substitute for η in (A.15) and solve for ψ_A.

Referring back to Fig. A.1, it is now necessary to find the coordinates of points A', F', G', H' and K', in order to check the slopes of the lines A'F', F'G', G'H' and H'K' for a given numerical problem. If these slopes are found to be equal, then points A', F', G', H' and K' are collinear.

Given $\delta = 10^\circ$, $\varphi = 20^\circ$ and $c = 165$ psf. Then, $m = \tan\varphi = 0.364$, $n = \tan\delta = 0.1763$ and $A = 1 + n^2 = 1.031$

Circle O_1:

The coordinates of center O_1 are (60, 0); the coordinates of point A are (0, 165). From Eq. (A.9), $\sigma_{A'}$ can be determined

$$\sigma_{A'} = \sigma_{01} + \sqrt{F_A - E_A^2} \qquad \sigma_{01} = 60$$

$$F_A = \frac{(m\sigma_{01} + c)^2}{1 + m^2} = \frac{(0.364 \times 60 + 165)^2}{1 + (0.364)^2}$$

$$= 30800$$

$$E_A^2 = (n\sigma_A + c)^2 = (165)^2 = 27,300$$

Therefore:

$$\sigma_{A'} = 60 + \sqrt{30800 - 27,300} = 119.2 \text{ psf}$$

The coordinates of A' are then (119.2, 165)

Circle O_2

The coordinates of center O_2 are (236, 0); the coordinates of point F can be calculated from (A.6b) and (A.7).

$$\sigma_F = \frac{B_F - \sqrt{B_F^2 - AD_F}}{A}$$

$$B_F = \sigma_{02} - nc = 236 - 0.1763 \times 165 = 206.9$$

$$A = 1 + n^2 = 1 + (0.1763)^2 = 1.031$$

$$D_F = \sigma_{02}^2 + c^2 - \frac{(m\sigma_{02} + c)^2}{1 + m^2}$$

$$= (236)^2 + (165)^2 - \frac{(0.364 \times 236 + 165)^2}{1.132} = 27300$$

Therefore,

$$\sigma_F = \frac{206.9 - \sqrt{(206.9)^2 - 1.031 \times 27300}}{1.031} = 83.2 \text{ psf.}$$

$$\tau_F = n\sigma_F + c = 0.1763 \times 83.2 + 165$$

$$= 179.65 \text{ psf}$$

The coordinates of point F are (83.2, 179.65)

$$\sigma_{F'} = \sigma_{02} + \sqrt{F_F - E_F^2}$$

$$F_F = \frac{(m\sigma_{02} + c)^2}{1 + m^2} = 55600$$

$$E_F^2 = (\tau_F)^2 = 32200$$

Then

$$\sigma_{F'} = 236 + \sqrt{55600 - 32200} = 389 \text{ psf.}$$

The coordinates of point F' are (389, 179.65).

Circle O_3:

The coordinates of center O_3 are (500, 0).

$$\sigma_G = \frac{B_G - \sqrt{B_G^2 - AD_G}}{A}$$

$$B_G = 500 - 29.1 = 470.9$$

$$D_G = (500)^2 + (165)^2 - \frac{(0.364 \times 500 + 165)^2}{1.132}$$

$$= 170800$$

Then

$$\sigma_G = \frac{470.9 - \sqrt{(470.9)^2 - 1.031 \times 170800}}{1.031} = 249 \text{ psf.}$$

$$\tau_G = n\sigma_G + c = 0.1763 \times 249 + 165 = 208.8 \text{ psf.}$$

$$\sigma_{G'} = \sigma_{03} + \sqrt{F_G - E_G^2}$$

$$F_G = \frac{(m\sigma_{03} + c)^2}{1 + m^2} = 106400$$

$$E_G^2 = \tau_G^2 = (208.8)^2 = 43600$$

$$\sigma_{G'} = 500 + \sqrt{106400 - 43600} = 751 \text{ psf.}$$

The coordinates of G' are (751, 208.8).

Circle O_4:

The coordinates of center O_4 are (1000, 0)

$$\sigma_H = \frac{B_H - \sqrt{B_H^2 - AD_H}}{A}$$

$$B_H = 1000 - 29.1 = 970.9$$

$$D_H = (1000)^2 + (165)^2 - \frac{(0.364 \times 1000 + 165)^2}{1.132} = 780200$$

$$\sigma_H = \frac{970.9 - \sqrt{(970.9)^2 - 1.031 \times 780200}}{1.031}$$

$$= 580 \text{ psf.}$$

$$\tau_H = n\sigma_H + c = 0.1763 \times 580 + 165 = 267 \text{ psf.}$$

$$\sigma_{H'} = \sigma_{04} + \sqrt{F_H - E_H^2}$$

$$F_H = 247000$$

$$E_H^2 = \tau_H^2 = 71300$$

$$\sigma_{H'} = 1000 + \sqrt{247000 - 71300} = 1419 \text{ psf.}$$

The coordinates of H' are (1419, 267).

Circle O_5:

The coordinates of center O_5 are (2000, 0).

$$\sigma_K = \frac{B_K - \sqrt{B_K^2 - AD_K}}{A}$$

$$B_K = \sigma_{05} - nc = 2000 - 29.1 = 1970.9$$

$$D_K = (2000)^2 + (165)^2 - \frac{(0.364 \times 2000 + 165)^2}{1.132} = 3,323,200$$

$$\sigma_K = \frac{1970.9 - \sqrt{(1970.9)^2 - 1.031 \times 3323,200}}{1.031} = 1260 \text{ psf.}$$

$$\tau_K = 0.1763 \times 1260 + 165 = 387 \text{ psf.}$$

$$\sigma_{K'} = \sigma_{05} + \sqrt{F_K - E_K^2}$$

$$F_K = 704,000$$

$$E_K^2 = \tau_K^2 = 150,000$$

$$\sigma_{K'} = 2000 + \sqrt{704000 - 150000} = 2745 \text{ psf.}$$

The coordinates of K' are (2745, 387).

Checking the slopes of lines A'F', F'G', G'H' and H'K', it is found that:

$$\tan \alpha_{A'} = \frac{179.69 - 165}{389 - 119.2} = 0.0543$$

$$\alpha_{A'} = \tan^{-1} 0.0543 \approx 3^\circ - 10'$$

$$\tan \alpha_{F'} = \frac{208.8 - 179.65}{751 - 389} = 0.0805$$

$$\alpha_{F'} = \tan^{-1} 0.0805 \approx 4^\circ - 35'$$

$$\tan \alpha_{G'} = \frac{267 - 208.8}{1419 - 751} = 0.08712$$

$$\alpha_{G'} = \tan^{-1} 0.08712 \approx 5^\circ - 0'$$

$$\tan \alpha_{H'} = \frac{387 - 267}{2745 - 1419} = 0.09049$$

$$\alpha_{H'} = \tan^{-1} 0.09049 \approx 5^{\circ}\text{-}10'$$

This result reveals that line A'K' can be approximated by a straight line between F' and K'. Apparently, a significant deviation occurs only in circles very near the origin. Therefore, the straight line assumption for the locus of the shearing stresses for cohesive elements taken at the toe of retaining walls of different heights when plotted on Mohr's circles is found to be reasonable, justifying the graphical procedure described in Article 4.2.

Case 2: Passive Case of Failure

Due to the similarity in the nature of this problem and that for the active case, no analytical investigation is presented. A graphical solution is shown in Fig. A.3, in which it is seen that the locus of the shearing stresses deviates significantly from a straight line only at points A' and F'. Since these two points have very small abscissa, they represent the vertical stresses of very low retaining walls. Soils engineers are usually interested in intermediate and high retaining walls. For the correspondingly large normal stresses the associated shearing stresses can be considered to be located on the nearly straight portion of the locus, G'K'.

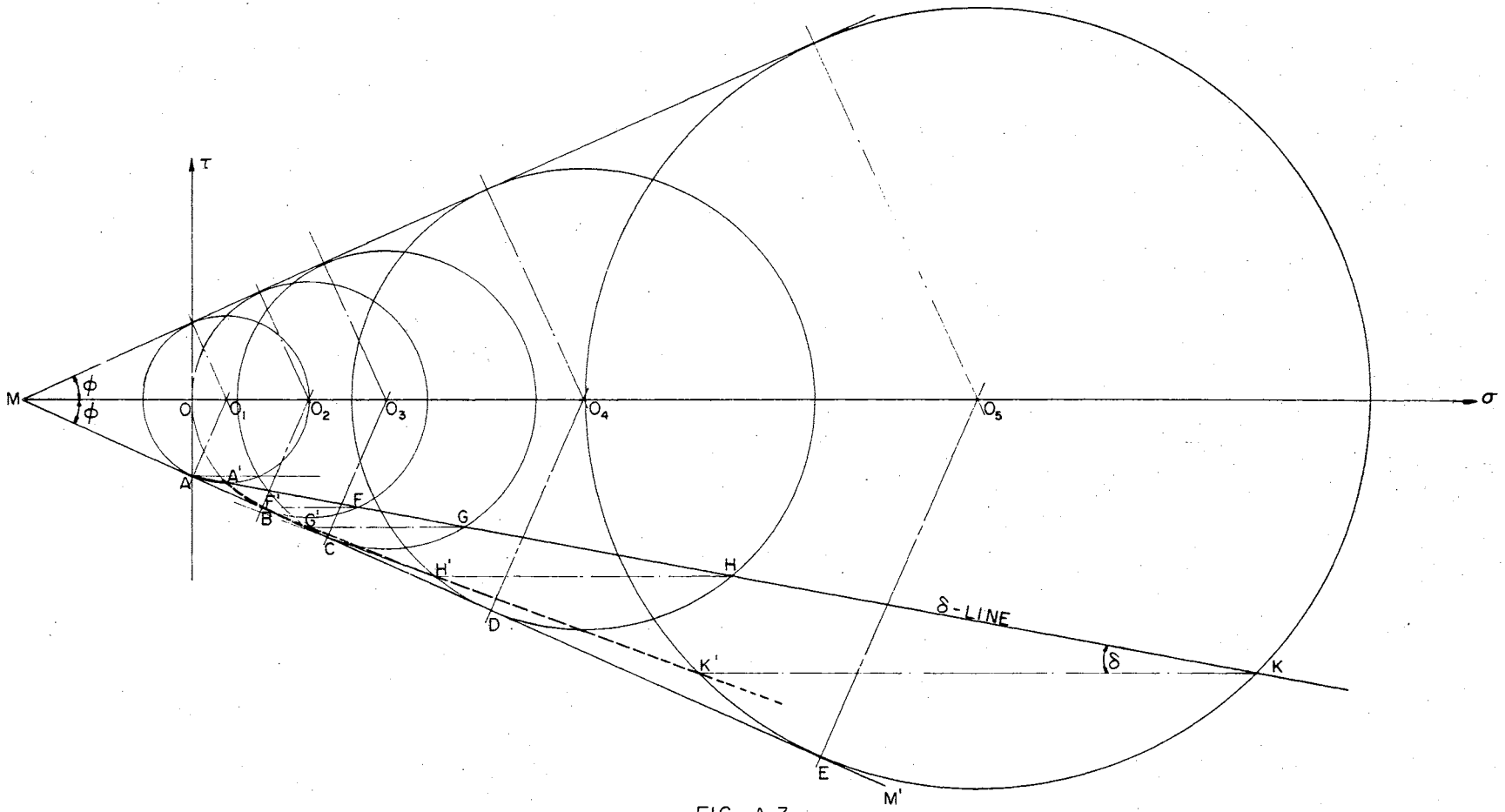

FIG. A.3

COHESIVE SOIL, PASSIVE CASE: GRAPHICAL DETERMINATION OF THE LOCUS OF THE SHEARING STRESSES ACTING ON THE VERTICAL AND HORIZONTAL PLANES OF ELEMENTS TAKEN AT THE TOES OF DIFFERENT HEIGHT RETAINING WALLS.

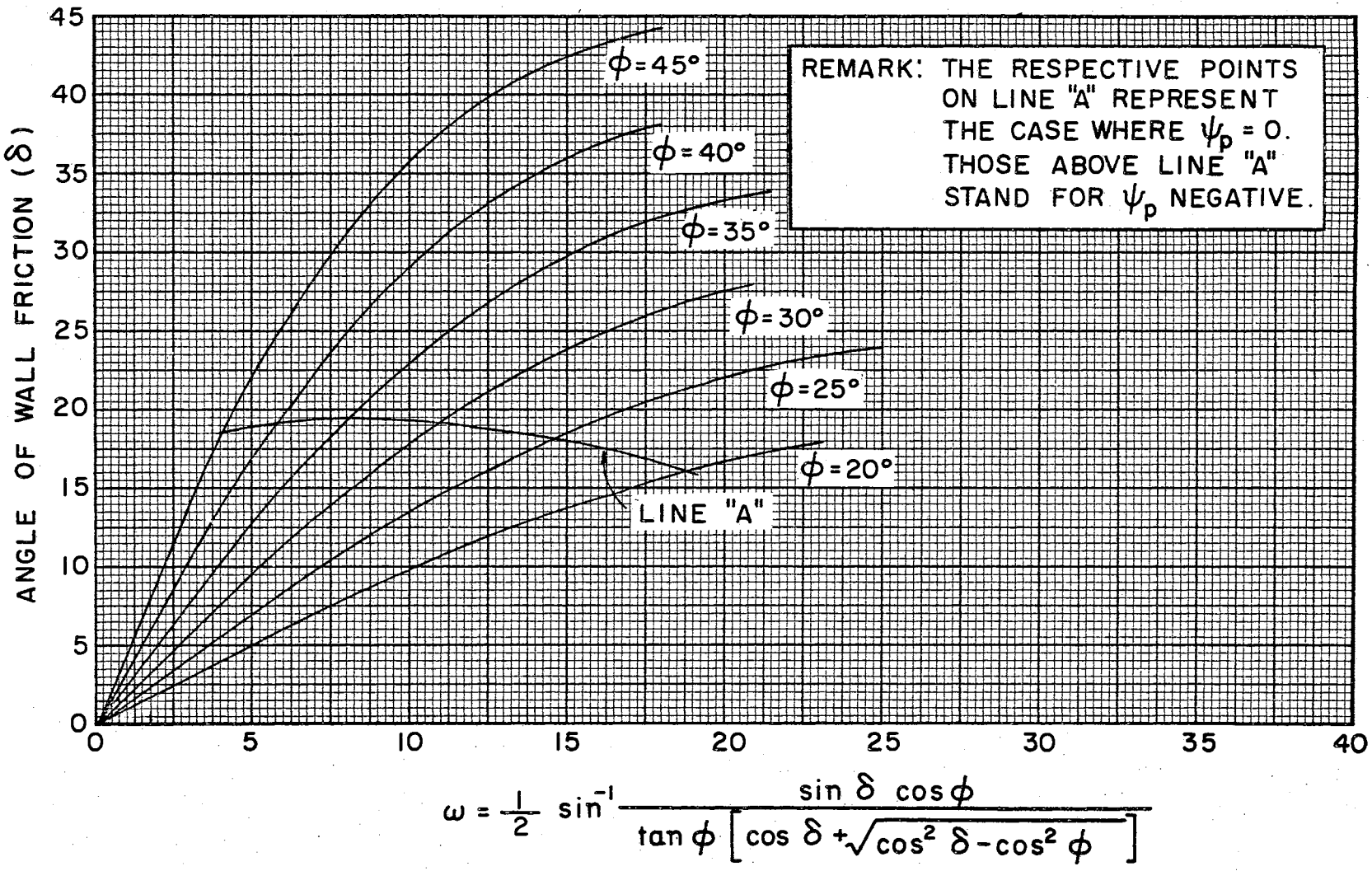

FIG. I- δ-ω RELATION FOR COHESIONLESS SOIL

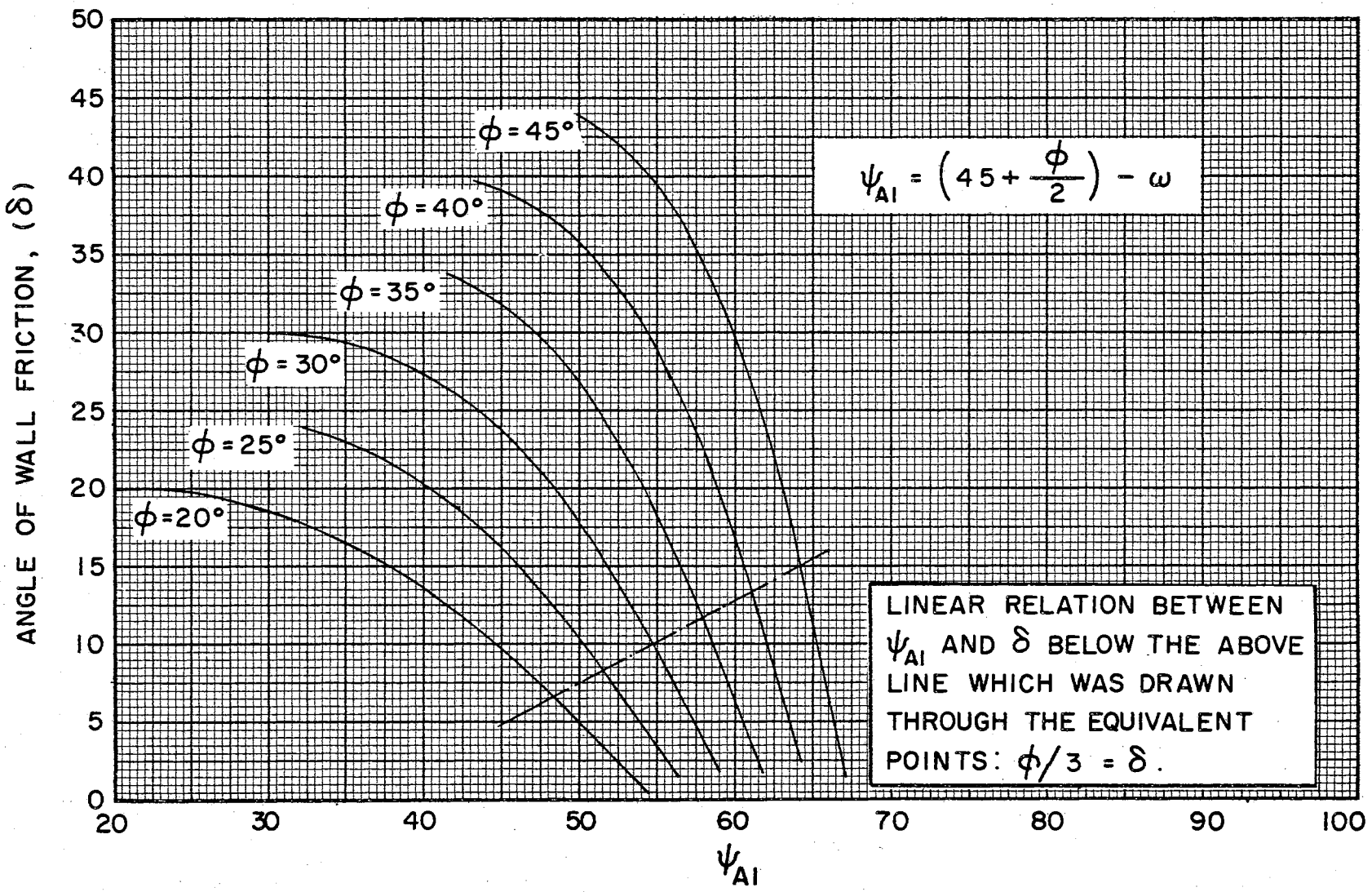

FIG. II- δ-ψ_{AI} RELATION FOR COHESIONLESS SOIL

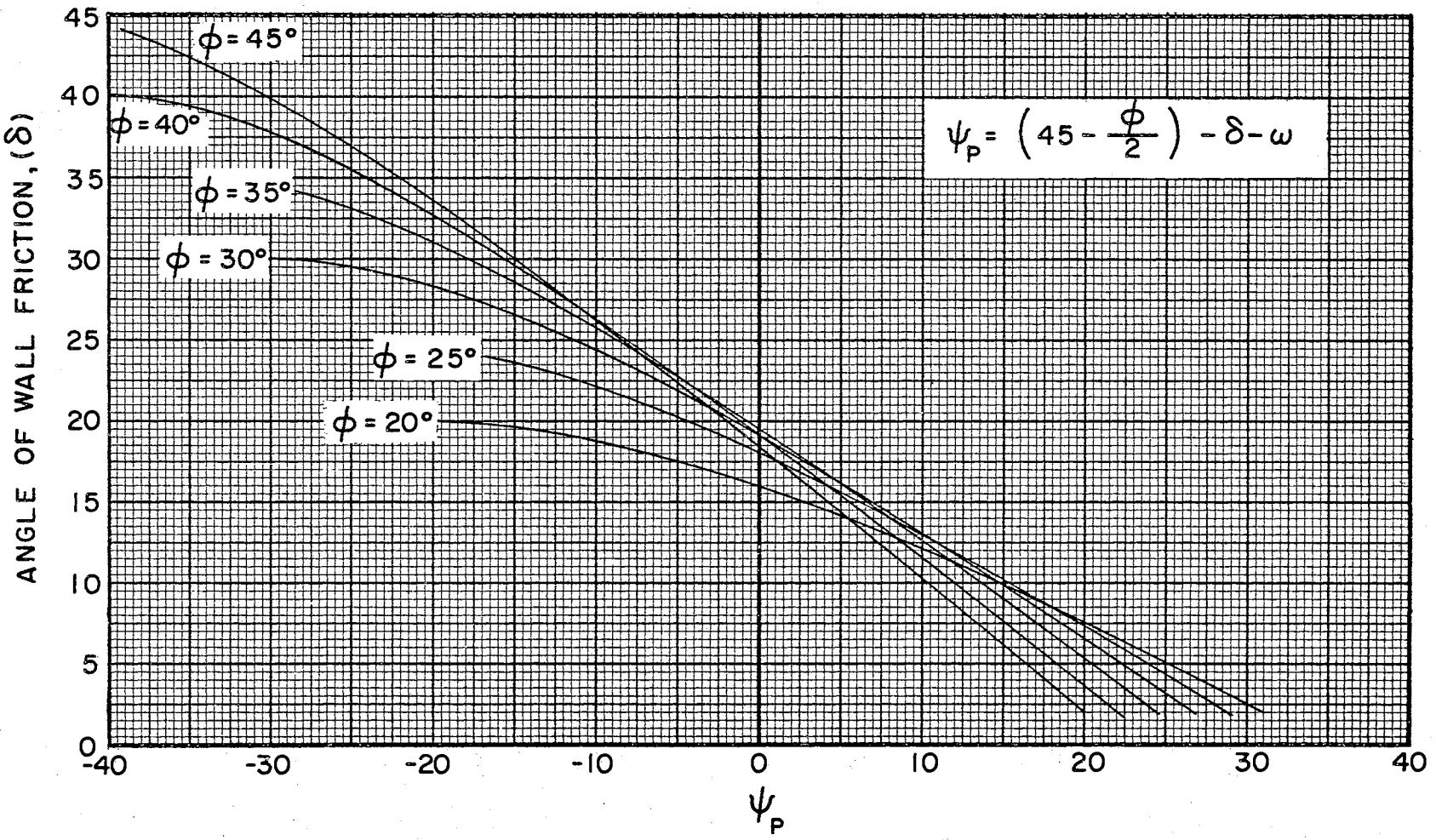

FIG. III - δ-ψ_p RELATION FOR COHESIONLESS SOIL.

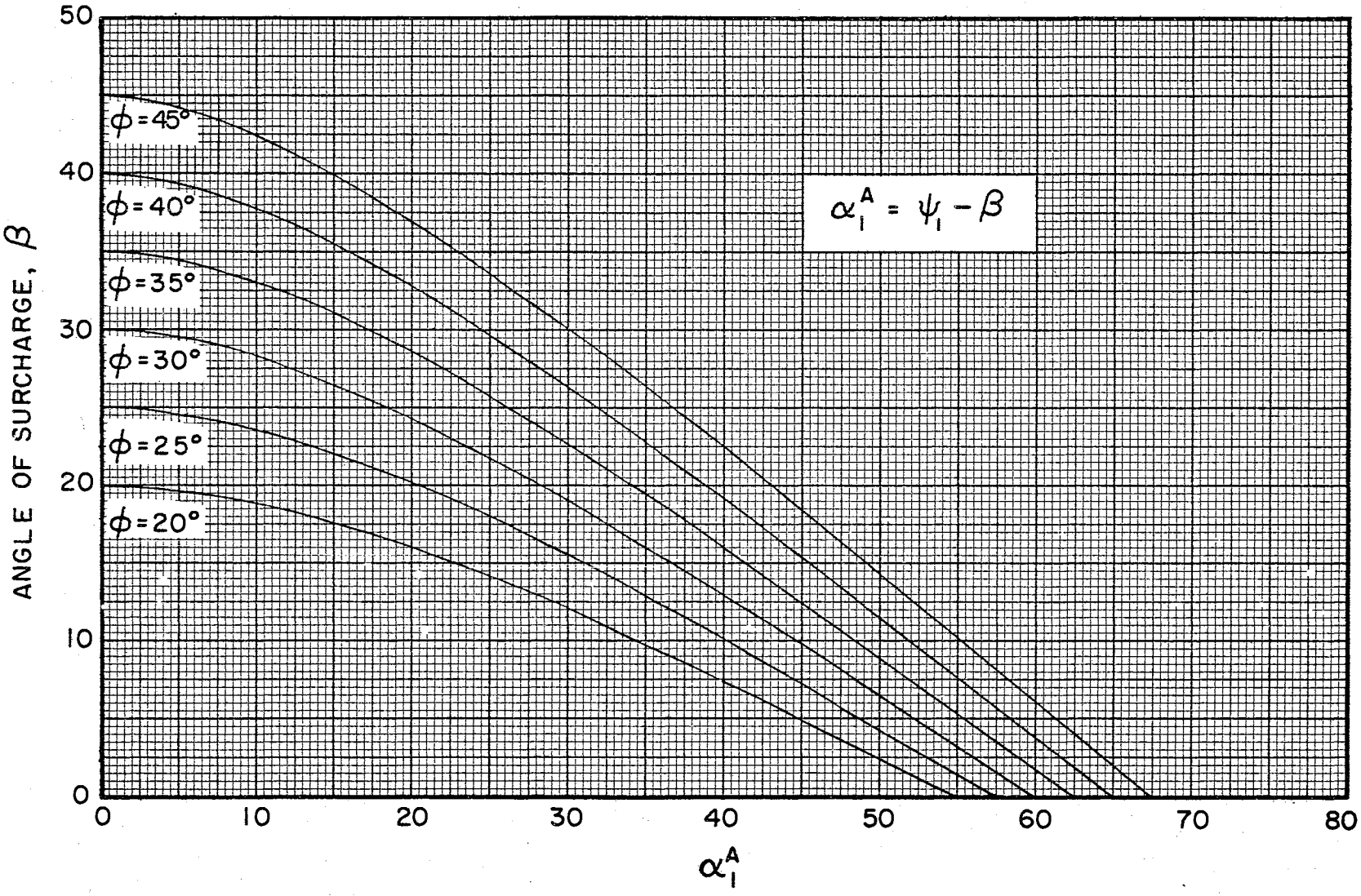

FIG. IV - $\beta - \alpha_1^A$ RELATION FOR SEMI-INFINITE SLOPING COHESIONLESS MASS

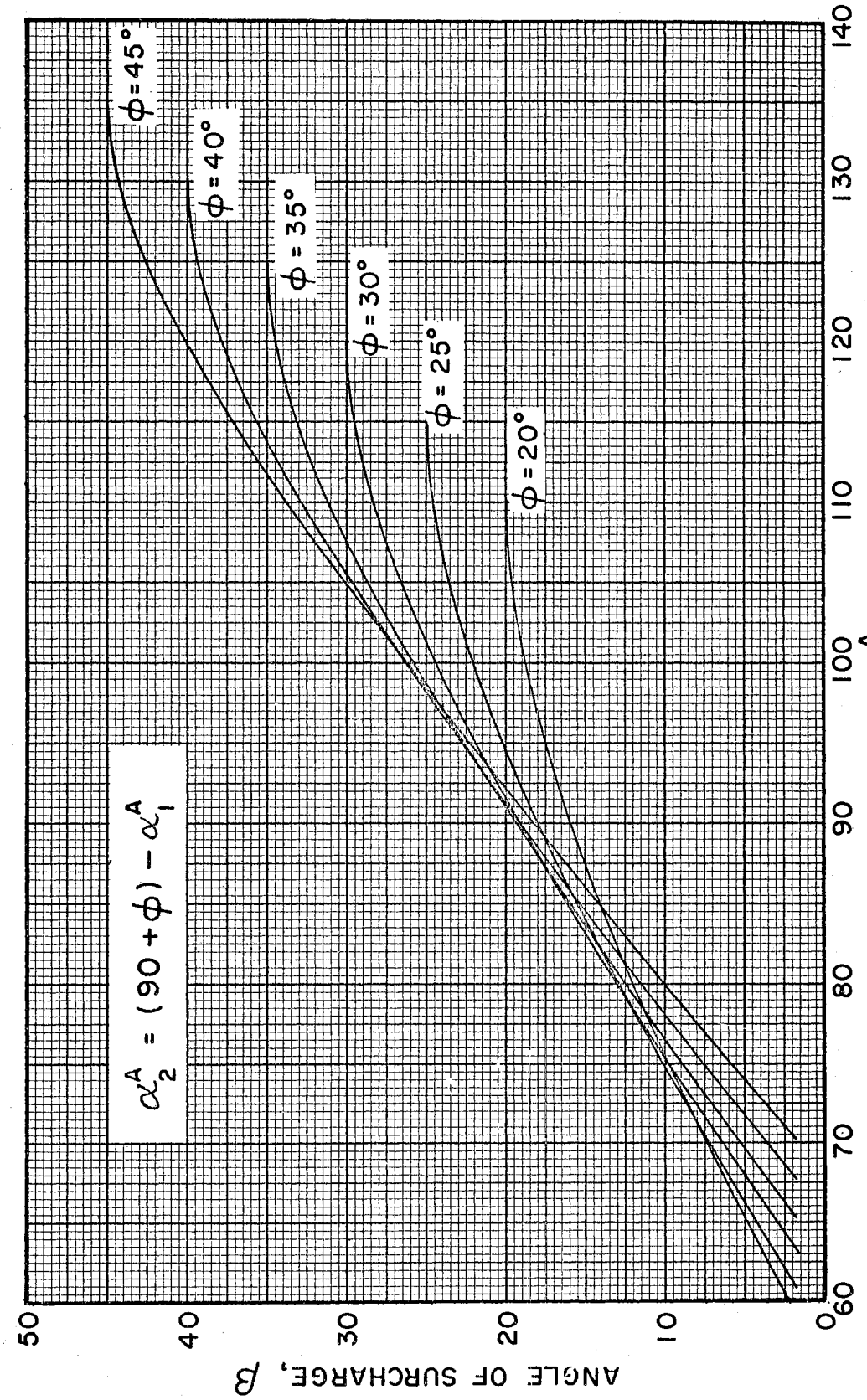

FIG. V - β - α_2^A RELATION FOR SEMI-INFINITE SLOPING COHESIONLESS MASS

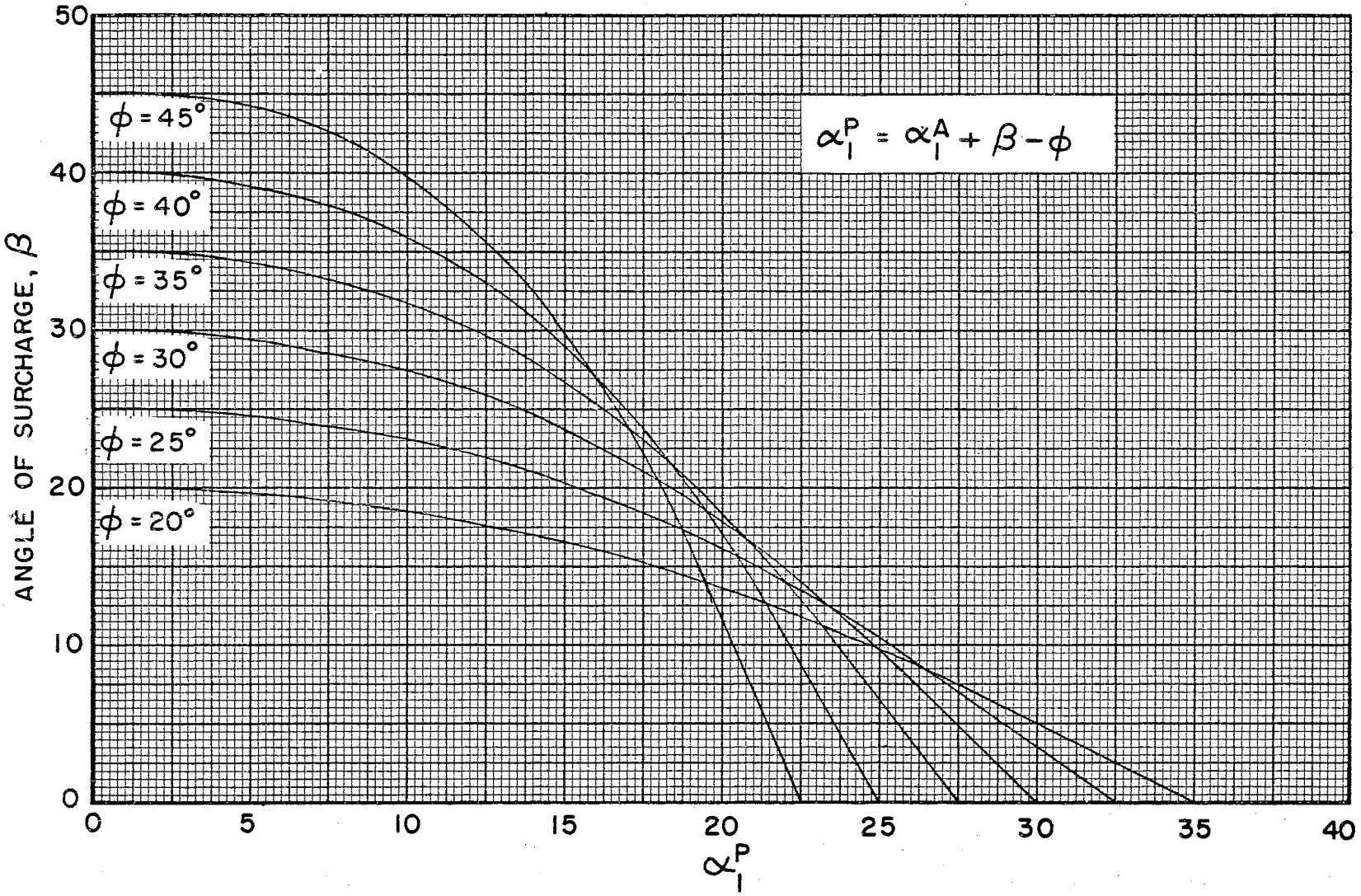

FIG. VI - $\beta - \alpha_1^P$ RELATION FOR SEMI-INFINITE SLOPING COHESIONLESS MASS

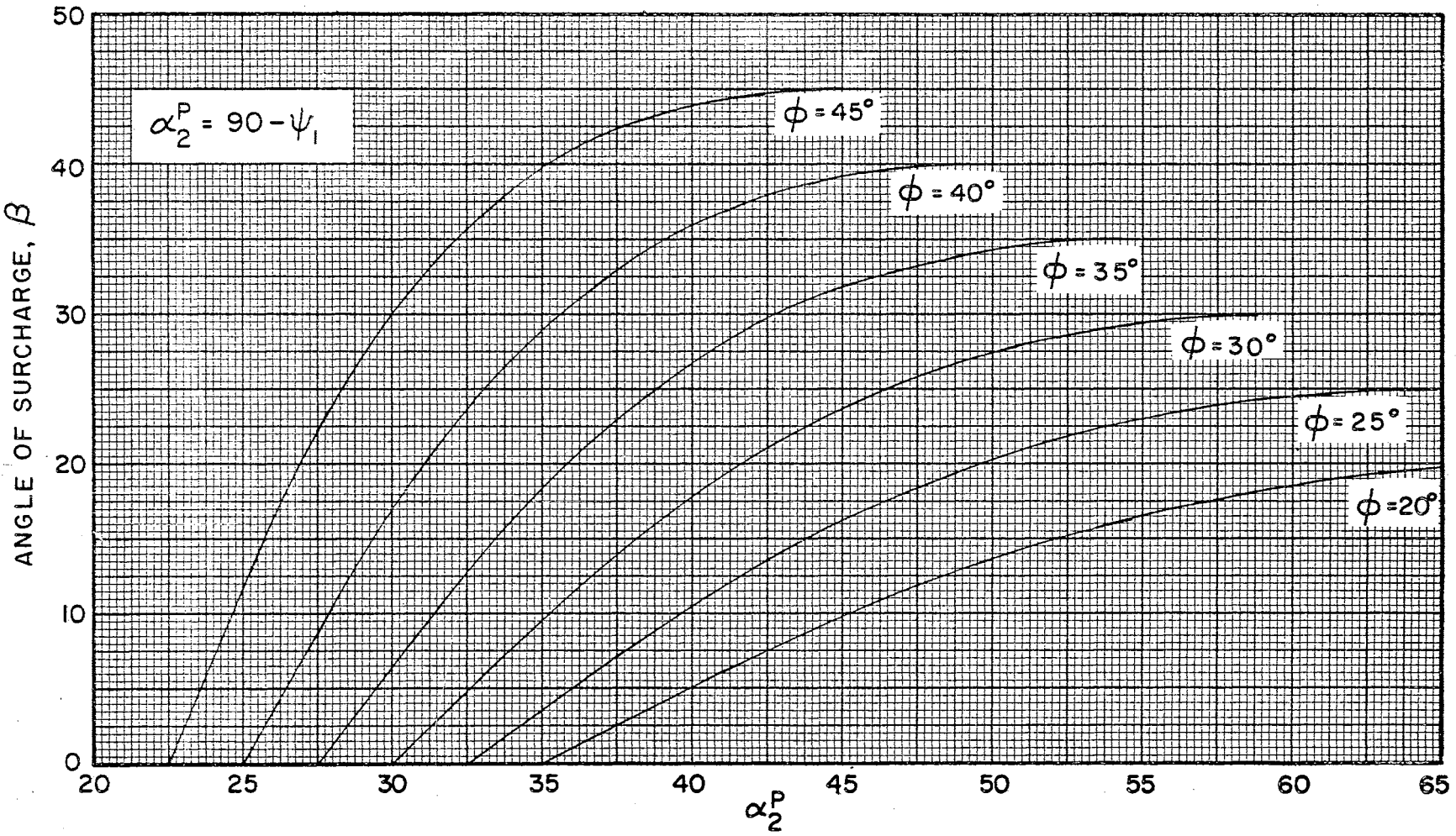

FIG. VII - $\beta - \alpha_2^P$ RELATION FOR SEMI-INFINITE SLOPING COHESIONLESS MASS

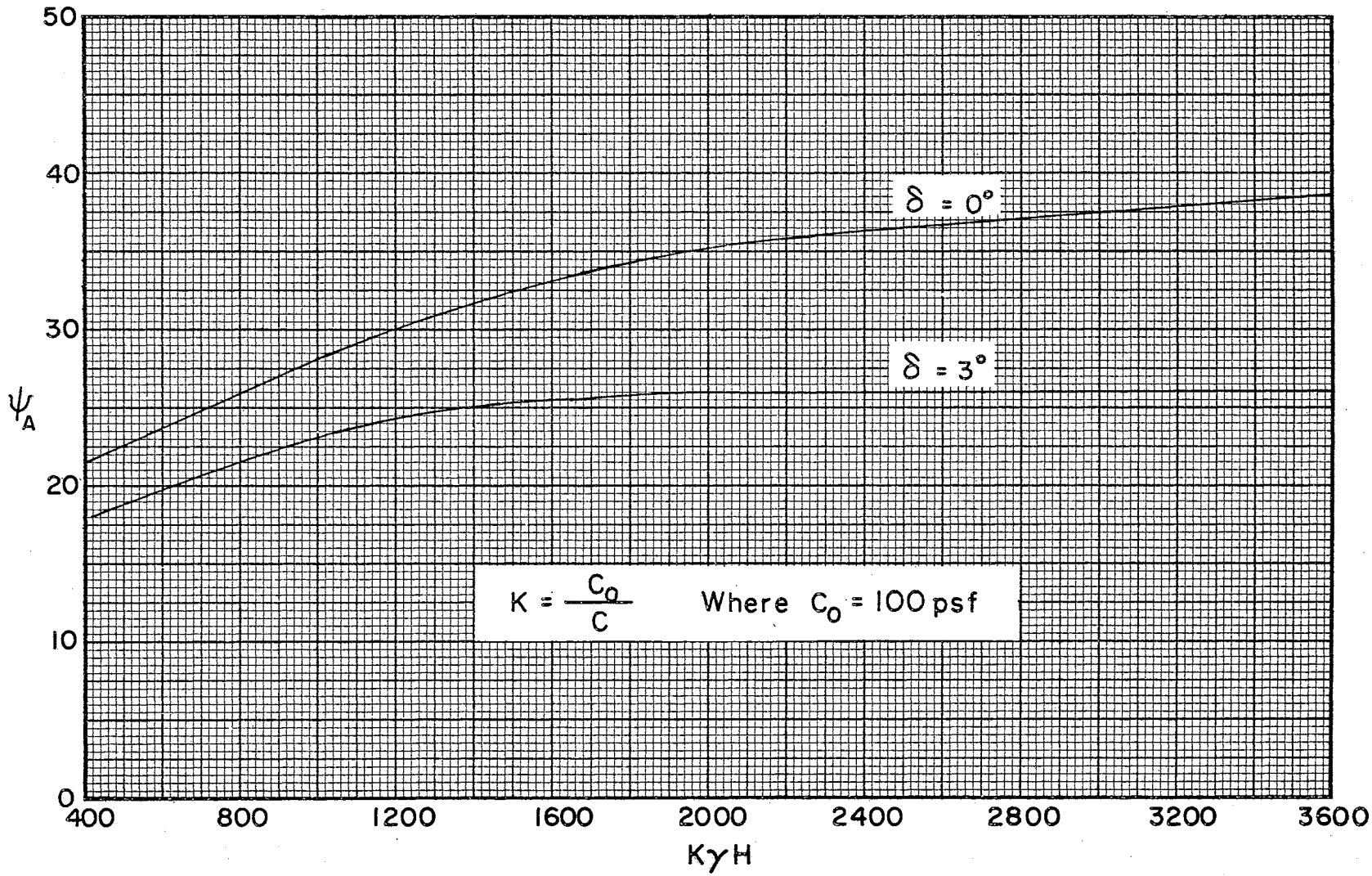

FIG. VIII - GRAPHS FOR DETERMINING ψ_A IN COHESIVE SOIL WHEN $\phi = 5°$

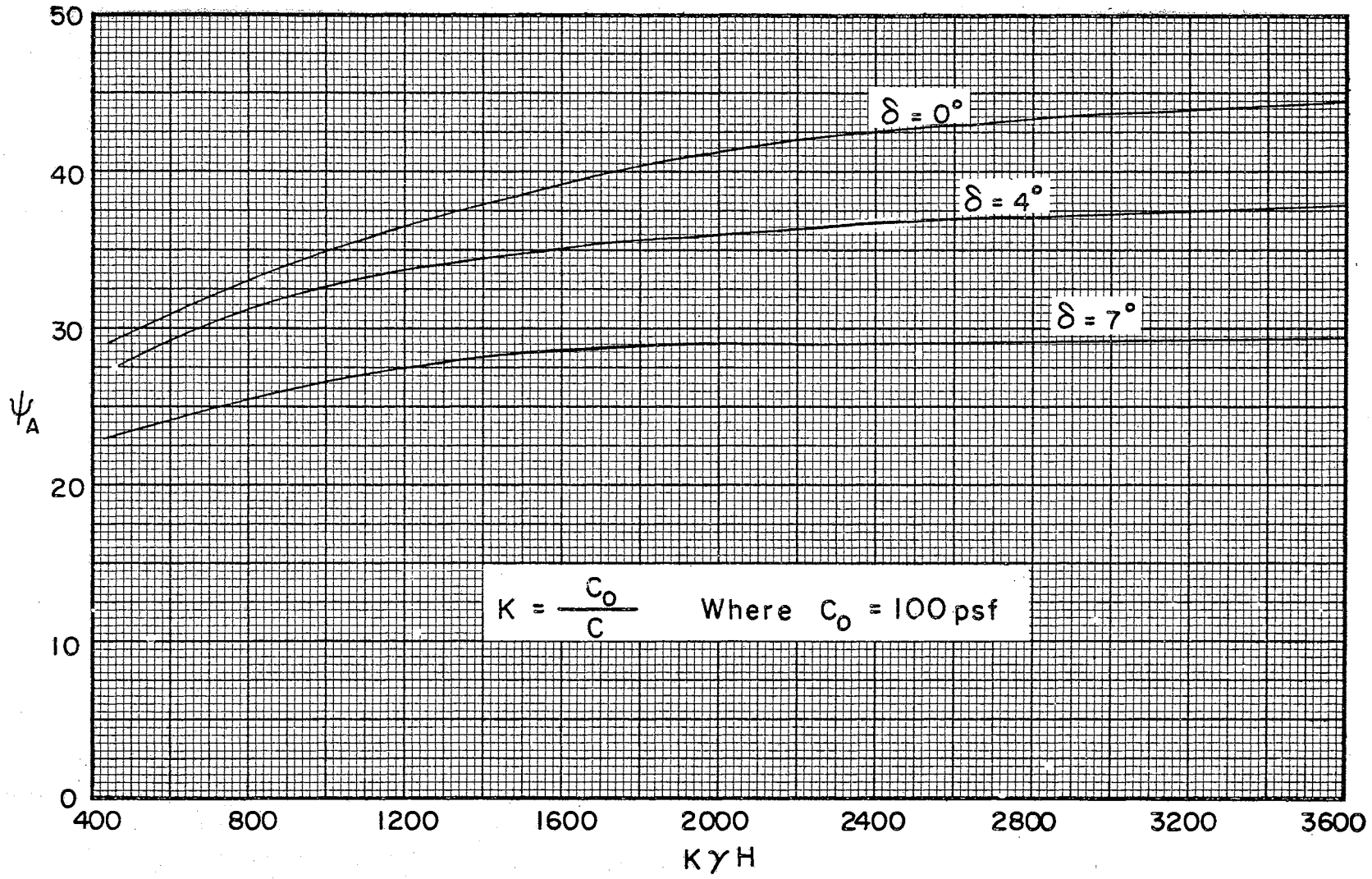

FIG. IX - GRAPHS FOR DETERMINING ψ_A IN COHESIVE SOIL WHEN $\phi = 10°$

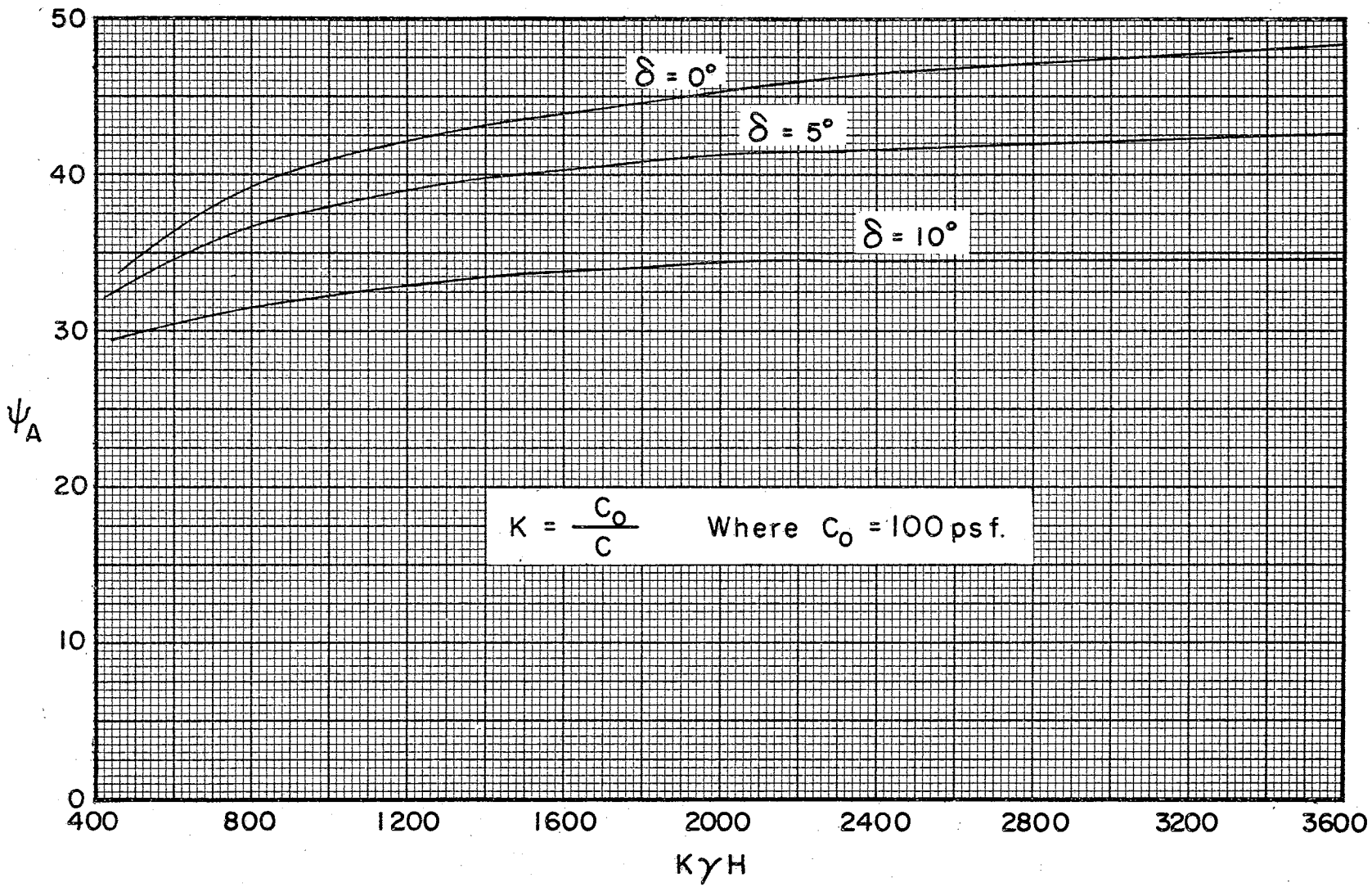

FIG. X - GRAPHS FOR DETERMINING ψ_A IN COHESIVE SOIL WHEN $\phi = 15°$

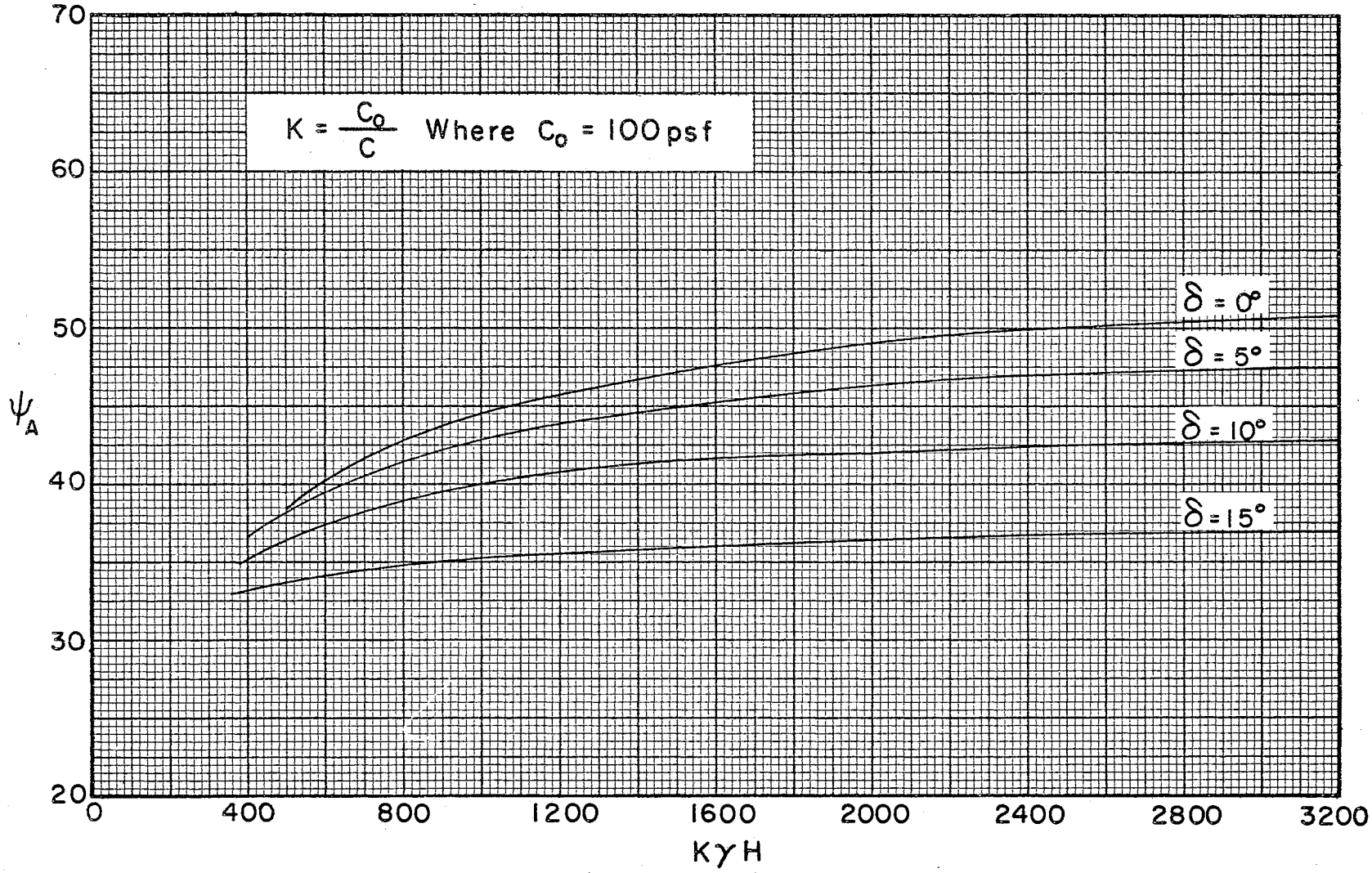

FIG. XI - GRAPHS FOR DETERMINING ψ_A IN COHESIVE SOIL WHEN $\phi = 20°$

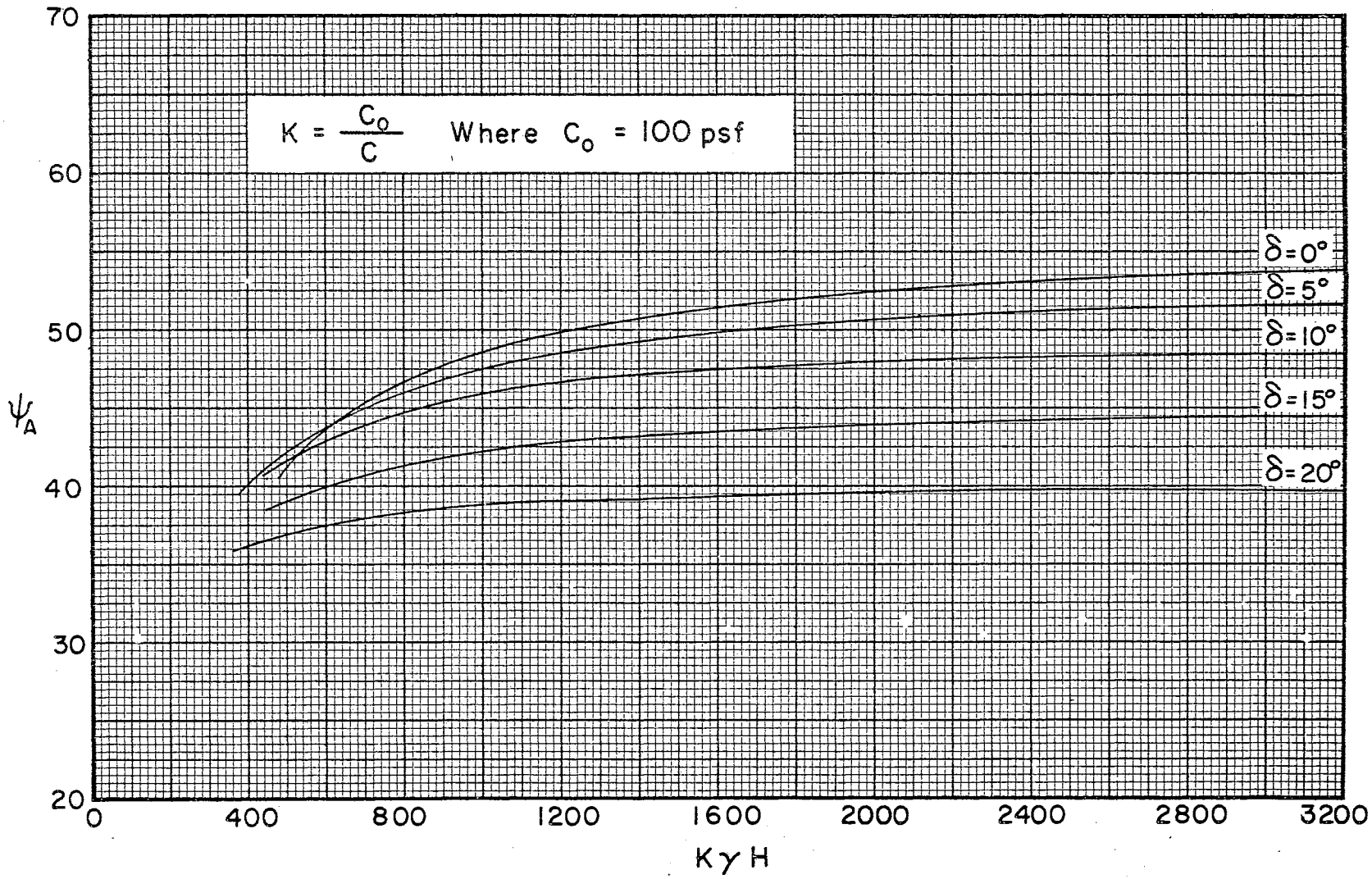

FIG. XII - GRAPHS FOR DETERMINING ψ_A IN COHESIVE SOIL WHEN ϕ = 25°

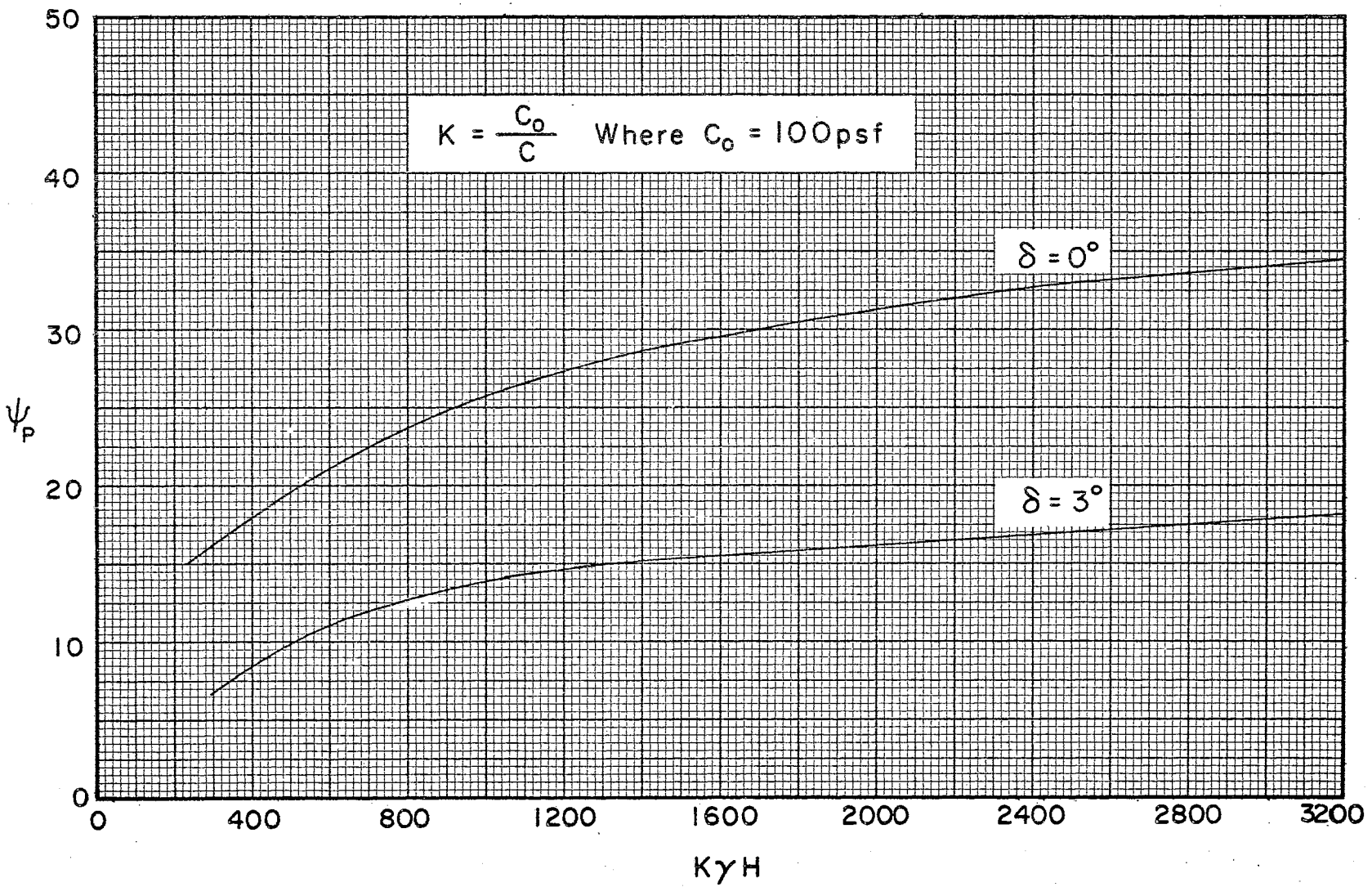

FIG. XIII - GRAPHS FOR DETERMINING ψ_p IN COHESIVE SOIL WHEN ϕ = 5°

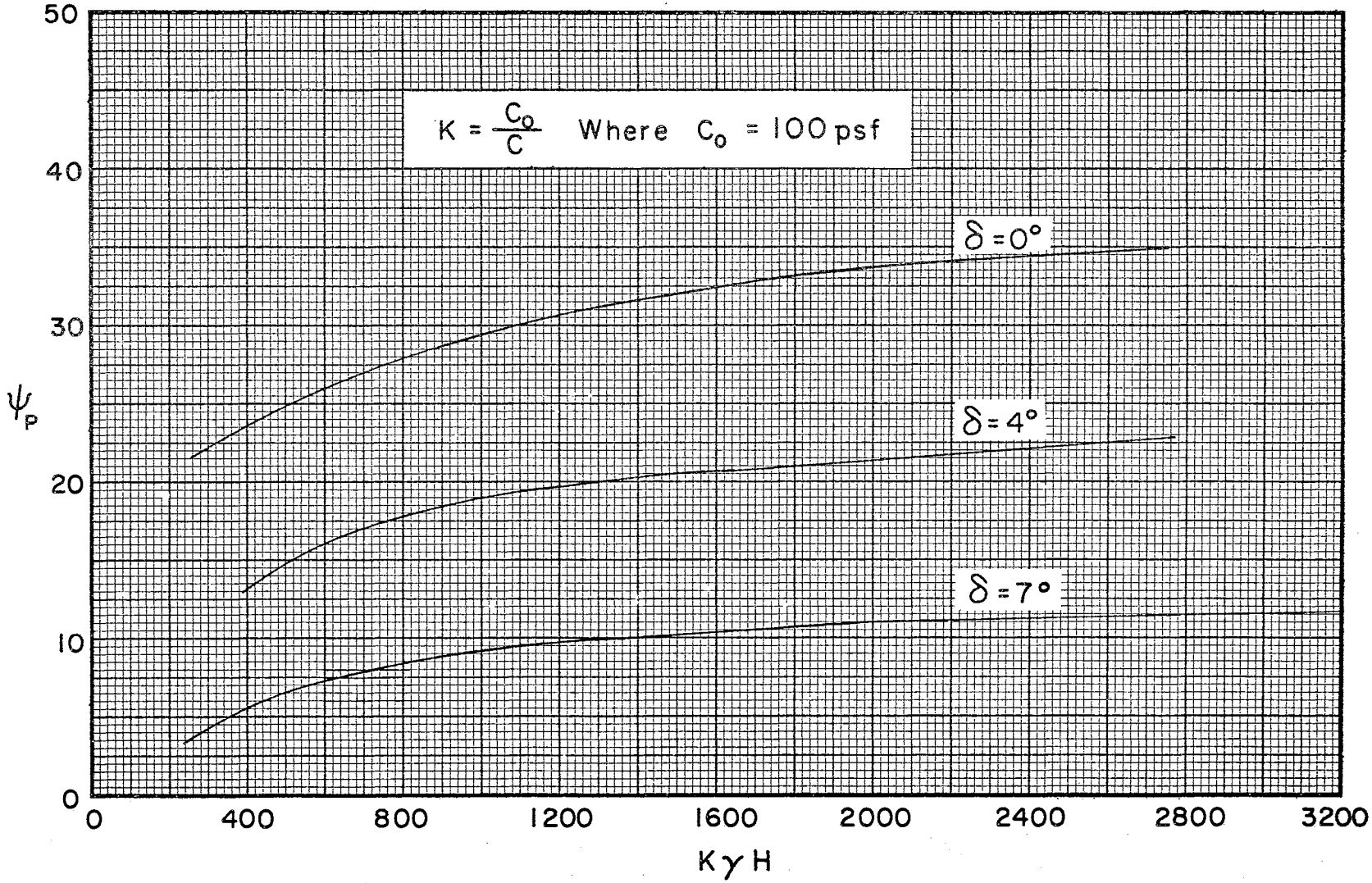

FIG. XIV - GRAPHS FOR DETERMINING ψ_p IN COHESIVE SOIL WHEN ϕ = 10°

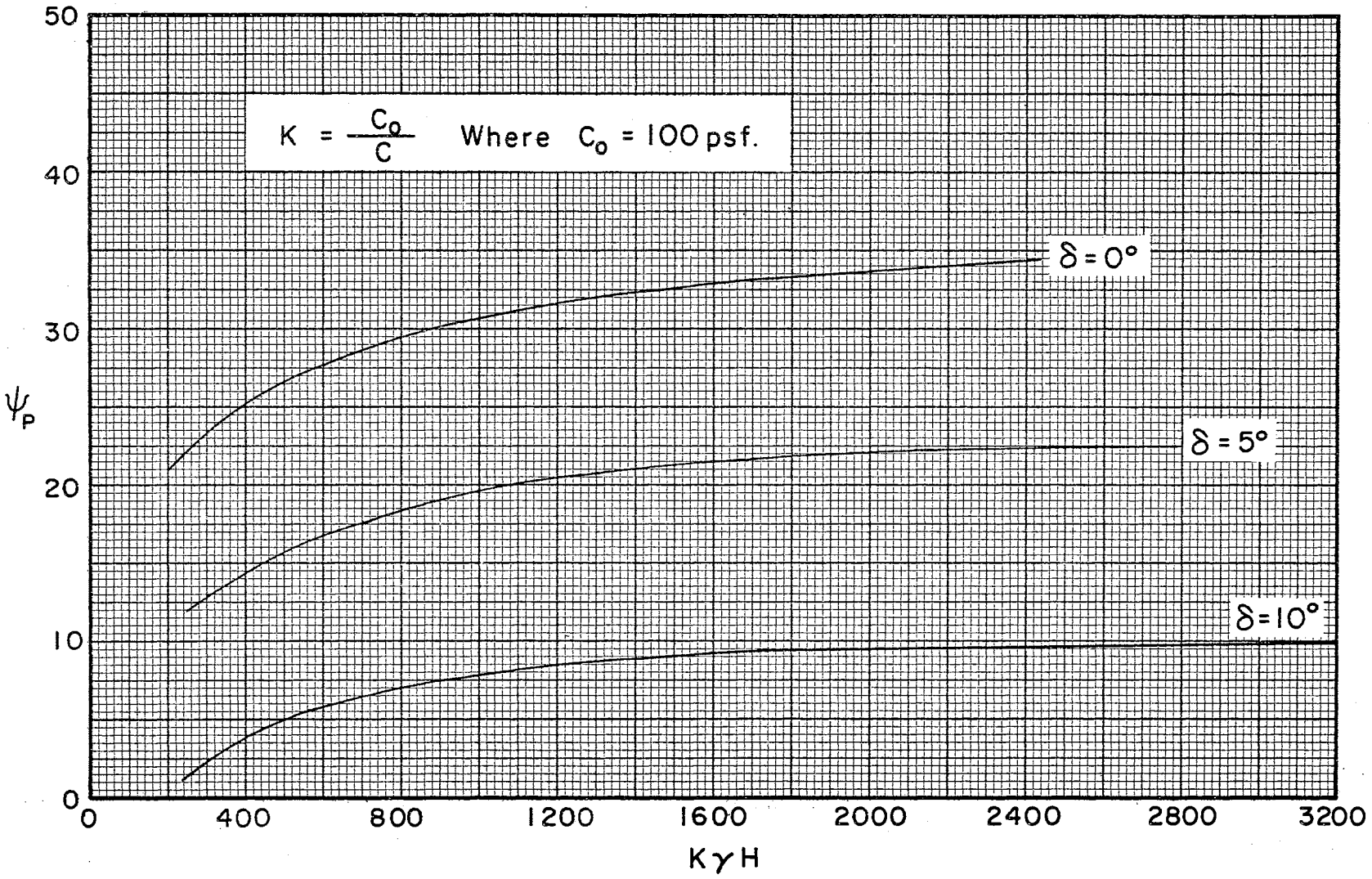

FIG. XV - GRAPHS FOR DETERMINING ψ_p IN COHESIVE SOIL WHEN ϕ = 15°

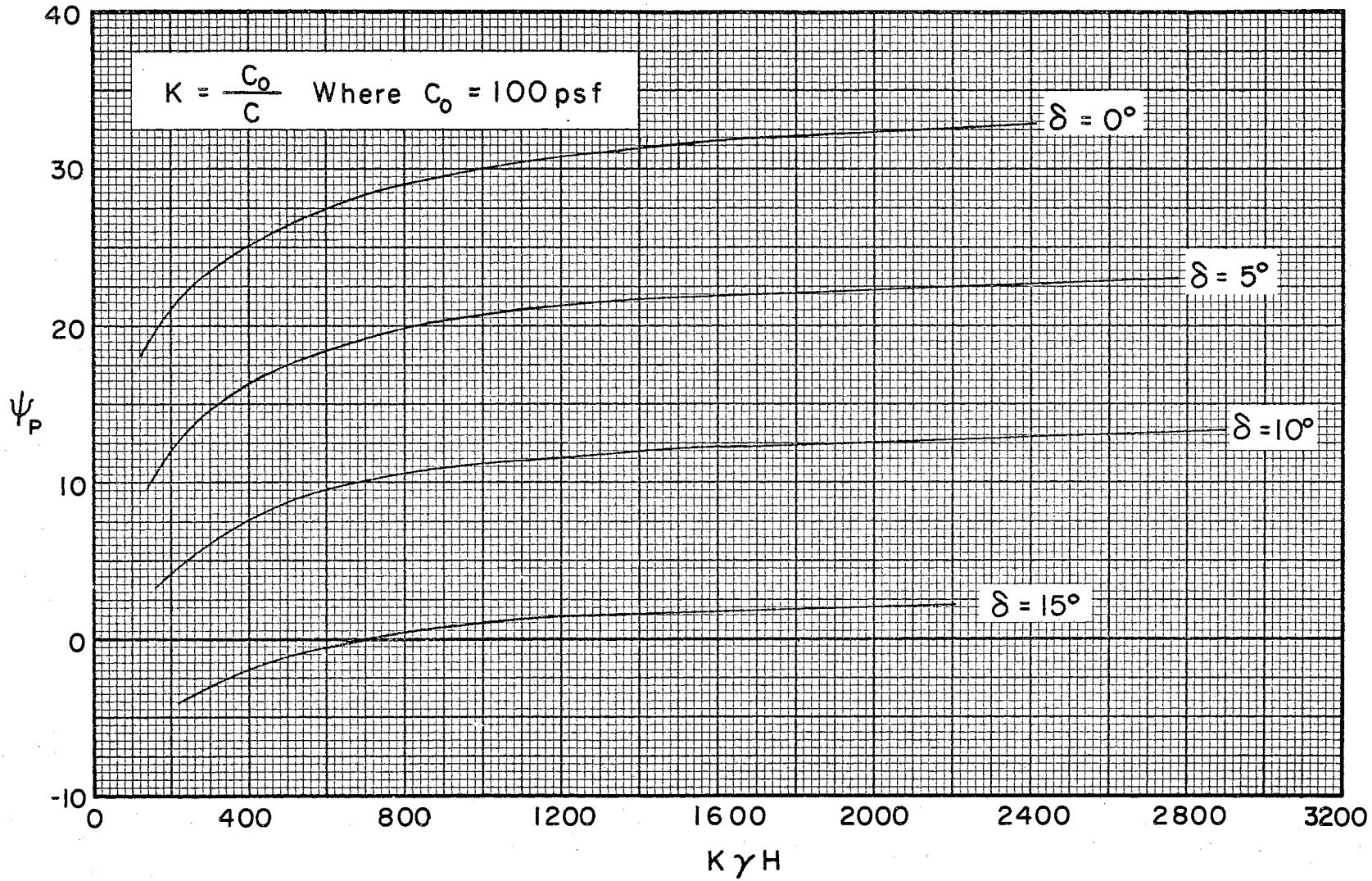

FIG. XVI – GRAPHS FOR DETERMINING ψ_p IN COHESIVE SOIL WHEN ϕ = 20°

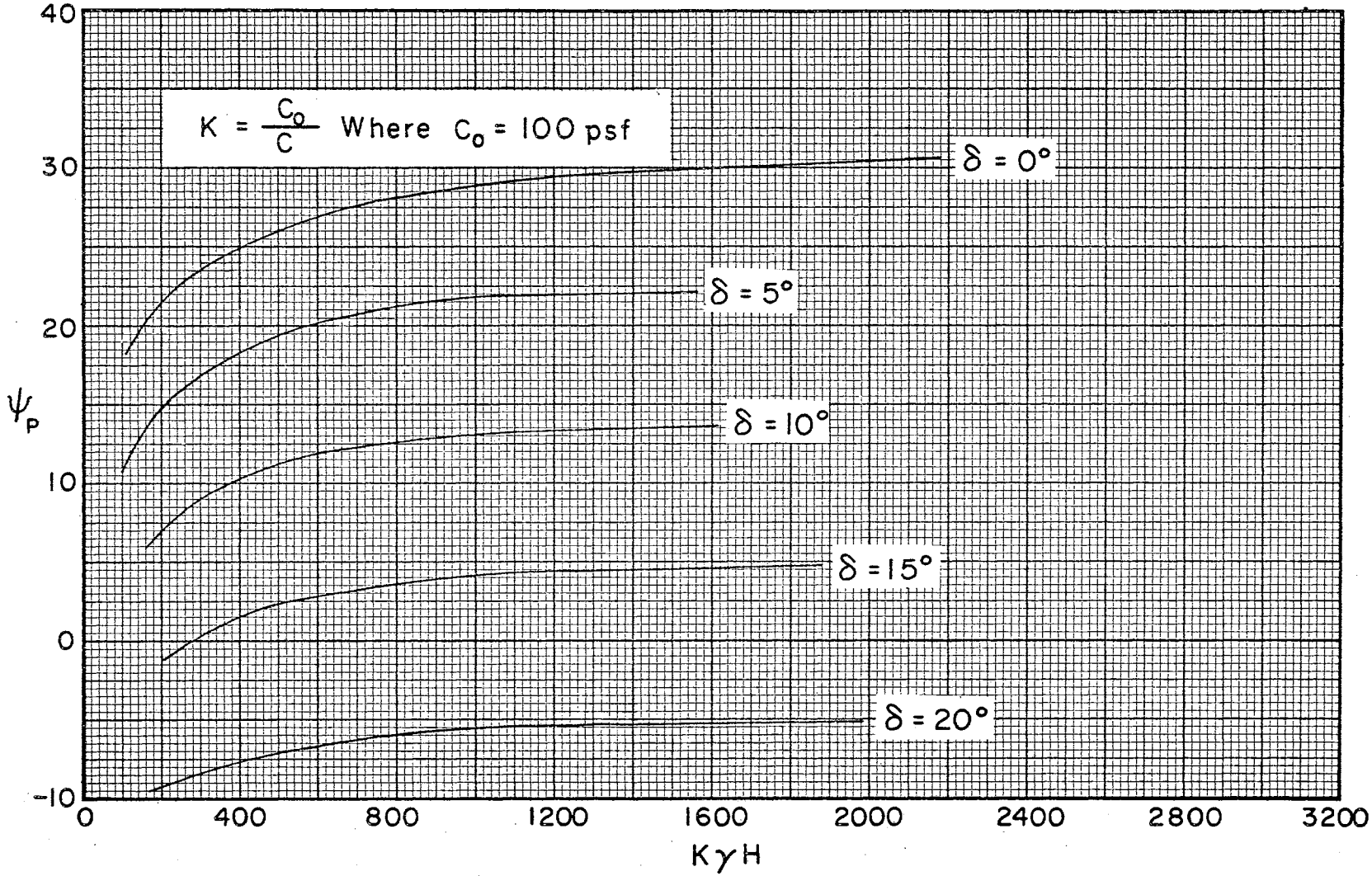

FIG. XVII - GRAPHS FOR DETERMINING ψ_p IN COHESIVE SOIL WHEN $\phi = 25^\circ$

VITA

Assad Faiez Abdul-Baki

Candidate for the Degree of

Doctor of Philosophy

Thesis: A DIRECT METHOD FOR THE DETERMINATION OF EARTH PRESSURES ON RETAINING WALLS

Major Field: Engineering

Biographical:

Personal Data: Born November 16, 1931, at Ainbal, Lebanon, the son of Faiez and Hind Abdul-Baki.

Education: Graduated from Collège De La Sagesse, Beirut, Lebanon, in May, 1950. Received the degree of Bachelor of Science in Mechanical Engineering from Oklahoma State University in May, 1955. Received the degree of Master of Science in Civil Engineering from Oklahoma State University in August, 1956. Completed requirements for the Doctor of Philosophy degree in August, 1965.

Professional Experience: Bridge Designer, Clarkeson Consulting Engineers, Albany, New York, 1956-57. Bridge Designer, Tippets-Abbett McCarthy-Straton, Beirut, Lebanon, 1957-58. Structural Designer, Dar Al-Handassah, Consulting Engineers, Beirut, Lebanon, 1958-62, in charge of the layout and structural design of a 90 M.W. power station. Graduate Assistant in the Civil Engineering Department at the Oklahoma State University from September, 1962, to date.

Organizations: Registered Professional Engineer in Lebanon; Associate Member of American Concrete Institute.